COMPUTATIONAL CHEMISTRY STUDIES OF [1,7] SIGMATROPIC HYDROGEN SHIFT IN Z,Z-1,3,5-HEPTATRIENE SYSTEMS AND ESTERIFICATION REACTIONS

BY

MACHARIA KIBE GODFREY (MSc-Kenyatta University)
(REG. NO I84/15169/2004)

DEPARTMENT OF CHEMISTRY

A THESIS SUBMITTED IN PARTIAL FULFILLMENT OF THE REQUIREMENTS FOR THE AWARD OF THE DEGREE OF DOCTOR OF PHILOSOPHY OF KENYATTA UNIVERSITY

March 2009

DECLARATION

This thesis is my original work and has not been presented for a degree in any other University or any award.

Macharia Kibe Godfrey
Department of chemistry

Signed ……. Date……

We confirm that the work reported in this thesis was carried out by the candidate under our supervision.

Prof. M. S. Rajab
Department of chemistry
Kenyatta University

Signed ……. Date……

Prof. G. K. Muthakia
Department of chemistry
Kenyatta University

Signed ……. Date……

DEDICATION

To my wife Catherine Njeri, our children, Ruth Nyawira and Victor Macharia.

ACKNOWLEDGEMENTS

First of all I would like to express my gratitude to my supervisors Prof. M. S. Rajab, and Prof. G. K. Muthakia for sparking my interest in both quantum mechanical calculations and computational chemistry, encouraging me to study molecular modeling, developing my skills in and love for research by offering valuable insights and direction, generously giving their time to help me with everything, and being wonderful and supportive PhD advisors and a real joy to work with. Their experience and optimistic encouragement has been of great help and inspiration throughout the past years.

Secondly, I would to sincerely thank Prof. H. G. Kruger, of University of KwaZulu-Natal, for giving me kick start in computational. He also allowed me to visit his laboratory in South Africa. The hospitality of Sandrak Naicker family who accompdated me in South Africa is highly appreciated. They treated me as one of their family.

I am grateful to Kenyatta University for the sponsorship of my study through a staff development program and providing supportive and condusive environment full of intellectual challages and stimulations.

I am indebted to my friends Dr. A. K. Machocho, Dr. P. K. Tarus, Dr. E. O. Changamu and L. M. Gitu and to other friends that I have not properly acknowledged here, for unselfishly giving their quality time and offering prayers of support for me throughout my time at Kenyatta University.

Finally, if it were not for the heroic efforts of my wife Catherine Njeri and the (relative) patience of my children Ruth Nyawira and Victor Macharia- all who allowed me to spend a ridiculous number of hours over a keyboard in a non-communicative trance- I would most certainly never have accomplished anything.

Honour and glory to God, the Father Almighty, the Creator of heaven and earth, for showing His love, joy, peace, patience, kindness, goodness, faithfulness, gentleness, and self-control to me, without whose justification and righteousness I would not be writing this today.

TABLE OF CONTENTS

Page

LIST OF FIGURES

LIST OF TABLES

LIST OF SCHEMES

LIST OF ABBREVIATIONS AND SYMBOLS

Ψ	Wave function
3-21G	[Pople's basis set] (pronounced "three two one jee"). The core orbitals represented by three primitive GTOs , whereas the inner and outer valence orbitals consist of two and one Gaussians, respectively
6-31+G*	[Pople's basis set] defined as for 6-31G* with diffuse functions added
6-31G	[Pople's basis set] (pronounced "six three one jee") The core consists of 6 GTOs which are not split, whereas the inner and outer valence orbitals consist of three and one Gaussians, respectively
6-31G*	[Pople's basis set] defined as for 6-31G with polarization added
Ab initio	From the beginning
AM1	Austin Model 1
B3LYP	A density functional method due to Lee, Yang and Parr which incorporates a 3- parameter function due to Axel Becke
BFGS	Broyden-Fletcher-Goldfarb-Shanno method
BLYP	A density functional method due to Becke, Lee, Yang and Parr
BP86	A density functional method developed by Becke and Perdew In 1986
CAMD	Computer Aided Molecular Design
CAMM	Computer Aided Molecular Modeling
CASCF	Complete Active Space Self Consistent Field
CI	Configuration Interaction
CNDO	Complete Neglect of Differential Overlap
CPU	Central processing unit
DFT	Density Functional Theory
E_{el}	Pure electronic energy
FF	Force Field
FMO	Frontier Orbital Theory
GGA	Generalized Gradient Approximation
gjf	Gaussian job file
GTO	Gaussian Type Orbitals
$\hat{H}$	Hamiltonian
HF	Hartree-Fock
HOMO	Highest Occupied Molecular Orbital
HPT	1, 3, 5- Heptatriene
IRC	Intrinsic Reaction Coordinates
LCAO	Linear Combination of Atomic Orbitals
LDA	Local Density Approximation
LST	Linear Synchronous Transit
LUMO	Lowest Unoccupied Molecular Orbital
MCSCF	Multiconfiguration Self-Consistent Field
MEP	Molecular Electrostatic Potential
MINDO	Modified Intermediate Neglect of Differential Overlap
MM	Molecular Mechanics
MNDO	Modified Neglect of Diatomic Overlap

MO	Molecular Orbital
MP	Moller-Plesset
MP2	Second- order Moller-Plesset
MP4	Fourth- order Moller-Plesset
NBO	Natural Bond Orbital
NDDO	Neglect of Diatomic Differential Overlap
OPCP	Orbital Phase Continuity Principle
PES	Potential Energy Surface
PM3	Parametric Method Number 3
QM	Quantum Mechanics
QSAR	Quantitative Structure-Property Relationships
QST	Quadratic Synchronous Transit
RAM	Radom Access Memory
RHF	Restricted Hartree-Fock
SCF	Self Consistent Field
STO	Slater Type Orbitals
STQN	Synchronous Transit-Guided Quasi Newton
TS	Transition State
UHF	Unrestricted Hartree-Fock

LIST OF APPENDICES

Dirac's Famous Statement

"The underlying physical laws necessary for the mathematical theory of a large part of physics and the whole of chemistry are thus completely known, and the difficulty is only that the exact application of these laws leads to equations much too complicated to be soluble. It therefore becomes desirable that approximate practical methods of applying quantum mechanics should be developed, which can lead to an explanation of the main features of complex atomic systems without too much computation" (Paul Dirac, 1929)

ABSTRACT

Density functional theory has been used to study mechanisms of the reactions involving [1,7]-sigmatropic hydrogen shift in Z,Z-1,3,5-heptatriene systems, esterification of acetyl chloride with methanol and acid-catalyzed esterification of carboxylic acids with methanol. The calculations employed the B3LYP functional, with 6-31+G(d) basis sets. Mechanism routes were computed, with complete optimization of all intermediates and transition states. The effect of electron-donating and electron-withdrawing substituents in Z,Z-1,3,5-heptatriene systems was investigated. Analysis of the geometries, energies and electronic characteristics of the sigmatropic transposition compared to those of the unsubstituted cases provided insights into substituent effects of the reactions. The study revealed that the inductive and mesomeric effects of heteroatoms or heterosubstituents are of great importance in the energetics of the transformation. Steric effects also play an important role due to the geometrical constraints of the reaction. Generally increasing the electron density of the π system, decreases the electron density on the protropic proton resulting in the decrease of the activation energy. For the esterification of acetyl halides with methanol, the calculations suggest that the reaction proceeds through a loose transition state with a concerted S_N2 mechanism. The nucleophilic methanol attacks the carbonyl carbon at Bürgi-Dunitz trajectory and the interaction is subject to general base catalysis, either by a second molecule of methanol or a solvent molecule. This explains the mixed reaction kinetics observed from experimental data. The calculations suggest that the acid-catalyzed esterification of carboxylic acids with methanol involve interaction of both the proton and the counter ion. The calculated activation parameters in the solvent model are in excellent agreement with experimental results. The computational results for the methanolysis of acetyl chloride and acid-catalyzed esterification reactions call for a re-evaluation of some commonly accepted classical mechanistic pathways. For the reactions investigated in this study, the calculations revealed a new mechanistic insight of the reaction pathway.

CHAPTER ONE

1 INTRODUCTION

1.1 Computational Chemistry

Computational chemistry is a branch of chemistry that uses computers to solve real problems in chemistry, pharmaceutical, biotechnology and material science. It uses the results of theoretical chemistry, incorporated into efficient computer programs, to calculate the structures and properties of molecules and solids. Its results normally complement the information obtained by chemical experiments; it can in some cases predict hitherto unobserved chemical phenomena. It is widely used in the design of new drugs and materials (Clark, 1985; Hinchcliffe, 1996; Hirst, 1990).

Computational chemistry is capable of predicting many properties of molecules and reactions, including the following; molecular energies and structures, energies and structures of transition states, bond and reaction energies, molecular orbitals, vibrational frequencies, thermochemical properties, reaction pathways, spectroscopic quantities and numerous other molecular properties for systems in the gas phase and in solution, including the ground state and excited states (Cramer, 2004; Leach, 2001).

The methods employed cover both static and dynamic situations. In all cases the computer time increases rapidly with the size of the system being studied. That system can be a single molecule, a group of molecules or a solid. The methods are thus based on theories which range from highly accurate, but are suitable only for small systems, to very approximate, but

suitable for very large systems. The accurate methods used are called *ab initio* methods, as they are based entirely on theory from first principles. The less accurate methods are called empirical or semi-empirical because mathematical truncation or some experimental results, often from acceptable models of atoms or related molecules, are used along with the underlying theory.

Both of these approaches involve approximations, either as generalized forms of first principles equations optimized for computation, from systems with boundary conditions which limit the scope of computation to within a pre-defined window, or ultimately from the necessary approximation of quantum mechanics equations which have not been solved exactly except for single-electron systems (for example, the hydrogen atom). In practice, *ab initio* methods eventually converge towards the exact solution if all the approximations are made at a small enough magnitude.

1.2 Historical Development of Computational Chemistry

Building on the founding discoveries and theories in the history of quantum mechanics, the first theoretical calculations in chemistry were those of Walter Heitler and Fritz London in 1927 (Heitler and London, 1927). The books that were influential in the early development of computational quantum chemistry include: Linus Pauling and E. Bright Wilson's 1935 *Introduction to Quantum Mechanics – with Applications to Chemistry* (Pauling and Wilson, 1935), Eyring, Walter and Kimball's 1944 *Quantum Chemistry* (Eyring, *et al*., 1944), Heitler's 1945 *Elementary Wave Mechanics – with Applications to Quantum Chemistry* (Heitler, 1945), and later Coulson's 1952 textbook *Valence* (Coulson, 1952), each of which served as primary references for chemists in the decades to follow.

With the development of efficient computer technology in the 1940s, the solutions of elaborate wave equations for complex atomic systems began to be a realizable objective. In the early 1950s, the first semi-empirical atomic orbital calculations were carried out. Theoretical chemists became extensive users of the early digital computers. A very detailed account of such use in the United Kingdom is given by Smith and Sutcliffe (Smith and Sutcliffe, 1997). The first *ab initio* Hartree-Fock calculations on diatomic molecules were carried out in 1956 at the Massachusetts Institute of Technology (MIT), using a basis set of Slater orbitals. For diatomic molecules, a systematic study using a minimum basis set and the first calculation with a larger basis set were published by Ransil and Nesbet respectively in 1960 (Schaefer, 1984). The first polyatomic calculations using Gaussian orbitals were carried out in the late 1950s. The first configuration interaction (CI) calculations were carried out in Cambridge on the EDSAC computer in the 1950s using Gaussian orbitals by Boys and coworkers (Boys, *et al*., 1956). By 1971, when a bibliography of *ab initio* calculations was published (Richardson, *et al*., 1971), the largest molecules included were naphthalene and azulene (Buenker and Peyerimhoff, 1969; Preuss, 1968). Abstracts of many earlier developments in *ab initio* theory have been published by Schaefer (Schaefer, 1984).

In 1964, Hückel method calculations (using a simple linear combination of atomic orbitals method for the determination of electron energies of molecular orbitals of π electrons in conjugated hydrocarbon systems) of molecules ranging in complexity from butadiene and benzene to ovalene, were generated on computers at Berkeley and Oxford (Streitwieser, *et al*., 1992). These empirical methods were replaced in the 1960s by semi-empirical methods such as the complete neglect of differential overlap (CNDO) (Pople and David, 1970).

In the early 1970s, efficient *ab initio* computer programs such as ATMOL, GAUSSIAN, IBMOL, POLYAYTOM and GAMESS, began to be used to speed up *ab initio* calculations of molecular orbitals. Of these four programs, only GAMESS and GAUSSIAN, now massively expanded, is still in use, but many other programs are now in use. At the same time, the methods of molecular mechanics, such as MM2, were developed, primarily by Norman Allinger (Allinger, 1977).

One of the first mentions of the term "computational chemistry" can be found in the 1970 book *Computers and Their Role in the Physical Sciences* by Sidney Fernbach and Abraham Haskell Taub, where they state "It seems, therefore, that 'computational chemistry' can finally be more and more of a reality" (Fernbach and Taub, 1970). During the 1970s, widely different methods began to be seen as part of a new emerging discipline of *computational chemistry*. The *Journal of Computational Chemistry* was first published in 1980.

1.3 Concepts of Computational Chemistry

Computational chemistry involves a mathematical description of systems of chemical species. The goal is to solve the complex equations such as Schrödinger equation for electronic and nuclear motion which accurately describe natural phenomena. In a practical application of computational chemistry, mathematical equations or algorithms are devised to quantitatively describe the physical and chemical phenomena (for example, energy states, structures, reactivity, positions and momenta of atoms) that occur in a particular system. These algorithms are then programmed in the appropriate computer languages and linked together so that the many millions of calculations required to effectively describe the phenomena can be quickly computed. For example, it might be necessary to calculate billions of integrals to accurately describe the repulsion of electrons in a complex molecule.

The end result is a set of computational tools that predict the characteristics and behaviour of the chemical system.

The term theoretical chemistry may be defined as a mathematical description of chemistry, whereas computational chemistry is usually used when a mathematical method is sufficiently well developed that it can be automated for implementation on a computer. Note that the words *exact* and *perfect* do not appear here, as very few aspects of chemistry can be computed exactly. However, almost every aspect of chemistry can be described in a qualitative or approximate quantitative computational scheme.

Molecules consist of nuclei and electrons, so the methods of quantum mechanics apply. Computational chemists often attempt to solve the non-relativistic Schrödinger equation, with relativistic corrections added, although some progress has been made in solving the fully relativistic Schrödinger equation. In principle, it is possible to solve the Schrödinger equation in either its time-dependent or time-independent form, as appropriate for the problem at hand; in practice, this is not possible except for very small systems. Therefore, a great number of approximate methods strive to achieve the best trade-off between accuracy and computational cost. Accuracy can always be improved with greater computational cost. Significant errors can present themselves in *ab initio* models comprising of many electrons, due to the computational expense of full relativistic-inclusive methods. This complicates the study of molecules interacting with high atomic mass unit atoms, such as transitional metals and their catalytic properties. Present algorithms in computational chemistry can routinely calculate the properties of molecules that contain up to about 40 electrons with sufficient accuracy. Errors for energies can be less than a few kJ/mol. For geometries, bond lengths can be predicted within a few picometres and bond angles within 0.5 degrees. The treatment

of larger molecules that contain a few dozen electrons is computationally tractable by approximate methods such as density functional theory (DFT). There is some dispute within the field whether or not the latter methods are sufficient to describe complex chemical reactions, such as those in biochemistry. Large molecules can be studied by semi-empirical approximate methods. Even larger molecules are treated by classical mechanics methods that employ what is called molecular mechanics (MM). In QM/MM methods, small portions of large complexes are treated quantum mechanically (QM), and the remainder is treated approximately (MM).

In theoretical chemistry, chemists, physicists and mathematicians develop algorithms and computer programs to predict atomic and molecular properties and reaction paths for chemical reactions. Computational chemists, in contrast, may simply apply existing computer programs and methodologies to specific chemical questions. There are two different aspects to computational chemistry:

Computational studies can be carried out in order to find a starting point for a laboratory synthesis, or to assist in understanding experimental data, such as the position and source of spectroscopic peaks. Computational studies can be used to predict the possibility of so far entirely unknown molecules or to explore reaction mechanisms that are not readily studied by experimental means. Thus, computational chemistry can assist the experimental chemist or it can challenge the experimental chemist to find entirely new chemical objects.

Several major areas may be distinguished within computational chemistry:

- The prediction of the molecular structure of molecules by the use of the simulation of forces, or more accurate quantum chemical methods, to find stationary points on the energy surface as the position of the nuclei is varied.
- Storing and searching for data on chemical entities (chemical databases, chemoinformatic).
- Identifying correlations between chemical structures and properties (quantitative structure-activity relationships - QSAR and quantitative structure-property relationships – QSPR).
- Computational approaches to help in the efficient synthesis of compounds.
- Computational approaches to design molecules that interact in specific ways with other molecules (for example drug design).

1.4 Molecular Modeling

Molecular modeling is the science or art of representing molecular structures numerically and simulating their behaviour with the equations of quantum and classical physics and it is one of the fastest growing fields in science. Consequently, it is now becoming very useful to simulate experiments by computer before doing the laboratory bench work. The computer model is able to display the results on a visual unit for further modification, correction or study (Leach, 2001).

Modeling techniques are widespread in their use and have become more and more important in widely varying fields of chemistry, ranging from small organic molecules to proteins, polymers, inorganic solids and liquids. Molecular modeling varies from building, visualizing and comparing molecules to performing complicated and time demanding calculations on complex molecular system.

Practical application of these techniques has grown dramatically in areas such as pharmaceutical drug design, biotechnology, chemical engineering and organic synthesis in the last three decades. Molecular modeling can help in the interpretation and understanding of experimental results, and in some cases suggest the appropriate directions for further experiments. It has been employed widely as a tool in the prediction of physical-chemical properties; for example, quantitative structure-property relationships (QSPR) studies can predict conformations and relative molecular stability of compounds and the viability of some transformations (Hyde and Livingstone, 1988). Over the years, the advent of faster computers and more reliable software packages have simplified the handling of complex molecules, drastically cutting down computer time and increasing reliability of the results obtained. As such, molecular modeling has become both practical and convenient, and could eliminate the need for costly and time consuming experiments.

1.5 Computer-Aided Molecular Modeling (CAMM)

Computer aided molecular modeling is the investigation of molecular structures and properties using computational chemistry and graphical visualization techniques. Comparison with experimental data, where available, is important to guide both laboratory and computational work.

Most molecular modeling work involves three stages; Selecting a suitable model to describe intra- and inter-molecular interactions in the system (quantum mechanics and molecular mechanics), performing the calculation, and analyzing the results.

CAMM covers a range of techniques that has been used by chemists, physicists or biologists to simulate and then predict molecular properties. There is a growing interest in applying modeling techniques to other areas of science, for example, polymer or catalyst science. A basic overview of the various areas in industrial research suitable for CAMM has been presented by Dearing (Dearing, 1988).

CAMM techniques are used to process, investigate, or predict molecular properties: providing structural information, determinations of properties by force-field calculations and molecular electronic properties by quantum mechanical methods, using molecular dynamics calculations on molecular motions, predicting protein folding and revealing the diversity of molecular properties.

Computer-aided molecular design (CAMD) involves all computer-aided techniques used to discover, design and optimize compounds with desired structures and properties (Hopkinson and Judson, 1989).

1.6 Computational Chemistry and Experiment

Computational chemistry will never be a full replacement for doing experiments, but can often supplement experimental work. Very often neither experiment nor computational chemistry can by itself give the desired full insight. In many cases one must therefore piece together whatever information and conclusion that can be drawn from either source. Sometimes computational chemistry can be used to calculate properties that are not at all available from experimental work, while some issues can be difficult both in the laboratory and on the computer. When working with results from modeling and the laboratory one should have a feeling for the quality of the data from different sources.

Computational chemistry has grown as a field very quickly, and many researchers are perhaps not fully aware of the potential of its methods. On the other hand there has been the impression that researchers sometimes are more aware of the limitations of the tools they work with, than that of other methods, and may come to overestimate the quality of the work in a different field. In the field of three reactions investigated in this study there is as noted in chapter two considerable amounts of experimental data. On the other hand it must also be noted that the systems in the process display considerable complexity. Given the complexity of the system, the amount of experimental data available must actually be considered to be rather sparse. The mechanism of these systems also present challenges for computational chemistry work. The absence of experimental data at the molecular level also means that it can be difficult to validate models being used and conclusions drawn regarding the nature of the system. The approach in this work has therefore been somewhat pragmatic. The most effort has been put into areas where computational chemistry was thought to give the most valuable new insight, whereas some aspects have been approached tentatively.

1.7 Theoretical Organic Chemistry

Theoretical organic chemistry encompasses a wide range of topics, spanning from high level electronic structural calculations of simple organic molecules using well-established *ab initio* MO or DFT techniques to computer simulations of chemical reactions and interaction in solution.

Theoretical treatments of organic molecules may be roughly classified in terms of electronic structure theories and empirical force fields. The former describe an organic system by quantum chemical methods which include HF theory, post-Hartree-Fock methods, DFT and

MCSCF techniques. On the other hand, semi-empirical force fields represent a molecular system by van der Waals spheres and partial atomic charges, and the potential energy surface is simply expressed by empirical potential functions.

The following section gives a brief description of the three systems investigated in the present study by computational methods.

1.8 Thermal [1,7]-Sigmatropic Hydrogen Shifts

Sigmatropic rearrangements are those reactions in which a sigma (σ) – bond (in other words a substituent) moves across a conjugated system to a new site. The thermal [1,5]- and [1,7]-sigmatropic hydrogen shifts are subsets of pericyclic processes first systematically defined in 1965 by Woodward and Hoffmann, (Woodward and Hoffmann, 1965) (Figure **1.8.1**). The classic metabolic transformation of previtamin D, to vitamin D_3 is a pivotal event in calciferol (vitamin D) biosynthesis (Blondin, *et al*., 1964) and can be considered to be an example of a biological [1,7]-sigmatropic hydrogen shift.

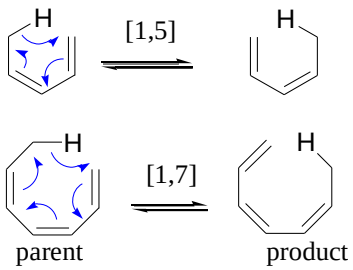

Figure 1.8.1: [1,5] and [1,7]- sigmatropic H shift.

In the present study, the effect on rate enhancement or retardation by substituent groups in Z,Z-1,3,5-heptatriene systems and related heteroanalogues was investigated by computational method.

1.9 Esterification of Acetyl Chloride with Methanol

The alcoholysis of acyl chlorides reaction is useful to convert alcohols into their esters which are frequently used as solvents, fragrances and additives to drugs and perfumes as well on an industrial scale.

According to the classical mechanism(Scheme **1.9.1**) (March, 1992), the nucleophilic alcohol adds to acyl chloride, to form a tetrahedral intermediate with subsequent loss of hydrogen chloride. This simple concept has been challenged by experimental findings that concurrent second-order and third-order contributions to the overall kinetics (Willms, *et al*., 2000; Willms, *et al*., 2000) (first- and second-order with respect to alcohol) take place.

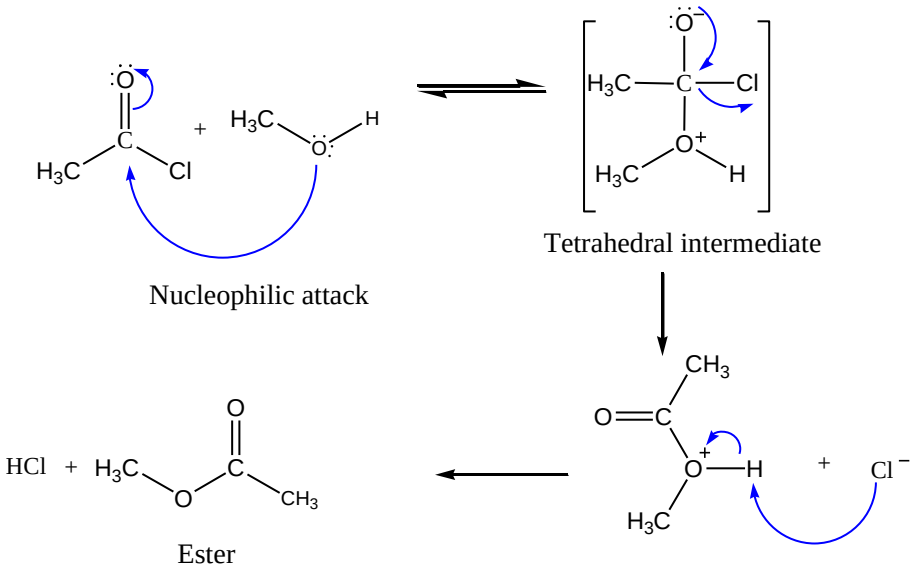

Scheme 1.9.1 Classical mechanism for methanolysis of acetyl chloride. (March, 1992)

The present study applied computational methods to verify the mechanism of esterification of acetyl chloride with methanol.

1.10 Acid-Catalyzed Esterification

Esterification of carboxylic acids with alcohols is one of the most general and widely used reactions of considerable industrial interest due to the enormous practical importance of organic ester products. The ester products include environmentally friendly solvents, flavors, pharmaceuticals, plasticizers, polymerization monomers and emulsifiers in the food, cosmetic and chemical industries (Altiokka and Citak, 2003; Ayturk, *et al*., 2003). Recently, a growing interest in ester synthesis has been further stimulated due to the great promise shown by long chain mono alkyl esters as fuels for diesel engines (Aafaqi, *et al*., 2004; Lotero, *et al*., 2005).

1.10.1 Mechanism of Acid-Catalyzed Esterification

Esterification can take place without adding catalysts due to the weak acidity of carboxylic acids themselves (autocatalysis). But the reaction is extremely slow and requires several days to reach equilibrium at typical conditions. Either homogenous mineral acids, such as H_2SO_4, HCl or HI, or heterogeneous solid acids, such as various sulfonic resins, have been shown to be able to effectively catalyze the reaction.

The ester formations involve reaction of protonated acid. It is now generally accepted that this protonation takes place on the carbonyl oxygen (Stewart and Yates, 1960). Bender (Bender, 1960) has formulated a mechanism for these reactions involving six stages. Most of these stages occur relatively rapidly, and for the purpose of this study only two of them will be discussed (Scheme **1.10.1**). Protonation of the acid takes place in a fast reversible step and the rate-limiting reaction involves reaction of the protonated species with the methanol. The intermediate so formed then undergoes a series of fast reactions (proton shifts and loss of a molecule of water) to give ester.

The catalysts essentially promote the protonation of the carbonyl oxygen on the carbonyl group thereby activating nucleophilic attack by an alcohol to form a tetrahedral intermediate.

Classical textbooks (Maitland, 1997; Solomons and Fryhle, 2004) teach slight variations of a linear stepwise mechanism for esterification of an acid with an alcohol, where solvent molecules readily transfer protons from one oxygen atom to another, (scheme **1.10.1**).

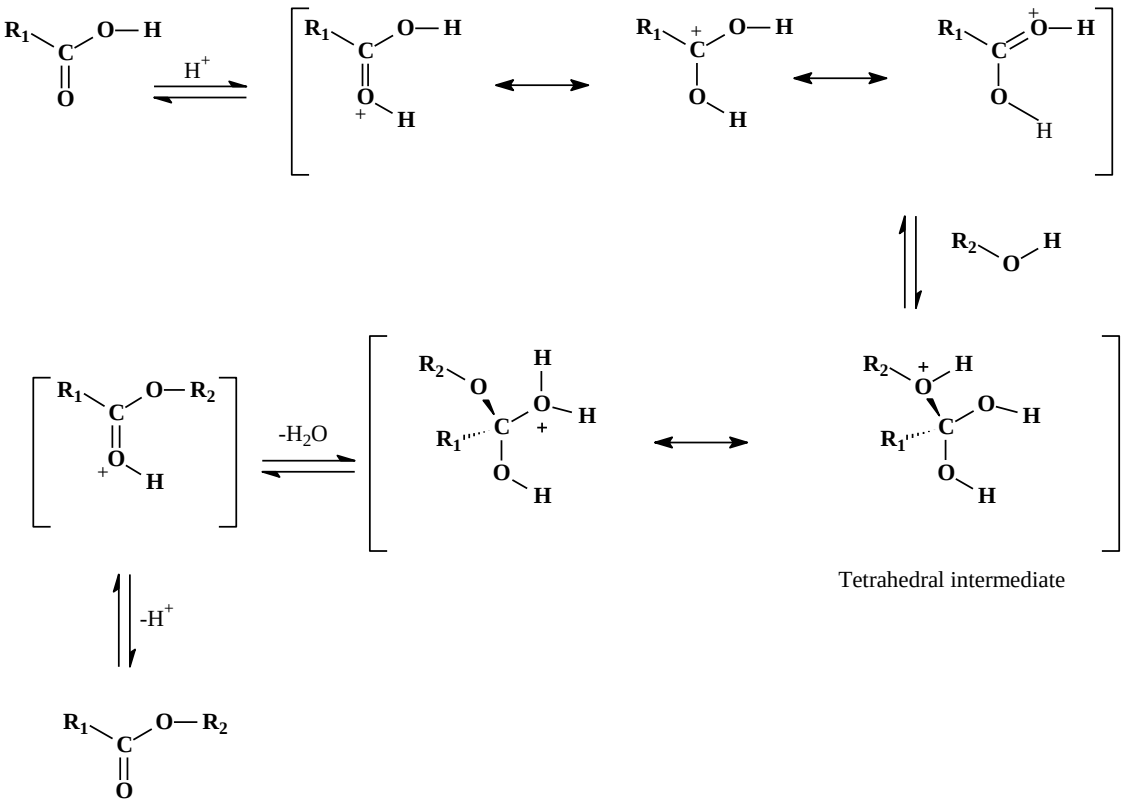

Scheme 1.10.1 Classical mechanism of esterification.

This mechanism, fails to take into account the role of the counter ion in the reaction. This study demonstrated the role of counter ion in acid-catalyzed esterification using computational methods.

1.11 Problem Statement

Despite the wide use of the computational chemistry techniques, there are problems which include:

i. Inconsistencies in the large theoretically generated parameters from the myriad of computational software in the market.

ii. Some structures predicted in the literature are inconsistent with the current knowledge.

iii. Paucity of computational methods to predict the course and outcome of reactions.

1.12 Justification

The following are the challenges that face modern chemists:

- Chemical structure and reactivity investigation with molecular mechanics, quantum chemistry and molecular dynamics methods.
- Modeling of bioorganic compounds such as proteins, enzymes and nucleic acids.
- Developing new algorithms for modeling chemical and biological phenomena.
- Prediction of physical-chemical properties with Quantitative Structure-Property Relationships (QSPR).
- Quantitative Structure-Activity Relationships (QSPR) models for biological activity, toxicity, mutagenicity and carcinogencity.
- Computer-aided synthetic transformation.

1.13 Hypothesis

Computational chemistry can be used to predict structure, properties and activities of molecules, which normally agree with experimental data.

1.14 General Objectives

The primary purpose of this study was to use theoretical calculations and molecular modeling to investigate the mechanism of the following reactions: [1,7]- sigmatropic hydrogen shift of Z,Z-1,3,5-heptatriene systems, esterification of acetyl chloride with methanol, and acid-catalyzed esterification of carboxylic acids with methanol.

1.14.1 Specific Objectives

The specific objectives of the study were:

A To investigate the effect on rate enhancement or retardation by substituent groups in Z,Z-1,3,5-heptatriene systems and related heteroanalogues using computational methods.

B To apply computational methods to verify the mechanism of esterification of acetyl chloride with methanol.

C To investigate the role of the counter ion in acid-catalyzed esterification reactions using computational methods.

In this study, computational methods, in particular DFT, have been employed to study three classes of organic reactions; thermal [1,7]-sigmatropic hydrogen shifts of Z,Z-1,3,5-heptatriene systems, esterification of acetyl chloride with methanol, and acid-catalyzed esterification of carboxylic acids with methanol. Methods derived from quantum mechanics,

statistical mechanics, thermodynamics and classical electrostatics have been used. These results were validated by comparison with experimentally derived data.

The following chapter gives a literature review of these three reactions and details of the applied computational methods.

CHAPTER TWO

2 LITERATURE REVIEW

2.1 Computational Chemistry Techniques

Computational chemistry is the study of molecular systems by computational techniques. These techniques include quantum chemistry, molecular dynamics and Monte Carlo, combinations of them, and, data mining and informatics. The field of computational chemistry has had extensive impact in the area of drug design, material science, environmental chemistry and chemical engineering.

Computational chemistry simulates chemical structures and reactions numerically, based in full or in part on the fundamental laws of physics. It allows chemists to study chemical phenomena by running calculations on computers rather than examining reactions and compounds experimentally. Some methods can be used to model not only stable molecules, but also short-lived, unstable intermediates and even transition states. In this way, they can provide information about molecules and reactions which is impossible to obtain through observation. Computational chemistry is therefore both an independent research area and a vital adjunct to experimental studies. The term covers a fairly broad range of theories and methods.

The various methods of computational chemistry can be thought of as offering a toolbox. For different problems studied choices must be made as to what methods are best suited. In the present work several different issues related to the three reactions have been studied. In

studying these problems an eclectic approach has been chosen; namely to attempt to find the method best suited to each problem.

As a result a fairly large number of methods have been employed. And these methods again draw on different fields of theory. No attempt will be made to cover the underlying theory in any detail here. The present chapter will rather focus on introducing the various branches of computational chemistry in general terms. The introduction is intended to give general insight into the various methods, in particular their strengths, weaknesses and limitations. In addition the terminology to be used in the following chapters will be introduced. The section gives a brief presentation of the main elements of computational chemistry.

2.2 An Overview of Computational Chemistry

There are two broad areas within computational chemistry devoted to the structure of molecules and their reactivity: molecular mechanics (MM) and quantum mechanics (QM). They both perform the same basic types of calculations:

- Computing the energy of a particular molecular structure (spatial arrangement of atoms or nuclei and electrons). Properties related to the energy may also be predicted by some methods.
- Performing geometry optimizations, which locate the lowest energy molecular structure in close proximity to the specified starting structure. Geometry optimization depend primarily on the gradient of the energy- the first derivative of energy with respect to atomic positions.
- Computing the vibrational frequencies of molecules resulting from interatomic motion within the molecule, called evaluating the Hessian. Frequencies depend on

the second derivative of the energy with respect to atomic structure, and frequency calculations may also predict other properties which depend on second derivatives.

These sections provide an overview of the fundamental equations that are used in the construction of computational models. In some sense these sections are historical. However, in order to appreciate differences between modern computational models, and the range over which they may be applicable, it is important to understand the foundation on which all of them are built. There are roughly four different "flavours" to computational chemistry, namely: *ab initio* methods, semi-empirical methods, density functional theory and molecular mechanics/molecular dynamics. Section 2.3 covers the molecular mechanics, section 2.4.1 focuses on approximations inherent in the so called semi-empirical models. Section 2.4.2 describes the *ab initio* approach.

2.3 Molecular Mechanics (MM)

Molecular mechanics uses the laws of classical physics to explain and interpret the structure and properties of molecules. Molecular mechanics methods are available in many computer programs, including MM3, HyperChem, Quanta, Sybyl and Alchemy. There are many different molecular mechanics methods. Each one is characterized by its particular force field. A force field has these components:

- A set of equations defining how the potential energy of a molecule varies with the locations of its component atoms.
- A series of atom types, defining the characteristic of an element within a specific context. Atom types prescribe different characteristics and behaviour of an element depending upon its environment. For example, a carbon atom in a carbonyl group is

treated differently from one bonded to three hydrogens. The atom type depends on hybridization, charge and the types of other atoms to which it is bonded.

- One or more parameter sets that fit the equations and atom types to experimental data. Parameter sets define force constants, which are values used in the equations to relate atomic characteristics to energy components, and structural data such as bond lengths and angles.

MM is a classical model that calculates the forces between all atoms in a system, both bonded and nonbonded, to determine the potential energy for nuclear motion. It is based on an empirical force field that involves extensive optimization of parameters to fit experimental data. The potential energy V, is divided into various contributions;

$$V = V_{str} + V_{\varphi} + V_{vdW} + V_{es} + V_{\omega} \qquad (2.3.1)$$

where V_{str} is the bond-stretching potential, $V\varphi$ is the bond-bending potential, V_{vdW} and V_{es} describe nonbonded interactions arising from van der Waals forces and electrostatic forces, respectively and V_{ω} is a torsional potential for molecules containing a single bond.

The force constants, van der Waals parameters, partial charges, and other parameters are adjusted to fit known geometries, energies and vibrational spectra of small molecules. In a MM calculation, an initial guess for the geometry of the system is made. The potential is then minimized through a gradient search method to determine the equilibrium structure and heat of formation. Knowledge of V for nuclear motion also permits the vibrational spectra to be calculated. The partition of the potential into the various terms in eqn. (2.3.1) allows individual contributions to total energy from the various types of interactions to be examined, which can provide useful insight within the limits of the model. There are several flavors of MM available, such as the MM2 and MM3 methods. While the quality of MM calculations is variable, the main advantage of the technique is that it is extremely fast compared to more

advanced computational methods. Hence, it has found wide usage in theoretical treatments of very large biological systems for which even semi-empirical methods would be unwieldy. MM is not suitable for calculating reaction thermochemistry, involving bond breaking and making, since it is a classical method.

Molecular mechanics calculations don't explicitly treat electrons in molecular systems. Instead, they perform computations based upon the interactions among the nuclei. Electronic effects are implicitly included in force fields through parameterization.

This approximation makes molecular mechanics computations quite inexpensive computationally, and allows them to be used for very large systems containing many thousands of atoms. However, it also carries several limitations as well. Among the most important are these:

- Each force field achieves good results only for a limited class of molecules, related to those for which it was parameterized. No force field can be generally used for all molecular systems of interest.
- Neglect of electrons means that molecular mechanics methods cannot treat chemical problems where electronic effects predominate. For example, they cannot describe processes which involve bond formation or bond breaking. Molecular properties which depend on subtle electronic details are also not reproducible by molecular mechanics methods.

2.4 Quantum Mechanical Methods

Quantum methods are used for the theoretical investigation of molecular properties which depend on the electronic structure of the system. This method uses quantum mechanics

rather than classical physics as the basis for its computations. The basis of these methods is the time independent nonrelativistic Schrödinger equation (Schrödinger, 1926).

$$\hat{H}\Psi = E\Psi \qquad (2.4.0)$$

where $\hat{H}$ is the Hamiltonian operator, E the energy and Ψ the wavefunction of the system under consideration. However, exact solution to the Schrödinger equation (eqn. 2.4.0) either analytically or numerically for systems of interest are not computationally practical. Quantum mechanics methods are characterized by their various mathematical approximations to its solution. There are two major classes of electronic structure methods, semi-empirical and *ab initio* methods.

Semi-empirical and *ab initio* methods differ in the trade-off made between computational cost and accuracy of the results. Semi-empirical calculations are relatively inexpensive and provide reasonably qualitative descriptions of molecular systems and fairly accurate quantitative predictions of energies and structures for systems where good parameter sets exist.

In contrast, *ab initio* computations provide high quality quantitative predictions for a broad range of systems. They are not limited to any specific class of systems. Early *ab initio* programs were quite limited in size of system they could handle. However this is not true for modern *ab initio* programs. On a typical workstation, Gaussian 03 can compute the energies and related properties for systems containing a dozen heavy atoms in just a few minutes. It can handle jobs of up to a few hundreds atoms, and can predict the structures of molecules having as many as a hundred atoms on the same size computer system. Correspondingly larger systems can be handled on supercomputer systems based upon their specific CPU

performance characteristics. Semi-empirical methods and *ab initio* methods are discussed in details in the next two sections.

2.5 Semi-Empirical Methods

Semi-empirical methods, such as Austin Model 1 (AM1), Modified Intermediate Neglect of Differential Overlap (MINDO/3) and Parametric Method Number 3 (PM3), implemented in programs like MOPAC, AMPAC, HyperChem and Gaussian uses parameters derived from experimental data to simplify the computation. They solve an approximate form of the Schrödinger equation that depends on having appropriate parameters available for the type of chemical system under investigation. Different semi-empirical methods are largely characterized by their different parameter sets.

While the quality of the results is varied, all of these methods can be studied. In addition, semi-empirical models can perform very well for systems for which they have been optimized. They are not so successful in difficult cases, such as radical and ionic species or transition states.

Most semi-empirical models involve an approximation that neglects, to some extent, the overlap of atomic orbitals in a molecule. The Austin Model 1 (AM1) semi-empirical method is a variant of the Neglect of Diatomic Differential Overlap approach (NDDO). The overlap approximation states that for integrals that contain the atomic orbitals (AOs), f_i,

$$f_r^*(1) f_s(2) d\tau = 0 \qquad (2.5.1)$$

if r and s are centered on different atoms, even if they are bonded.

In addition, only the valence electrons are treated with a minimal basis set (only a few AOs per atom). The core electrons and the nuclei are approximated as an average potential in which the valence electrons move. The parameters in the model have been optimized to reproduce gas phase heat of formation, equilibrium structures, dipole moments and ionization potentials for molecules containing H, B-F, Si-Cl, Zn, Ge, Br, Sn and I. It performs best for molecules containing first row atoms only, but is less successful for systems that incorporate atoms from the second row and beyond. The quality of the AM1 method is suitable for rough calculations of organic molecules and the results may be used as the starting point for higher level calculations. The AM1-AM2 model is an extended version of AM1 that has also been parameterized to reproduce aqueous heats of solvation for neutral species. The incorporation of solvation effects in *ab initio* methods is usually relatively difficult and this is an advantage of the semi-empirical approach.

The Parametric Method Number 3 (PM3) method is similar to AM1 but has an improved parameterization and has been extended to include heavier atoms. In general, PM3 gives improved results over AM1 for molecules containing second row atoms and heavier. It also gives a better account of hydrogen bonding. Still, the typical errors in bond lengths and angles are about twice as large as those resulting from low level (3-21G) *ab initio* calculations.

2.6 *Ab Initio* Theory

Ab initio methods, unlike either molecular mechanics or semi-empirical methods, use no experimental parameters in their computations. Instead, it is based upon the fundamental laws of quantum mechanics and uses a variety of mathematical transformation and

approximation techniques to solve the fundamental equations. This section provides an introductory overview of the theory underlying *ab initio* quantum mechanical methods.

The starting point for any quantum mechanical theory is the Schrödinger equation

$$\hat{H}\Psi = E\Psi \tag{2.6.1}$$

Where, $\hat{H}$ is the Hamiltonian of the system, Ψ is the wave function and E is the energy. The typical form of the Hamiltonian operator takes into account five contributions to the total energy of the systems: the kinetic energies of the electrons and nuclei, the attraction of the electrons to the nuclei, and interelectronic and internuclear repulsions.

$$\hat{H} = -\sum_i \frac{\hbar^2}{2m_e}\nabla_i^2 - \sum_k \frac{\hbar^2}{2m_k}\nabla_k^2 - \sum_i \sum_k \frac{e^2 Z_k}{r_{ik}} + \sum_{i<j} \frac{e^2}{r_{ij}} + \sum_{k<l} \frac{e^2 Z_k Z_l}{r_{kl}} \tag{2.6.2}$$

Where *i* and *j* run over electrons, *k* and *l* run over nuclei, ħ is Plank's constant divided by 2π, m_e is the mass of an electron, m_k is the mass of the nucleus *k*, ∇^2 del, is the Laplacian operator, e the charge on the electron, Z is an atomic number and r_{ab} is the distance between particles a and b. Ψ is a function of 3n coordinates where n is the total number of particles (nuclei and electron), for example, the x, y and z Cartesian coordinates specific to each particle. In Cartesian coordinates, the Laplacian has the form

$$\nabla_i^2 = \frac{\partial^2}{\partial x_i^2} + \frac{\partial^2}{\partial y_i^2} + \frac{\partial^2}{\partial z_i^2} \tag{2.6.3}$$

2.7 The Born-Oppenheimer Approximation

The Born-Oppenheimer approximation (Born and Oppenheimer, 1927) simplifies the general molecular problem by separating nuclear and electronic motions. This approximation is reasonable since the mass of a typical nucleus is thousands of times greater than that of an

electron. The nuclei move very slowly with respect to the electrons, and the electrons react essentially instantaneously to changes in nuclear position. Thus, the electron distribution within a molecular system depends on the positions of the nuclei and not on their velocities. Hence the application of the Born-Oppenheimer approximation yields the electronic Schrödinger equation:

$$H_{el}\Psi_{el} = E_{el}\Psi_{el} \qquad (2.7.1)$$

The Born-Oppenheimer approximation has a very profound consequence, it enables the calculation of potential energy surface (PES). The PES is the surface defined by pure electronic energy (E_{el}) over all possible nuclear coordinates. Equilibrium and transition state geometries are critical points on the PES.

$$E_{tot} = E_{el} + \sum_{A=1}^{M}\sum_{B>A}^{M}\frac{Z_A Z_B}{R_{AB}} \qquad (2.7.2)$$

A many-electron wavefunction can be approximated as a Slater determinant, which is composed of one-electron functions, so-called spin-orbitals. With the assumption that each electron moves in the "effective field" due to the nuclei and N–1 electrons, the N-electron eigenvalue problem is reduced to N one-electron eigenvalue problems. Taking the orthogonality of the spin orbitals into account, is arrived at the Hartree-Fock (HF) equations (in canonical form) (Fock, 1928; Hartree, 1928).

$$F\psi_i = \varepsilon_i\psi_i \qquad (2.7.3)$$

where F is an effective one-electron Fock operator, ψ_i a spin-orbital and ε_i the respective orbital energy. For a closed-shell system the Fock operator is written as:

$$F = H^{core} + \sum_{i=1}^{N/2}\left\{2J_i - K_i\right\} \qquad (2.7.4)$$

where J_i and K_i are the Coulomb and exchange operator respectively. H^{core} is the core Hamiltonian operator, which represents the kinetic energy of the electrons and the electronuclear interactions.

The Hartree-Fock (HF) eigenfunctions ψ_i an be expressed by a linear combination of atomic orbitals (LCAO), ϕ_μ □ ("basis functions"):

$$\psi_i = \sum c_{\mu i} \phi_\mu \qquad (2.7.5)$$

which leads to the generalized eigenvalue problem (*Roothaan-Hall* equation), (Hall, 1951; Roothaan, 1951)

$$FC = SCE \qquad (2.7.4)$$

where F corresponds to the Fock matrix, C is the orbital coefficient matrix, S the overlap matrix and E the diagonal matrix of orbital energies.

The *Roothaan-Hall* equations have a non-trivial solution only if the following secular equation is satisfied:

$$\det\left|F - \varepsilon S\right| = 0 \qquad (2.7.5)$$

This equation cannot be solved directly because the Fock matrix elements F_{ij} involve Coulomb and exchange integrals which themselves depend on the spatial wavefunctions. Therefore a self-consistent field (SCF) approach is used, which iteratively improves the coefficients C_{ja} until convergence has been reached. Scheme 2.7.1 below represents the flow chart of the HF-SCF procedure.

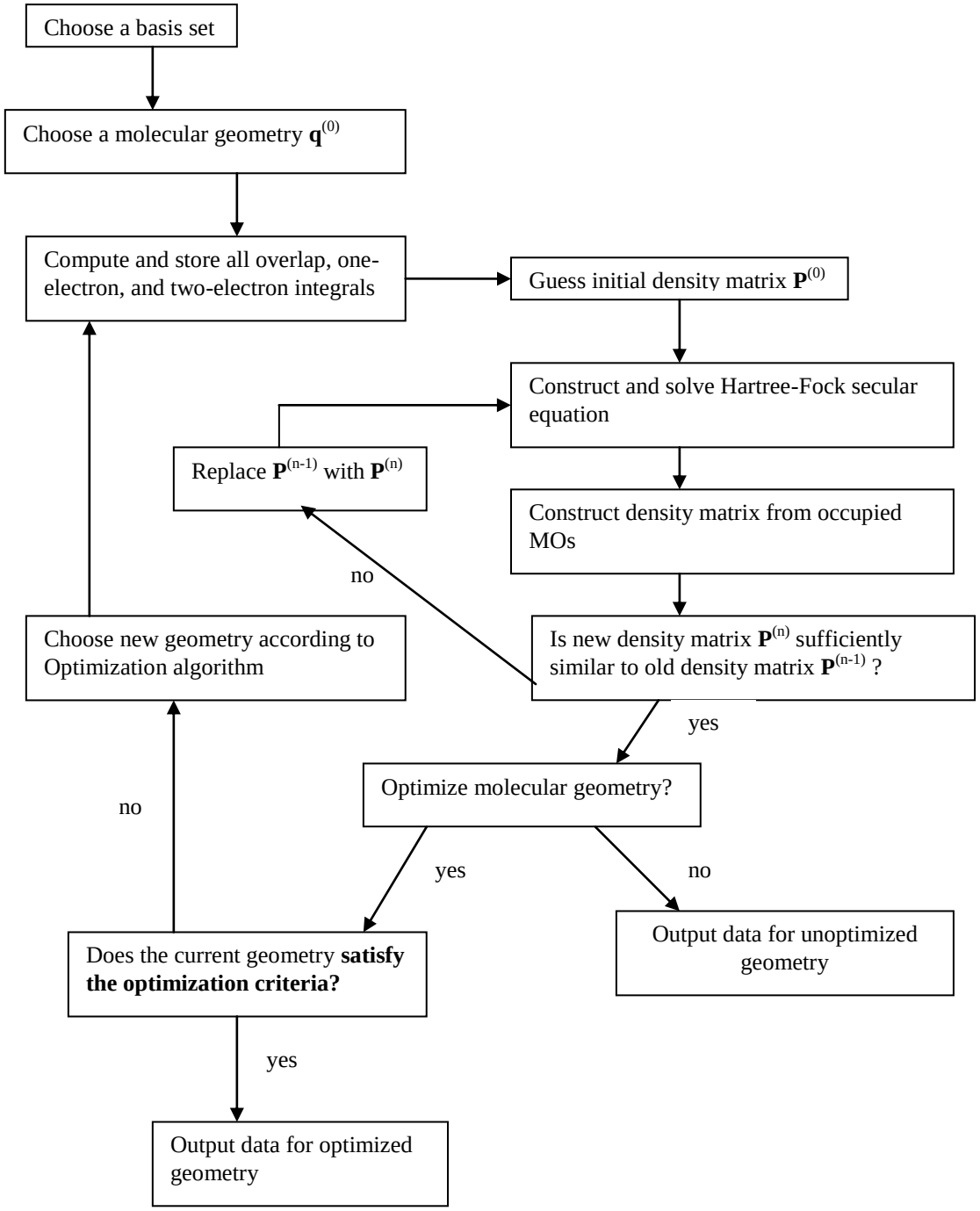

Scheme 2.7.1: Flow chart of the HF-SCF procedure.

The correlated *ab initio* methods go beyond the Hartree-Fock (HF) approximation, and include the effects of electron correlation by a variety of techniques, for instance by perturbation theory or by variational theory. These methods are accurate and widely used by quantum chemists today. However, there are practical limitations, because the computational effort is extremely high for large molecules.

2.8 Density Functional Theory (DFT)

An alternative to *ab initio* methods that has been growing in popularity over the past decade is density functional theory (DFT). In wavefunction-based *ab initio* theory the full N-electron wavefunction is calculated, whereas DFT focuses on the total energy and the one-electron density distribution. One of the most important reasons for the success of DFT is that it includes the electron correlation in an effective manner. The central underlying idea is the relationship between total energy and electron density. In 1964, Hohenberg and Kohn showed that the electron density $\rho(r)$ uniquely defines the ground-state energy *E* and other properties of a system (Hohenberg and Kohn, 1964). Therefore, *E* is a unique functional of $\rho(r)$.

In DFT the energy functional is written as a sum of two terms:

$$E[\rho(r)] = \int V_{ext}(r)\rho(r)dr + F[\rho(r)] \qquad (2.8.1)$$

The first term arises from the interaction of the electrons with an external potential $V_{ext}(r)$. $F[\rho(r)]$ is the sum of the kinetic energy of the electrons and the contribution from interelectronic interactions. There is a constraint on the electron density as the number of electrons (N) is fixed. In order to minimize the energy, this constraint is introduced as Lagrangian multiplier (μ), leading to:

$$\frac{\delta}{\delta\rho(r)}\left[E[\rho(r)] - \mu\int \rho(r)dr\right] = 0 \qquad (2.8.2)$$

$$\left(\frac{\delta E[\rho(r)]}{\delta\rho(r)}\right)_{V_{ext}} = \mu \qquad (2.8.3)$$

where μ is the chemical potential of the electrons for a given external potential. According to Kohn and Sham (Kohn and Sham, 1965) the term $F[\rho(r)]$ in eqn. (2.8.4) can be approximated by:

$$F[\rho(r)] = E_{KE}[\rho(r)] + E_H[\rho(r)] + E_{XC}[\rho(r)] \tag{2.8.4}$$

where $E_{KE}[\rho(r)]$ is the kinetic energy of a system of non-interacting electrons with the same density $\rho(r)$ as the real system. $E_H[\rho(r)]$ is the electron-electron Coulombic energy, and the so-called exchange-correlation functional $E_{KE}[\rho(r)]$ contains contributions from exchange and correlation (plus kinetic energy corrections). Kohn-Sham orbitals $\psi_i(r)$ are introduced to evaluate the kinetic energy $E_{KE}[\rho(r)]$. The full expression for the energy of an N-electron system within the Kohn-Sham scheme reads:

$$\begin{aligned} E[\rho(r)] = \sum_{i=1}^{N} \int \psi(r) \left(-\frac{\nabla^2}{2} \right) \psi_i(r) dr + \frac{1}{2} \iint \frac{\rho(r_1)\rho(r_2)}{|r_1 - r_2|} + \\ E_{XC}[\rho(r)] - \sum_{A=1}^{M} \int \frac{Z_A}{|r - R_A|} \rho(r) dr \end{aligned} \tag{2.8.5}$$

The density $\rho(r)$ of the system is obtained from the Kohn-Sham orbitals:

$$\rho(r) = \sum_{i=1}^{N} |\psi_i(r)|^2 \tag{2.8.6}$$

A variational treatment leads to the one-electron Kohn-Sham equations:

$$\left\{ -\frac{\nabla_1^2}{2} - \left(\sum_{A=1}^{M} \frac{Z_A}{r_{1A}} \right) + \int \frac{\rho(r_2)}{r_{12}} dr_2 + V_{XC}[r_1] \right\} \psi_i(r_1) = \varepsilon_i \psi_i(r_1) \tag{2.8.7}$$

where ε_i are the orbital energies. V_{Xc} is known as the exchange-correlation potential, which is the derivative of the exchange-correlation energy with respect to the electron density.

The Kohn-Sham equations are solved self-consistently: an initial guess of the density is fed to eqn. (2.8.6) from which a set of orbitals are obtained, leading to an improved density, which is used for the second iteration, and so on until convergence is achieved. The exchange-correlation functional is *a priori* unknown in density functional theory. The simplest approximation considers the homogeneous, uniform electron gas, where the electron density is constant throughout the space. The exchange-correlation energy for the uniform electron gas can be written as:

$$E_{Xc}^{LDA} = E_X^{LDA} + E_C^{LDA} \tag{2.8.8}$$

The first term, comprising the exchange energy, has the form,

$$E = -\frac{9}{4\alpha_{ex}}\left(\frac{3}{4\pi}\right)^{1/3}\sum_r \int \left[\rho_1^r(r)\right]^{4/3} dr \tag{2.8.9}$$

where α_{ex} is the exchange scale factor, with the theoretical value of 2/3. The second term, the correlation energy, is represented as,

$$E_X^{LDA} = \int \rho_1(r_1)\varepsilon_c\left[\rho_1^{\alpha}(r), \rho_1^{\beta}(r_1)\right] dr_1 \tag{2.8.10}$$

where $\varepsilon_c\left[\rho_1^{\alpha}, \rho_1^{\beta}\right]$ represents the correlation energy per electron with ρ_1^{α} and ρ_1^{β} being the respective α - and β - spin densities.

Ceperley and Alder (Ceperley and Alder, 1980) determined the correlation energy of a uniform electron gas using Monte Carlo methods. In order to use these results in DFT calculations, suitable analytic interpolations have been determined by Vosko, Wilk and Nusair (VWN) (Vosko, *et al*., 1980). The representation of the exchange-correlation energy by equations (2.8.8-2.8.10) has been coined the local density approximation (LDA).

The most notorious shortcoming of the LDA is its tendency to overestimate binding energies. The obvious reason is that the electron distribution in molecules is far from a uniform electron gas. To remedy some of the deficiencies in LDA, the functionals have been refined by considering the gradient of the charge density, $\nabla\rho(r)$, in corrections to the LDA:

$$E_{XC}[\rho] = \int \rho\varepsilon_{XC}\rho F(\rho, \nabla\rho)dr \qquad (2.8.11)$$

where $F(\rho, \nabla\rho)$ is termed a gradient or 'non-local' correction, since the potential now depends not only on the electron density, but also on its gradient (Parr and Yang, 1989). The resulting generalized gradient approximation (GGA) functionals offer significant improvements over LDA and are widely used in computational chemistry. One prominent example is the BP86 functional (Becke, 1988; Perdew, 1986) which has become the workhorse for many applications in organometallic chemistry. The performance of GGA functionals can often be further improved by the admixture of some Hartree-Fock exchange, typically of the order of 20%. The most popular of the hydrid functionals is B3LYP (Becke, 1993; Lee, *et al*., 1988; Perdew, 1986) which is currently the preferred choice for DFT calculations in organic chemistry. Further information about the merits of different functionals can be found in reviews and monographs on DFT (Koch and Holthausen, 2000; Parr and Yang, 1989; Ziegler, 1991).

2.9 Basis Sets

The basis sets are the mathematical functions from which the wave function is constructed. The full HF wave function is expressed as a Slater determinant formed from the individual occupied MOs. In the abstract, the HF limit is achieved by use of an infinite basis set, which necessarily permits an optimal description of the electron density. In practice, however, one cannot make use of an infinite basis set. The number of two-electron integrals increases as

N^4 where N is the number of basis functions. So keeping the total number of basis functions to a minimum is computationally attractive. In addition, however, it can be useful to choose basis set functional forms that permit the various integrals appearing in HF equations to be evaluated in a computationally efficient fashion. Thus a larger basis set can still represent a computational improvement over a smaller basis series if evaluation of the greater number of integrals for the former can be carried out faster than the latter.

The choice of a basis set is critical to efficient computation. One choice for the basis functions is a Slater – Type Orbital (STO) which is similar to a hydrogen atom atomic orbital. While Slater Type Orbitals are very accurate, they are unwieldy to integrate and are not good basis sets for complicated systems. STO have the functional of the form shown in equation (2.9.1)

$$\chi_{\zeta,n,l,m}(r,\theta,\varphi) = NY_{l,m}(\theta,\varphi)r^{n-1}e^{-\zeta r} \qquad (2.9.1)$$

An alternative choice for the basis that results in more facile integration is a Gaussian–Type Function (GTF) sometimes called Gaussian – Type Orbital (GTO). A Cartesian Gaussian centered on an atom a will have the form (equation 2.9.2)

$$\chi_{\zeta,n,l,m}(r,\theta,\varphi) = NY_{l,m}(\theta,\varphi)r^{2n-2-l}e^{-\zeta r^2} \qquad (2.9.2)$$

N is a normalization constant and $Y_{l,m}$ are spherical harmonic functions. The exponent, ζ , determines the orbital extent, or size.

The GTF's can be combined to approximate a particular atomic orbital.

$$\chi_r = \sum_u d_{ur} g_u \qquad (2.9.3)$$

where the g_u are referred to as primitive Gaussians and the χ_r are termed contracted Gaussians.

To approximate an atomic s–orbital, only s–type Gaussian functions are combined, and likewise for the other atomic orbitals. The coefficients, d_{ur}, are fixed to yield a best fit, usually to a STO. Gaussian – type functions are not accurate as STO's since they do not yield a "cusp" (discontinuous derivative) at the origin and so a number of GTF's must be combined to yield a satisfactory representation of the atomic orbital. However, this difficulty is offset by the computational efficiency with which integrals involving products of Gaussian functions may be evaluated.

2.9.1 Selection of Basis Sets

There are a number of different types of basis sets that are used in modern *ab initio* calculations, depending on the complexity of the problem and the desired level of accuracy. Usually, a larger basis set consisting of more basis functions will yield increased accuracy. A minimal basis is one that is composed of a single basis function for each atomic orbital. An example of a minimal basis set is the STO – 3G which represents each atomic Slater – type orbital (the contracted Gaussian) as a sum of three primitive Gaussians.

A split – valence basis set treats the core and atomic orbitals differently and includes more diffuse Gaussian functions with a smaller orbital exponent (e.g. 6-31G).

Polarization basis sets include extra basis functions of higher angular momentum to account for the polarization of atomic charge in a molecule. For example, the 6-31G*, or 6-31G(d), basis set adds a d – type orbital to all heavy atoms (everything but H and He).

To provide more accurate descriptions of anions, or neutral molecules with unshared pairs, basis sets may be augmented with so-called diffuse functions. The presence of diffuse functions is symbolized by the addition of a plus sign, +, to the basis set designator: 6-31+G. (Since these are s and p orbitals, the symbol goes before the G.) Again, a second + implies diffuse functions added to hydrogens; however, little improvement in results is noted for this addition unless the system under investigation includes hydride ions.

The SCF approximation does not include the effects of electron correlation which arise due to instantaneous Coulombic interactions between electrons. This deficiency can be remedied by implementing improvements to the HF method. One approach is to use Configuration Interaction (CI) methods which mix excited state electronic configurations into the wave function to further minimize the energy. CI methods are not very efficient for ground state calculations but are extensively used for evaluations of electronically excited states. The Møller-Plesset (MP) method uses perturbation theory to improve the wave function. The perturbation treatment is usually carried out to second-order (MP2) or higher MP3, MP4) but not beyond fourth-order. The computation effort for MP5 increases and actual calculations are only possible for small systems. There is very little experience with performance of MPn beyond MP4. The MP method is more efficient than the CI calculations and is more commonly used for ground state calculations. However, the MP energy is not variational and may not yield an upper bound to the true energy.

The basis set of the current study has the keyword 6-31+G(d). For all atoms in the studied system, the core orbitals are represented by contraction of six gaussian functions, the compact

part of the valence orbitals are contractions of three gaussian functions and the diffuse part of the valence are represented by one gaussian function. Additionally, polarization functions and diffuse functions are used in the basis set of each atom excluding the hydrogen atom. Supplementing polarization function has been proved particularly useful when hydrogen acts as a bridging atom, such as the transition structures of the systems of current interest; while using diffuse functions helps dealing with anions and molecules containing lone pairs. Moreover, this basis sso has been proved efficient in previous studies (Leach, 2001).

2.10 Geometry Optimization

The way the energy of a molecular system varies with small changes in its structure is specified by its potential energy surface (PES). A potential energy surface is a mathematical relationship linking molecular structure and the resultant energy.

Geometry optimizations usually attempt to locate global minima on the potential energy surface, thereby predicting equilibrium structures of molecular systems. Optimizations can also locate transition structures. A geometry optimization begins at the molecular structure specified as its input, and steps along the potential energy surface. It computes the energy and the gradient at that point, and then determines how far and in which direction to make the next step. The gradient indicates the direction along the surface in which the energy decreases most rapidly from the current point as well as the steepness of that slope.

Most optimization algorithms also estimate or compute the value of the second derivative of the energy with respect to the molecular coordinates, updating the matrix of force constant (known as the Hessian). These force constants specify the curvature of the surface at that point, which provides additional information useful for determining the next step.

2.10.1 Minima

Stable molecules and intermediates in reactions correspond to minima on the potential energy surface, the lowest one being the *global energy minimum*, while the others are called *local minima*. From a mathematical standpoint, a function *f*, which depends on one or more independent variables, x_1, x_2,…x_i has a minimum when the first derivative of the function with respect to each of the variables is zero and the second derivatives are all positive:

$$\frac{\partial f}{\partial x_i} = 0; \frac{\partial^2 f}{\partial x_i^2} > 0 \qquad (2.10.1)$$

The function to be optimized and its derivatives are calculated with a finite precision, which depends on the computational implementation. In practice the geometry optimization is considered converged if the gradient is reduced below a suitable "cut-off" value. There are a number of well-established optimization methods for finding minima which are usually classified by the required input information: Zero-order methods need only the values of the function itself (for example., grid searches), first-order methods make use of the function and its gradient (*e.g.*, steepest descent and conjugate gradient methods), and second-order methods require the function as well as the first and second derivatives (for example., Newton-Raphson methods). With increasing order, the computational effort in the quantum-chemical calculation and the rate of convergence in the geometry optimization normally both increase so that a compromise is needed for best overall performance. The computational aspect of calculating the Hessian, is often encountered in electronic structure calculations. Here the calculation of the second derivative matrix can be an order of magnitude more demanding than calculating the gradient. In such cases, and *updating* scheme may be usedinstead. The idea is to start off with an approximation to the Hessian, maybe just a unit matrix. The initial step will thus resemble a steepest descent step. As the optimization

proceeds, the gradients at the previous and cuurent points are used for making the Hessian a better approximation for the actual system. After two steps, the updated Hessian is a rather good approximation to the exact Hessian in the direction defined by these two points. There are many such updating schemes, for example, energy optimization first-order quasi-Newton methods with names *Broyden-Fletcher-Goldfarb-Shanno* (BFGS) updating scheme is generally used as implemented in the Gaussian code (M. J. Frisch, *et al*., 2003). For minimizations, the BFGS update is usually preferred, as it tends to keep the Hessian positive definite.

2.10.2 Transition States

Transition states are usually characterized by one imaginary frequency since they are first-order saddle point. The transition state structure connects the reactant and the product (Figure 2.10.1).

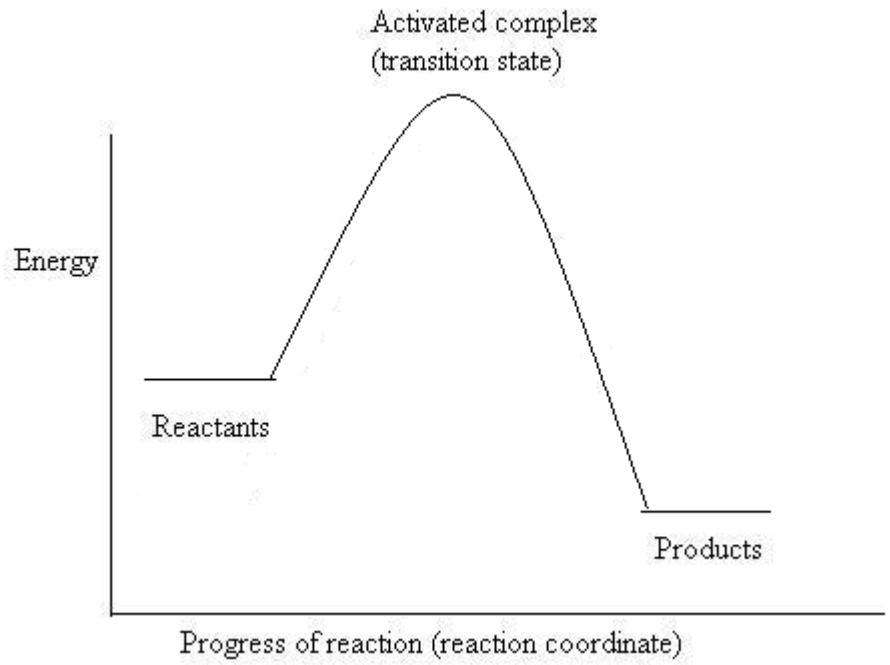

Figure 2.10.1: Reaction progress potential energy surface.

Transition states are generally much more difficult to locate than minima, because one needs to find a maximum in one (and only one) direction, and minima in all other directions. At a first-order saddle point, the first derivatives of the potential function with respect to the coordinates are all zero, and the energy passes through a maximum (negative curvature) for movement along the pathway that connects two minima, but is minimal for displacements in all other directions perpendicular to the path (positive curvature). The linear synchronous transit algorithm (LST) (Halgren and Lipscomb, 1977), which searches for a maximum along a linear path between reactants and products, is one of the methods to get near to the transition state, but it often leads to structures with two or more negative eigenmodes. This problem is effectively handled by using the quadratic synchronous transit method (QST) (Halgren and Lipscomb, 1977), where the algorithm searches for a maximum along a parabola connecting reactants and products, and for a minimum in all directions perpendicular to the parabola. Bell and Crighton refined this approach, by looking for a maximum along a parabolic path between the reactants and products, (Bell and Crighton, 1984) while a minimum is found in the space conjugate (rather than orthogonal) to the path. A more recent variation of QST, implemented by Peng and Schlegel, (Peng and Schlegel, 1993) uses a circle arc instead of a parabola for interpolation and follows the tangent to the circle for guiding the search towards the transition state (TS) region. This approach is called Synchronous Transit-Guided Quasi Newton (STQN) method. This method has been used in this study as implemented in Gaussian program package(M. J. Frisch, *et al*., 2003) for locating transition states.

2.10.3 Intrinsic Reaction Coordinates (IRC)

In a given coordinate system, a reaction path is defined as the steepest descent path or minimum energy path from the transition state down to the reactants and products. If mass

weighted Cartesian coordinates are used, then this path is known as intrinsic reaction coordinates (IRC). Tracing the IRC in both directions establishes which minima are connected by a given transition state. Many different algorithms have been suggested for determining reaction paths. Widely used is the one by Gonzalez and Schlegel, (Gonzalez and Schlegel, 1989; Gonzalez and Schlegel, 1990) which is efficient and reliable, and remains stable even at larger step sizes. This algorithm has been used as implemented in the Gaussian code(M. J. Frisch, *et al*., 2003) whenever an IRC calculation was deemed necessary to confirm the nature of a given transition state.

2.10.4 Potential Energy Surfaces and Reaction Rates

Often in computational chemistry, the Born-Oppenheimer approximation applies which states that the wavefunctions of atomic nuclei and electrons can be separated. Since electrons move very fast, they are assumed to instantaneously adapt to every nuclear rearrangement. The potential energy of a molecular system can thus be described as a function of the coordinates of atomic nuclei, forming a multidimensional potential energy function, often called a potential energy surface (PES) (Leach, 2001). For chemical reactions, reactants and products states are found in minima on the surface and transition states correspond to saddle points. The difference in potential energy between a reactant state and its corresponding transition state (TS) is an activation barrier.

To validate a computational result one should compare the theoretical model to experimental data such as rate constants. However, a rate constant is a kinetic property, and it directly depends on a free energy barrier rather than a potential energy barrier. The relationship between the rate constant k of a chemical reaction step and its free energy barrier $\Delta G^{\ddagger}$ can be described by Erying's rate equation.

$$k = \frac{\kappa k_b T}{h} e^{-\Delta G^{\ddagger}/RT} C^{0(1-m)} \qquad (2.10.2)$$

Where κ is the transmission factor which varies between 0 and 1, k_b is the Boltzmann constant, T is the temperature, h is Plank's constant and R the gas constant. C^0 is a concentration factor, usually 1M, that defines the standard state, and m is the order of the reaction.

The exponential factor of equation 2.10.2 is the probability that the system reaches the transition state from the reactants state. The transmission factor κ is the probability that a molecule with forward velocity along the reaction coordinate in the transition state will proceed to form products instead of being reflected back to the reactants state. Classical transition state theory assumes that κ=1 but this is not necessarily the case. In addition, equilibrium constants K_{eq} can be expressed in terms of free energy differences, using the relation,

$$K = e^{-\Delta G^{\ddagger}/RT} \qquad (2.10.3)$$

where K_{eq} between two states is related to the standard free energy difference ΔG between the two states.

2.11 Population Analysis

In population analysis the electron density is partitioned among the nuclei, such that each nucleus is associated with a specific number of electrons and a net atomic charge. There are several methods used to calculate population analysis. For the purpose of this study, only two methods will be discussed briefly, Mulliken (Mulliken, 1955) and Natural Bond Orbital (NBO) analysis (Foster and Weinhold, 1980; Reed, *et al*., 1985).

In Mulliken population analysis (Mulliken, 1955), the electrons are divided between the atoms according to the degree to which different atomic orbital basis functions contribute to the total wavefunction. The starting point of this analysis is the equation which relates the total number of electrons to the density matrix and to the overlap integral.

$$N = \sum_{\mu=1}^{K} P_{\mu\mu} + 2\sum_{\mu=1}^{K}\sum_{\upsilon=\mu+1}^{K} P_{\mu\upsilon}S_{\mu\upsilon} \qquad (2.11.1)$$

Assuming that the basis functions are centered on atomic nuclei, the number of electrons associated with a particular atom can be obtained by summing over all basis functions centered on that atom. The net charge associated with an atom A is then given by:

$$N = Z_A - \sum_{\mu=1}^{K} P_{\mu\mu} + \sum_{\mu=1;\mu on A}^{K}\sum_{\nu=1;\nu\neq\mu}^{K} P_{\mu\nu}S_{\mu\nu} \qquad (2.11.2)$$

This population scheme is simple, but can depend strongly on the basis set, and a balanced basis set is needed to obtain meaningful results.

Natural Bond Orbital (NBO) analysis is used as a technique for studying hybridization and covalency effects in polyatomic wavefunctions (Foster and Weinhold, 1980; Reed, *et al*., 1985). The NBO for a localized σ bond σ_{AB} between atoms A and B is formed from orthonormal hybrids h_A, h_B (natural hybrid orbitals or NBOs):

$$\sigma_{AB} = C_A h_A + C_B h_B \qquad (2.11.3)$$

Natural hybrid orbitals are composed of natural atomic orbitals (NAOs), optimized for the chosen wavefunction. *Ab initio* wavefunctions transformed to NBO form are found to be consistent with Lewis structures and with the Pauling-Slater-Coulson picture of polarization and bond hybridization (Coulson, 1952; Pauling and Wilson, 1935; Slater, 1931). The transformation to NBOs provides orbitals, which are unoccupied and can be used to describe non-covalency effects.

These antibonds σ^*_{AB} are represented as:

$$\sigma^*_{AB} = C_B h_A + C_A h_B \tag{2.11.4}$$

Deleting these orbitals from the basis set and then recalculating the total energy gives the energy associated with the antibonds. Hence, decomposing the total energy *E* into components contributing for both covalent and noncovalent effects:

$$E = E_{\sigma\sigma} + E_{\sigma\sigma^*} \tag{2.11.5}$$

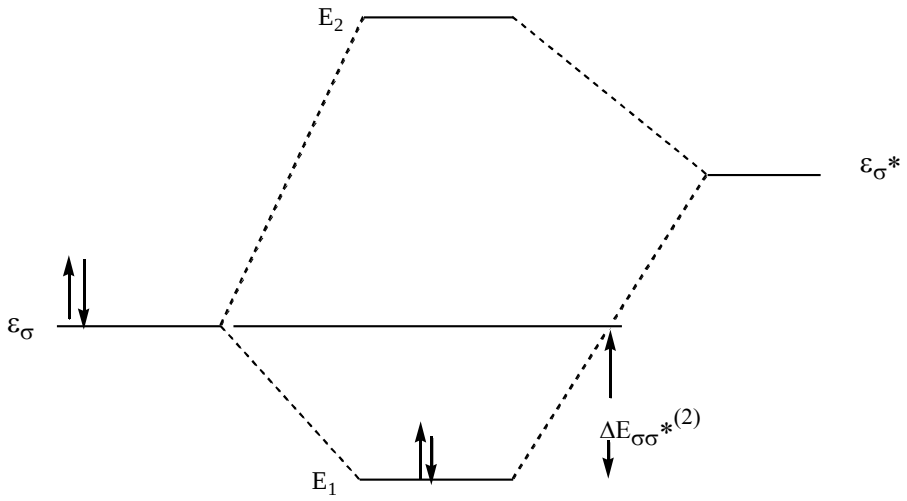

Figure 2.11.1: Perturbative donor-acceptor interaction, involving a filled orbital σ and an unfilled orbital σ*.

Figure **2.11.1**. displays the interaction of a filled σ orbital with the unfilled antibonding σ* orbitals of the Lewis structure. Estimates for the energy lowering $\Delta E^{(2)}_{\sigma\sigma^*}$ can be obtained from second-order perturbation theory:

$$\Delta E = -2\frac{\left\langle \sigma \middle| \hat{F} \middle| \sigma^* \right\rangle^2}{\varepsilon_{\sigma^*} - \varepsilon_\sigma} \tag{2.11.6}$$

where ε_σ and ε_{σ^*} are NBO orbital energies, and $\hat{F}$ is the Fock operator. The NBO perturbative analysis (eqn. 2.11.5) allows one to apply qualitative ideas of valence theory to describe the noncovalent energy lowering.

As the noncovalent delocalization effects (eqn. 2.11.6) are associated with $\sigma \to \sigma^*$ interactions between donor and acceptor orbitals, it can be appropriate to describe them as being of "donor-acceptor", "charge transfer", or generalized "Lewis base-Lewis acid" type. The quantity of charge *q* transferred in such interactions is given by:

$$q \cong \frac{\left|\Delta E^{(2)}_{\sigma\sigma^*}\right|}{\varepsilon^*_\sigma - \varepsilon_\sigma} \qquad (2.11.7)$$

The amount of charge transferred is typically much less than that required for formation of an ion pair. Hence, in a nutshell, NBO analysis emphasizes the importance of quantum mechanical orbital interaction and exchange effects in the non-covalent regime. This study used NBO analysis (rather than Mulliken analysis) for the interpretation of the computational results.

2.12 Molecular Orbitals- HOMO and LUMO

As long as the molecules whose interaction is to be considered are far apart, each has its own set of molecular orbitals (MO's) undisturbed by the other. These MO's form the unperturbed basis from which the interaction is to be evaluated. As the molecules approach sufficiently closely that overlap between their orbitals becomes significant, the new interaction constitutes a perturbation that mix orbitals of each molecule into those of the other. The strongest interactions will be between those orbitals that are close to each other in energy, but interaction between two filled levels will cause little change in the total energy because one

orbital moves down nearly as much as the other moves up. The significant interactions are therefore between filled orbitals of one molecule and empty orbitals of the other; furthermore, since the interaction is strongest for orbital pairs that lie closest in energy. The most important interactions are between the highest occupied molecular orbitals (HOMO) of one molecule and the lowest unoccupied molecular orbital (LUMO) of each other. These orbitals are sometimes referred to us the *frontier orbitals*. These orbital are discussed in details in sections 2.15 for [1,7] sigmatropic hydrogen shift and in sections 2.16 for esterification reactions.

2.13 Solvation Models

The importance of solvent effects in organic chemistry is emphasized by the fact that the vast majority of organic reactions are carried out in solutions and that processes related to life itself occur in aqueous environment. To characterize the reactivity of organic molecules and to predict the rates for organic reactions, it is essential to include solvent effects in the theoretical treatments. However, the inclusion of explicit solvent molecules means a significant increase in the size of the system, and requires a statistical mechanical description of the physical properties. Methods for the treatment of solvent effects may be divided into two categories: a continuum depiction of the solvent system characterized by its relative permittivity and a classical yet representation of the solvent molecules through the use of empirical potential functions. Continuum models have been used both in quantum mechanical calculations and in classical simulations of biological macromolecules and continue to enjoy popularity thanks to their computational efficiency. However, as the computational power increases, the advantages offered by continuum models will continue to diminish. Explicit solvent simulations may now be routinely carried out for large scale systems including solutions and biological molecules.

2.13.1 Continuum Solvation Models

One of the greatest challenges for computational chemist is to model organic reactions in a solvent environment, so as to mimic the reality in a reaction flask. Solvent molecules may directly interact with the solute, as in the case of ester hydrolysis, or they may not directly affect the solute but provide an environment that alters the behavior of the solute. The latter case can be described by continuum solvation models.

There have been several recent reviews on the theory and prospective applications of continuum models (Tomasi and Persico, 1994). Because of their computational simplicity and the possibility of parameterizing specific models, there has been significant refinement and improvement of continuum models in recent years. The following sections give brief description of polarizable continuum model (PCM).

The solvation free energy ΔG_{sol} is the free energy change to transfer a molecule from vacuum to solvent, which is represented as:

$$\Delta G_{sol} = \Delta G_{elec} + \Delta G_{vdw} + \Delta G_{cav} \qquad (2.13.0)$$

Where ΔG_{elec} represents the electrostatic part, arising due to the polarization of the medium under constant dielectric ε_s. ΔG_{vdw} is the van der Waals interaction between the solute and the solvent, which can further be divided into a repulsive term and an attractive dispersion term. ΔG_{cav} is the free energy required for cavity formation. Only ΔG_{elec} is treated by continuum solvation models.

In 1920, Born derived the electrostatic component of the free energy of solvation for placing a charge within a spherical solvent cavity (Born, 1920), which is obtained as the difference in the work done in charging the ion in the dielectric and *in vacuo*:

$$\Delta G = \frac{q^2}{2a}\left(1-\frac{1}{\varepsilon_s}\right) \qquad (2.13.1)$$

where *q* is the charge on the ion and *a* is the radius of the cavity. Onsager later extended this model to a dipole in a spherical cavity (Onsager, 1936).

Consider an isotropic liquid with solvent molecules undergoing random thermal motion, the average electric field at any point will be zero. However, the presence of solute will change this net orientation and hence the field induced by the introduction of the solute is referred as the "reaction field". In the "self-consistent reaction field method (SCRF)" the reaction field is incorporated into quantum mechanics by considering it as a perturbation of the Hamiltonian for an isolated molecule:

$$H_{tot} = H_o + H_{RF} \qquad (2.13.2)$$

where H_o is the Hamiltonian of the isolated molecule, and H_{RF} is the perturbation due to the reaction field (Tapia and Goscinski, 1975). The latter is given by

$$H = -\hat{\mu}^T \frac{2(\varepsilon_s - 1)}{(2\varepsilon_s + 1)a^3}\langle\psi|\hat{\mu}|\psi\rangle \qquad (2.13.3)$$

where $\hat{\mu}$ is the dipole moment operator and $\hat{\mu}^T$ is its transpose. The electrostatic contribution to the solvation free energy is obtained after solving for the wavefunction ψ of the modified Hamiltonian:

$$\Delta G_{elec} = \langle\psi|H_{tot}|\psi\rangle - \langle\psi_o|H_o|\psi_o\rangle + \frac{(\varepsilon_s - 1)}{(2\varepsilon_s + 1)a^3}\mu^2 \qquad (2.13.4)$$

The third term in eqn. (2.13.4) represents the work done in creating the charge distribution of the solute within the cavity in the dielectric medium.

The disadvantage of the original SCRF method is the use of a spherical cavity to represent all molecules. Tomasi (Tomasi, *et al*., 1981; Tomasi and Persico, 1994) devised a method for generating a realistic cavity shape of a molecule, using the van der Waals radii of the atoms of the solute. They coined this approach as "polarizable continuum" method (PCM), which has been implemented in various quantum mechanical programs. In PCM, ΔG_{elec} is computed numerically, because of the nonanalytical nature of the cavity shape. Since the wavefunction of the solute extends beyond the cavity, there are slight complications in PCM which can be handled in an approximate manner by scaling the charge distribution on the surface so that it is equal and opposite to the charge of the solute. Later, in 1993, Klamt and Schüürmann introduced COSMO ("conductor-like screening model") as an interesting variant of the PCM method (Klamt, *et al*., 1998; Klamt and Schüürmann, 1993; Schafer, *et al*., 2000). In this model, the cavity is considered to be surrounded by a conductor with infinite dielectric constant, which greatly simplifies the treatment of the screening effects and allows for an *a posteriori* correction to account for the finite dielectricity constant. COSMO is implemented in various quantum mechanical packages (for example., Gaussian(M. J. Frisch, *et al*., 2003) and Turbomole (Ahlrichs, *et al*., 1989). Some of the models used in SCRF are shown in Figure 2.6.1.

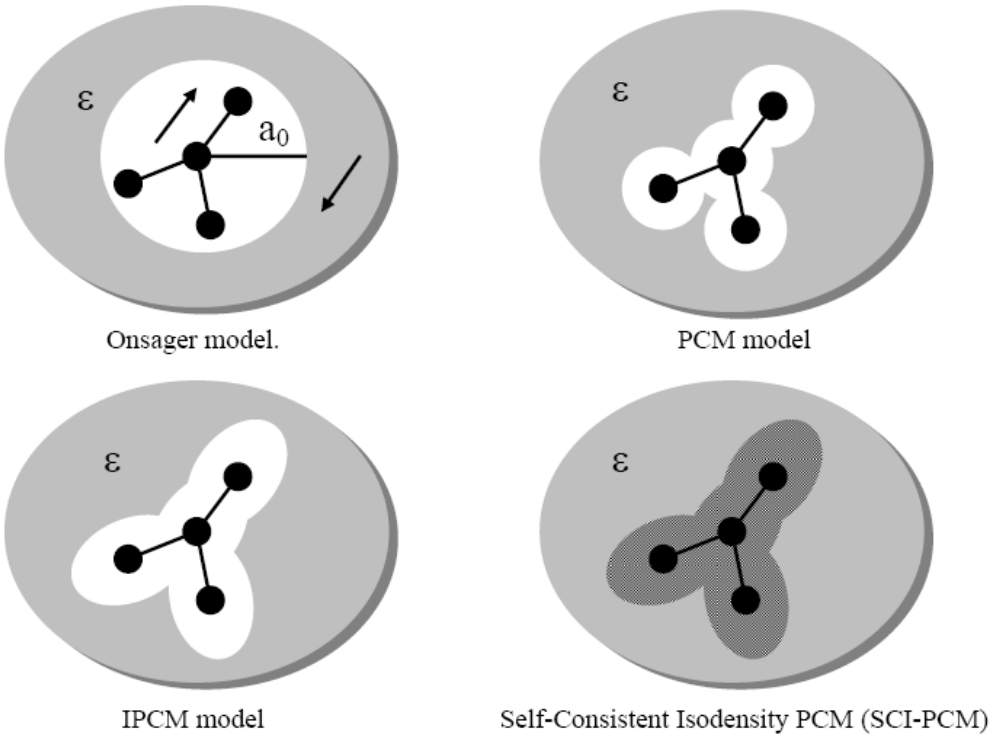

Figure 2.13.1: Simplified explanation of SCRF models.

The continuum solvation model used in this study is the so-called integral equation formalism polarizable continuum model (IEFPCM) (Cancès and Mennucci, 1998; Cancès, *et al*., 1997; Mennucci, *et al*., 1997), the most recent development of the largely diffused polarizable continuum model (PCM) method (Cammi and Tomasi, 1995; Tomasi, *et al*., 1981). This is an accurate continuum solvation model which uses a molecular-shaped cavity to define the boundary between solute and continuum dielectric and apparent surface charges to describe the electrostatic solvent effects. In the past few years, this model has been extended to evaluate solvent effects on molecular properties (Tomasi, *et al*., 2002).

2.14 Software

This study was carried out on a series of molecules using the GAUSSIAN 03 program installed on a Pentium IV desktop computer. The following section describes briefly the Gaussian 03 software.

2.14.1 The GAUSSIAN 03 Program

GAUSSIAN 03 (G 03) is a robust computational chemistry program that uses electronic structure modeling to investigate the chemical phenomena of interest. Gaussian 03 is capable of predicting many properties of molecules and reactions, including, molecular energies and structures, energies and structures of transition states, bond and reaction energies, molecular orbitals, vibrational frequencies, thermochemical properties, reaction pathways and numerous other molecular properties for systems in the gas phase and in solution, including the ground state and excited states. Gaussian 03 can serve as a powerful tool for exploring areas of chemical interest like substituent effects, reaction mechanisms, potential energy surfaces and excitation energies.

The input section to the GAUSSIAN 03 programs consists of the molecular charge and the multiplicity, the symbols of the constituent atoms and a definition of the molecular structure, either in the form of Cartesian coordinates or the Z-matrix notation, which define the molecular geometry in terms of bond lengths, bond angles and dihedral angles. The task to be performed, whether a single-point calculation, geometry optimization or frequency calculation, must also be specified, together with the appropriate basis set and the level of theory.

2.14.2 The GaussView Program

GaussView is a Graphical User Interface (GUI) program designed to simplify and extend the use of the Gaussian 03 program. In this study, Gaussview was used to build and edit molecules, set up and submit Gaussian jobs, and to display and use the results from the Gaussian jobs. However, GaussView is not directly integrated into the Gaussian program system, but acts as a front-end/back-end processor to facilitate its use on a desktop computer workstation. GaussView was also used to verify the animation of atoms associated with the negative eigenvalue of the different transition-states.

2.14.3 Thermochemistry in Gaussian 03

The equations used for computing thermochemical data in Gaussian 03 are equivalent to those given in standard texts on thermodynamics (partition functions equations in statistical mechanics) (McQuarrie and Simon, 1999). One of the most important approximations to be aware of is that all the equations assume non-interacting particles and therefore, apply only to an ideal gas. This limitation introduces some errors, depending on the extent that any system being studied is non-ideal. Further, for the electronic contributions, it is assumed that the first and higher excited states are entirely inaccessible. This approximation is generally not troublesome, but can introduce some errors for systems with low lying electronic excited states. Once these thermodynamic parameters are calculated, the potential energy surface can be obtained.

Having discussed the computational methods and software used the following sections in this chapter describe the three reactions studied.

2.15.0 Thermal [1,j]-Sigmatropic Hydrogen Shift

Interest in the study of concerted processes in organic chemistry has increased markedly since the development of the general theory of the principles of orbital symmetry by Woodward and Hoffmann (Woodward and Hoffman, 1970). Consequently, application of the rules governing orbital symmetry control in electrocyclic reactions, sigmatropic rearrangements, cycloaddition reactions, and cheletropic processes has contributed much to the understanding of the nature of the concerted reactions. Thermal and photochemical [1,j] sigmatropic rearrangement via either suprafacial or antarafacial pathways, and the resultant stereochemical consequences, is one of the more fascinating of these processes and has been subject of several early reviews (Frey and Walsh, 1969; Gilchrist and Storr, 1972; Gill, 1968; Hoffman and Woodward, 1968). This review will be limited to thermal [1,j] sigmatropic migrations (j=5,7] in neutral acyclic systems.

2.15.1 Theoretical Aspect of Sigmatropic Migration

The elementary theoretical framework governing sigmatropic migration has previously been described in details by Woodward and Hoffmann (Woodward and Hoffman, 1970). [1,j] hydrogen migration may be considered in terms of an interacting hydrogen atom and the HOMO of a polyene radical. The migrating H thus may participate in two possible transition state geometries, if orbital symmetry is to be maintained. In suprafacial migration, the migrating H maintains contact at all times with the same face of the π system, while in an antarafacial process the hydrogen must maintain contact with both faces of the π system simultaneously. This requirement makes [1,3] antarafacial hydrogen migration extremely difficult if not impossible.

If the migrating atom is capable of undergoing stereochemical inversion, then the selection rules allow two distinct suprafacial or antarafacial routes with attendant retention or inversion at the migrating centre (Scheme **2.15.1** and **2.15.2**).

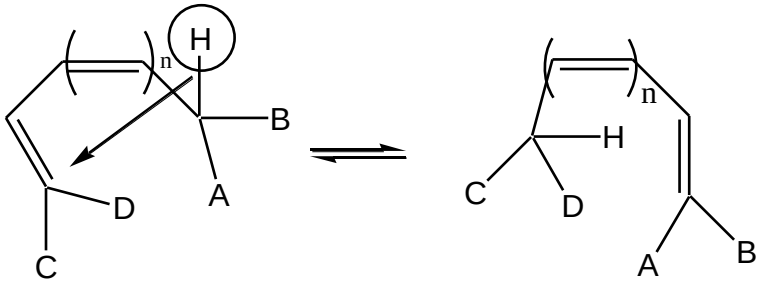

Scheme 2.15.1: Concerted sigmatropic suprafacial pathway (n=1,3…).

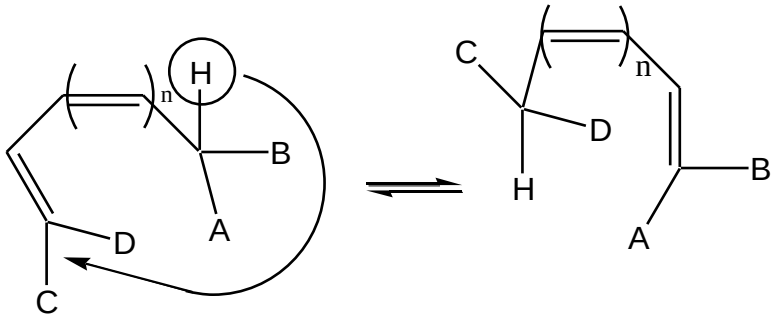

Scheme 2.15.2: Concerted sigmatropic antarafacial pathway (n=0,2,4..).

Thus for migrating groups other than hydrogen, [1,3] migrations become feasible. Selection rules for neutral [1,j] thermal migrations are summarized in table 2.15.1.

Table 2.15.1: Homo selection rules for [1,j] sigmatropic migration.

J	Allowed	Forbidden
3	Antara-rentention Supra-inversion	Antara-inversion Supra-retention
5	Antara-inversion Supra-retention	Antara-rentention Supra-inversion
7	Antara-rentention Supra-inversion	Antara-inversion Supra-retention

An alternative viewpoint of sigmatropic migration has been proposed by Zimmerman (Zimmerman, 1971) and discussed also by Dewar (Dewar, 1969; Dewar, 1971). Basically, this approach considers that thermal sigmatropic migration occurs via aromatic transition

states. Cyclic transition states may be classified as either aromatic or antiaromatic depending on the number of π electrons involved and whether the polyene follows Hückel (zero or even number of twists in cyclic array) or Möbius (odd number of twist) topology. Möbius transition states will be aromatic for 4n π electrons, with one sign inversion in the cycle, while Hückel transition states will be aromatic for (4n+2) π electrons, with no sign inversions. Thus [1,3] hydrogen migration, involving 4 π electrons, can only occur via a Möbius array, an antarafacial pathway. The [1,5] sigmatropic hydrogen migration, a (4n+2) π array follows a Hückel suprafacial pathway. The selection rules derived from application of the Hückel –Möbius concept are identical with those from HOMO approach, but seem preferable to some workers because they avoid the necessity of knowing the individual symmetries and HOMOs (table 2.15.2).

Table 2.15.2: Selection rules for thermal [1,j] sigmatropic migrations.

No. of electrons	System type	J	Allowed migration
4	Möbius	3	Antara-rentention Supra-inversion
6	Hückel	5	Antara-inversion Supra-retention
4n	Möbius	(4n-1)	Antara-rentention Supra-inversion
4n+2	Hückel	(4n+1)	Antara-inversion Supra-retention

Various orbital interaction schemes have been developed which extend the above arguments. Fukui has reviewed (Fukui, 1971) a method which considers the orbital interaction between the HOMO to predict the most favorable steric pathway. Goddard (Goddard, 1972) has proposed the orbital phase continuity principle (OPCP), an *ab initio* method which asserts that certain phase relationships must occur between the orbitals of the reactants and products for the reaction to be allowed. The results generally agree with the Woodward-Hoffmann

rules, and OPCP may also be applied to reactions involving no symmetry. Goddard's approach is based on a generalized valence-bond self-consistent field method and thus is the valence bond analog of the Woodward-Hoffmann MO approach. Finally Epiotis (Epiotis, 1973) has applied configuration interaction (CI) consideration in an effort to predict stereoselectivity in [1,3] and [1,5] shifts. Interestingly, he concludes that CI can affect [1,3] shifts and actually reverse stereoselectivity if groups of widely differing polarity are involved, but that [1,5] shifts are not affected. A generalization of this result is that CI is important for 4n processes, but not for 4n+2 aromatic arrays.

2.15.2 Nature and Conformation of Sigmatropic Transition States

Concerted migration of a σ bond between the termini of a polyenylic π-electron system implies the formation of a cyclic transition state. Thus a [1,5] migration proceeds via a cyclic six-membered transition state with suprafacial (allowed) geometry. It has been recognized that a *cis* configuration about the C_2-C_3 π bond is a necessary prerequisite, as a *trans* orientation would dictate a highly strained transition state (Frey and Walsh, 1969). Substituent groups will tend to occupy preferentially the more stable pseudo-ring positions.

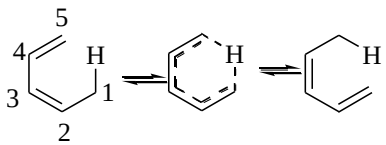

1 **2** **3**

Figure 2.15.1: Transition structure for [1,5]-H shift.

One of the first reported examples of a thermal [1,7] shift is the interconversion of vitamin D and precalciferol (Havinga and Schlatmann, 1961). If the migration follows a concerted path, the transition state must be coiled in a helical fashion to accommodate the antarafacial

geometry. Structure 2.15.2 is an envisioned transition state for acyclic antarafacial [1,7] sigmatropic migration of hydrogen.

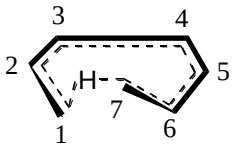

Figure 2.15.2: Transition structure for [1,7]-H shift.

In order to achieve this configuration, at least two double bonds must have the necessary cisoid configuration. If this condition is not met, then the more common [1,5] migration or some other pericyclic process may dominate (Heimgartner, *et al*., 1970). It appears that [1,7] H migration is actually favoured over [1,5] migration, all other factors being equal, with geometry being the deciding factor.

2.15.3 Experimental Work on [1,7]-H Shift

Although many early reviews categorize thermal [1,7]-H shift as rare, several reports indicate that [1,7]-H migration actually is preferable to [1,5] migration in systems where the two pathways are really competitive. When the geometry requirements for an antarafacial transition state are met, activation enthalpies ($\Delta H^{\ddagger}$~15-27 kcal/mol) are considerably less than for the corresponding [1,5] process. The highly ordered [1,7] transition state is characterized by a highly negative entropy of activation (-15 to -25 eu), which also distinguishes it from the less ordered [1,5] state.

The simplest literature example (Marvell, *et al*., 1973) is the postulated [1,7] H shift in the reversible isomerization of 2,4,6-octatriene (Scheme 2.15.3).

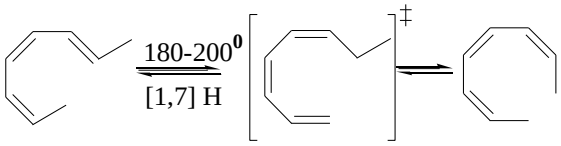

Scheme 2.15.3: Isomerization of 2,4,6-octatriene.

The intermediary *cis,cis*-1,3,5-octatriene is not detectable under the reaction conditions. By far the most extensive investigation of the [1,7]-H migration process has been carried out by Hansen, Schmid and coworkers (Heimgartner, *et al*., 1970; Heimgartner, *et al*., 1972). The reversibility of the [1,7] H migration was confirmed by deuterium substitution, which also confirm the [1,7] pathway as the main isomerization pathways. Activation parameters for reactions involving a concerted [1,7] H shift are listed in table 2.8.3.

Table 2.15.3: Experimental activation parameters for reactions involving a concerted [1,7] H shift.

Reaction	T range, K	LogA (sec^{-1})	$\Delta H^{\ddagger}$ Kcal/mol	$\Delta S^{\ddagger}$ Eu	Ref
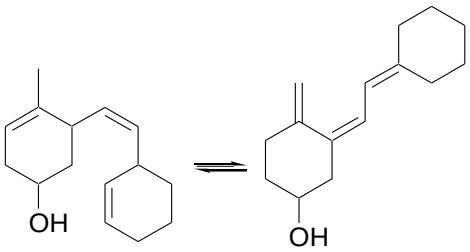	324-363 (Decalin)		20.9	-17.2	(Coutot and Rumin, 1970)
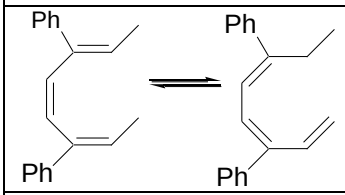	297-331 ($CDCl_3$)	9.5	18.5	-17.2	(Coutot and Rumin, 1970)
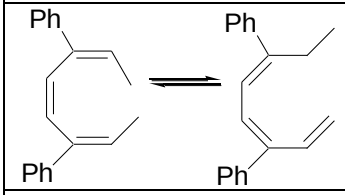	278-318 ($CDCl_3$)	7.8	14.9	-25.0	(Coutot and Rumin, 1970)
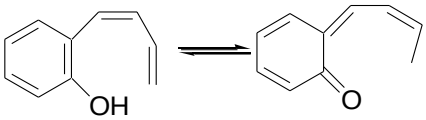	278-318 ($(CD_3)_2SO$)		23.0	-17.0	(Schweizer, *et al*., 1969)
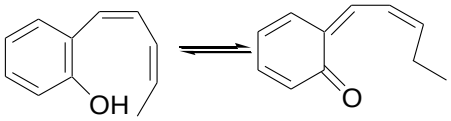	358-378 (octane)		24.9	-16.0	(Schweizer, *et al*., 1969)
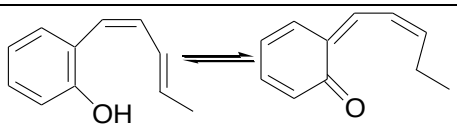	358-378 (octane)		26.1	-15.0	(Coutot and Rumin, 1970)

One of the key and final reaction of the *in vivo* and *in vitro* vitamin D synthesis is the thermal interconversion of previtamin D and vitamin D (Scheme 2.15.4) via the [1,7] antrafacial hydrogen shift (Havinga, 1973). These [1,7] shifts were thought to involve hydrogen transfers from one face to the other of the π system through a helical transition structure (Havinga and Schlatmann, 1961).

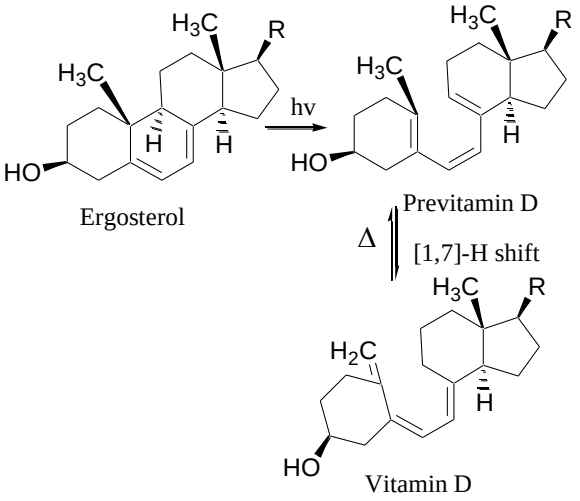

R=C_9H_{17}: vitamin D_2 series

R=C_8H_{17}: vitamin D_3 series

Scheme 2.15.4: Vitamin D synthesis.

Woodward and Hoffmann discussed the then known [1,5] and [1,7]-H shifts in 1965 in their seminal analysis and generalized formulation of sigmatropic reactions (Woodward and Hoffmann, 1965). They rationalized why [1,3] hydrogen shifts had not been observed, why [1,5] shifts should be suprafacial and were seen to be suprafacial, and deduced that [1,7-H shift should be antarafacial. These stereochemical characteristics of [1,5] and [1,7]-H shifts were later confirmed in an acyclic substituted pentadienyl (Roth, *et al*., 1970) and in heptadienyl reactants (Hoeger, *et al*., 1987; Hoeger and Okamura, 1985). This part of the background is of importance to the development of orbital symmetry theory for [1,7] hydrogen shifts. It rationalizes nicely the antarafacial stereochemistry invariably seen in cyclic and acyclic reactants.

2.15.4 Computational Chemistry Work on [i,j]-H Shift

Various computational studies have been done on [i,j]-H shift, the following section describes some selected pertinent studies.

The majority of calculations published in the past have been performed according to Hartree-Fock (HF) theory, which neglects correlation between electrons of opposite spin. The main limitation of HF theory is the one – electron nature of Fock operator. Thus, the calculated activation energies for pericyclic reactions are systematically too high and there could be systematic errors in geometries. Furthermore, the comparison between a concerted reaction and a possible stepwise mechanism involving a diradicaloid intermediate is generally not possible, because restricted Hartree-Fock theory (RHF) cannot be used for open- shell species, and the energies of the unrestricted HF (UHF) wave functions of the diradicaloid species are too low compared to RHF calculations on closed-shell species The inclusion of electron correlation by Møller- Plesset (MPn) perturbation theory or truncated configuration interaction (CI) calculations can address this problem. However, such calculations limit the size of the molecule to be studied practically to about 10 non- hydrogen atoms with current computers.

Recently, DFT has evolved as a viable alternative approach for molecular structure calculations. As has been pointed out, DFT- based methods include electron correlation explicitly in the exchange- correlation function at a moderate computational cost (Foresman and Frisch, 1996). These methods are therefore promising for highly accurate calculations of chemically interesting systems, as shown by a comparison of the results from DFT calculations with the extensive results from Hartree-Fock calculations and other MO- based methods (Houk, *et al*., 1992; Wiest and Houk, 1996).

Ab initio calculations of the [1,5]-H shift in (3*Z*)-penta-1,3-diene and other substituted pentadienes and heteroanalogues using the hybrid density functional B3LYP with the 6-31G* basis has been done (Saettel and Wiest, 2000). It was found that heteroatoms in (*Z*)-penta-1,3-diene have a substantial effect on the pericyclic [1,5]-H shift. As a general trend, electron-donating substituents increase the π electron density of the aromatic transition structure and stabilize it, decreasing the activation energy, whereas electron- withdrawing substituents have the inverse effect. The inductive and mesomeric effects of heteroatoms or heterosubstituents are of a great importance and in a continuous balance in the energetics of the transformation. Steric can also play an important role due to the geometrical constraints of the reaction.

The effects of fluorine and methoxy or acetoxy substituents at C-19 on the [1,7]-H migration in previtamin D analogs have been studied experimentally in the last twenty years by several groups in the USA and in Europe. In all theses studies, it has been found that a 19, 19-difluoro substitution completely inhibits the reaction, whereas a 19-methoxy (-acetoxy) substituents accelerates the conversion of previtamin D to vitamin D (Sicinski, 1992).

In spite of the experimental agreement, the mechanistic interpretations of these opposite effect were controversial. Sialom and Mazur (Sialom and Mazur, 1980) suggested two alternative explanations for the reaction acceleration effect of the 19-acetoxy substituent. One involves the electron donating property of the oxygen atom, which changes the electron distribution in the triene system, and the second is a steric effect that may destabilize the s-*cis* 6,7 conformation of the previtamin D molecule. The complete inhibition of thermal isomerization for 19, 19-difluoro substitution was explained by strong inductive effect of the fluorine atoms (Moriarty and Paaren, 1980) based on analogy to [1,5] shift reactions

(Breslow, *et al*., 1973) and assumptions that a localized positive charge on the terminal carbon atom of the triene system is involved in the transition structure for [1,7]-hydrogen migration. However, in other studies, it has been concluded that inductive effects do not play an important role in the stability of 19-acetoxy and 19-methoxy vitamin D analogs. Questions have also been raised as to whether the thermal stability of 19, 19-difluoroprevitamin D can be attributed to the strong inductive effect of the fluorine atoms.

The thermal [1,7]-sigmatropic hydrogen migration is considered to be a pivotal event in the metabolic production of vitamin D and has been utilized as the key step in the synthesis of several complex organic molecules. Although both the intramolecular and antarafacial nature of this process is established (Havinga, 1973), and the importance of the energies, nature and conformation of the transition state on the rates and product distribution has been recognized, there is no theoretical basis to predict the outcome of this process. This, together with our interest in the synthesis of useful chiral synthons employing the [1,7]-sigmatropic reaction as the key step, prompted us to develop a theoretical approach using molecular modeling as a predictive tool. This approach utilizes product like structures to evaluate relative transition-state energies as suggested by *ab initio* calculations. Such an approach could greatly simplify predictions, as it would allow energy calculations on fully developed structures by straightforward computational methods. The energies for structures representing both the starting material and product were allowed to minimize with appropriate restraints to ensure that the known stereoelectronic preferences necessary for a [1,7]-sigmatropic rearrangement are preserved.

2.16.0 Esterification

A nucleophilic substitution on the unsaturated carbon (e.g., the acyl carbon) is known to proceed via a tetrahedral intermediate (Scheme **2.16.1**).

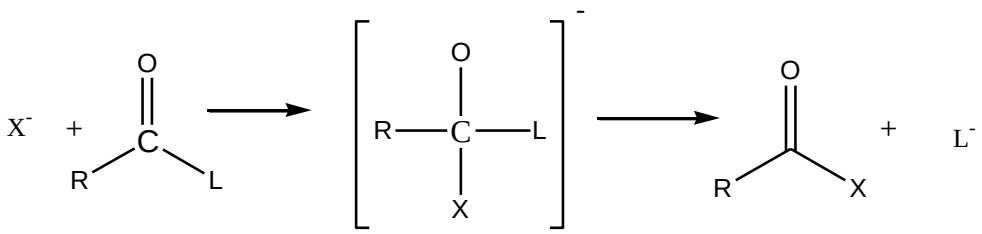

Scheme 2.16.1: Nucleophilic substitution on the unsaturated carbon.

The mechanistic details of the reactions like ester hydrolysis have been extensively investigated, because of the relevance to the enzymatic catalysis in reactions of carboxylic acids (Patai, 1966). The minimum-energy path of the gas-phase nucleophilic displacement on the acyl chloride has been investigated theoretically (Yamabe and Minato, 1983). The reaction is initiated by the formation of the π X---CH_3CO-C1 complex and takes place in a concerted manner. No tetrahedral intermediate was found.

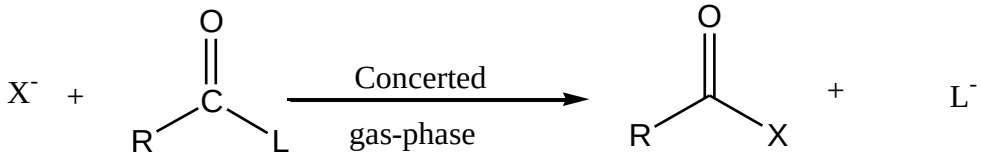

Scheme 2.16.2: Concerted nucleophilic substitution on the unsaturated carbon.

The order of the reactivity toward a nucleophile has been established experimentally (Figure **2.16.1**) (Hendrick, *et al*., 1970).

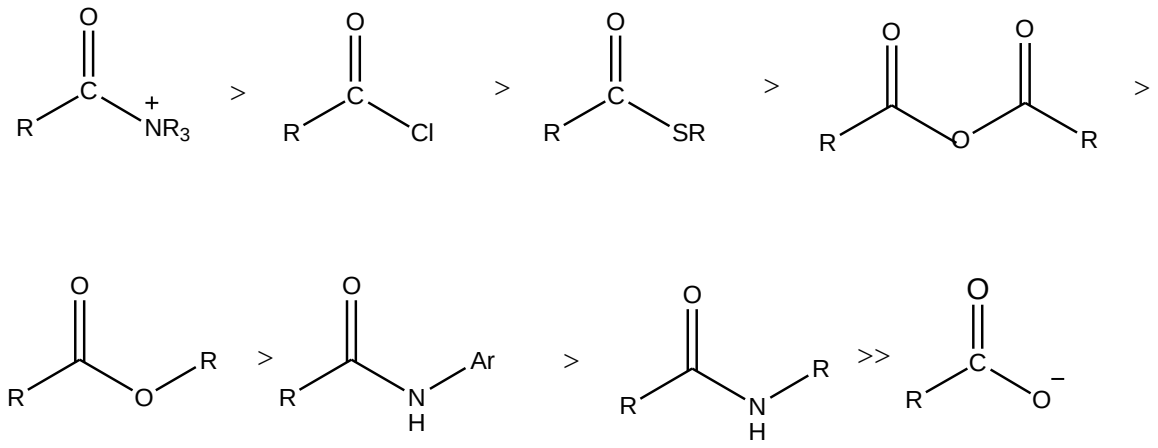

Figure 2.16.1: The order of the reactivity toward a nucleophile on the unsaturated carbon.

The order is explained in terms of both the activity of the leaving group (L), (the better the leaving group the faster is the reaction) and the extent of the conjugation to the carbonyl group. More systematic and uniform comparison may be made by applying the frontier orbital theory (Fukui, 1970).

The reactivity of carbonyl and aromatic compounds for the nucleophilic displacement has been investigated theoretically (Yamabe, *et al*., 1984). LUMO (lowest unoccupied MO) obtained by the mixing of the π* MO with the σ* MO is a uniform criterion of the relative reactivity of substrates. The presence or absence of the tetrahedral intermediate is found to depend on the energy difference between the π* and σ* MO's. Figure 2.16.2 displays the LUMO and (LU+1)MO and the easiness of concerted or tetrahedral intermediates reaction.

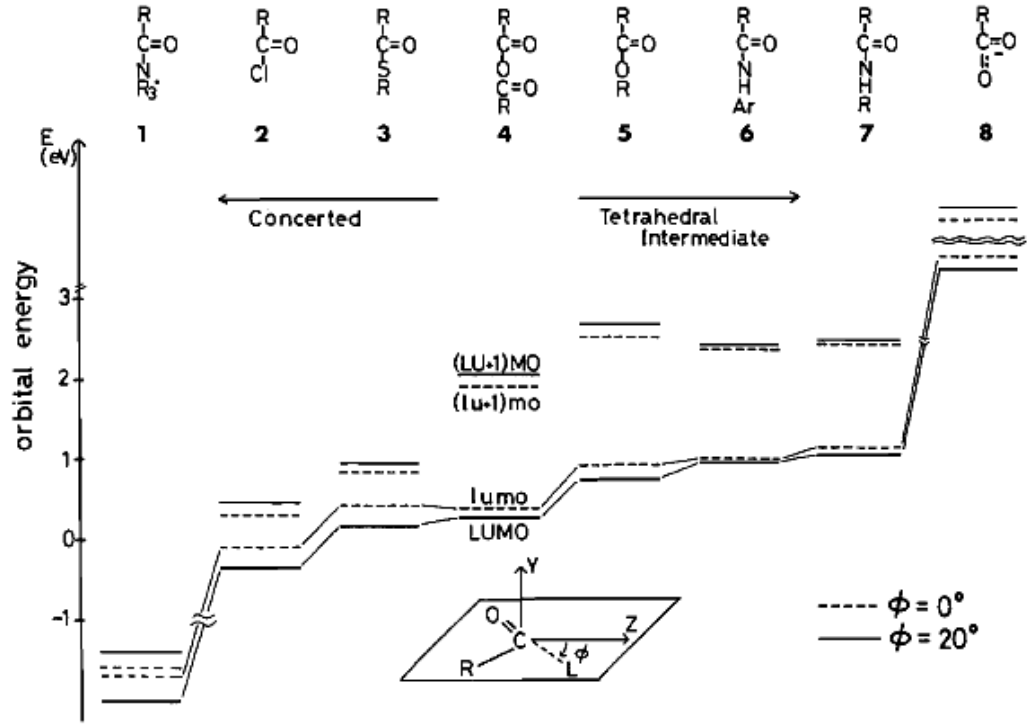

Figure 2.16.2: The unoccupied-orbital energies of carbonyl compounds computed with the MNDO MO method.

The broken levels, LUMO and (LU + 1)MO, are for the equilibrium geometry. The full-line levels, LUMO and (LU + 1)MO are for the bent-out geometry. LUMO means the lowest unoccupied MO, and (LU + 1)MO the second lowest unoccupied MO. Substituent R is the methyl group and Ar is the phenyl ring in the MO calculation.

Esterification is the general name for a chemical reaction in which two reactants (typically an alcohol and a carboxylic acid or acyl halide) form an ester as the reaction product. The esterification of a carboxylic acid with an alcohol is a reversible reaction (Eq 2.16.1) and can be accomplished only if a means is available to drive the equilibrium to the right.

$$RCOOH + R'OH \underset{}{\overset{H^+}{\rightleftharpoons}} RCOOR' + H_2O \qquad \text{Eq 2.16.1}$$

The reaction between acyl halides and alcohol (alcoholysis of acyl halides) is the best general method (Eq 2.16.2) for the preparation of esters (Sonntag, 1953).

$$RCOCl + R'OH \longrightarrow RCOOR' + HCl \qquad \text{Eq 2.16.2}$$

The reaction is of wide scope, and many functional groups do not interfere. A base is frequently (usually pyridine) added to combine with HX which is formed. A substantial number of different synthetic approaches have been suggested (Otera, 2003) to comply with modern standards of efficiency and atom economy. Chemoselectivity in reactions of esterification has been discussed by Melman and Nahmany (Melman and Nahmany, 2004). The review covered the preparative approaches for chemoselective acylation of hydroxyl groups in polyfunctional compounds. The following section gives the theoretical basis for esterification.

2.16.1 Theoretical Aspect of Esterification

The elementally theoretical framework governing esterification reactions is presented, with reference to reaction of methanol and acetyl chloride (methanolysis of acetyl chloride). The reaction may be considered in terms of interaction of the HOMO of the nucleophile and LUMO of the electrophile.

2.16.2 The Frontier Molecular Orbitals (FMOs)

The frontier molecular orbitals (FMOs) approximation can be employed in elucidating the molecular dynamics and interactions that occur during a reaction. The ground state configuration of CH_3COCl is:

$$\Psi(CH_3COCl)=(1s_O)^2(1s_C)^2(1s_O)^2(\sigma_{CH3})^2(\sigma_{CO})^2(\sigma_{Cl})^2(\pi_{CO})^2(n_O)^2(\pi^*_{CO})^0 .$$

Thus the shorthand notation for the ground state configuration is:

$\Psi(CH_3COCl)=K(\pi_{CO})^2(n_O)^2(\pi^*_{CO})^0$. Where K represent the "core" electron which are "tightly bound" to the molecular framework, that is, are close to and stabilized by the positive nuclear charge. Two relatively low-energy electronic transitions $(n \rightarrow \pi^*)$ and $(\pi \rightarrow \pi^*)$ (scheme 2.16.3) exist (Turro, 1978).

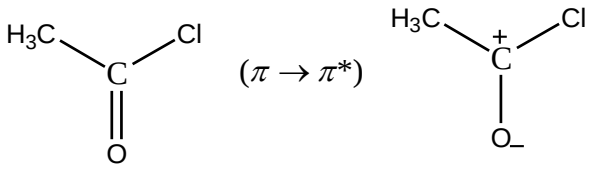

Scheme 2.16.3: $(\pi \rightarrow \pi^*)$ transition in acetyl chloride.

Since the second transition $(\pi \rightarrow \pi^*)$ is polarizable and zwitterionic in nature, it tends to undergo addition and substitution via a zwitterionic mechanism (Scheme 2.16.4).

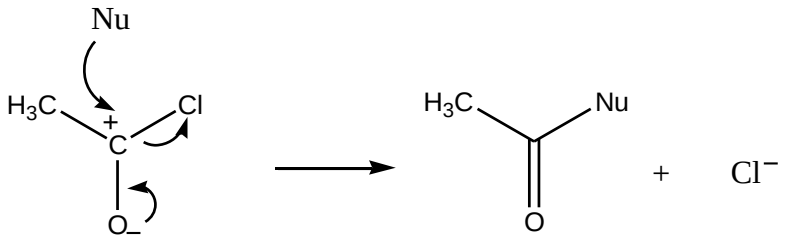

Scheme 2.16.4: Concerted S_N2 mechanism for the reaction of acetyl chloride with nucleophile.

Considering the energies of the orbitals involved, it is common knowledge that only the higher-energy filled orbitals (valence orbitals) and lower-energy (vacant) orbitals are most likely to be involved in reactions at ordinary temperatures (Figure 2.16.3).

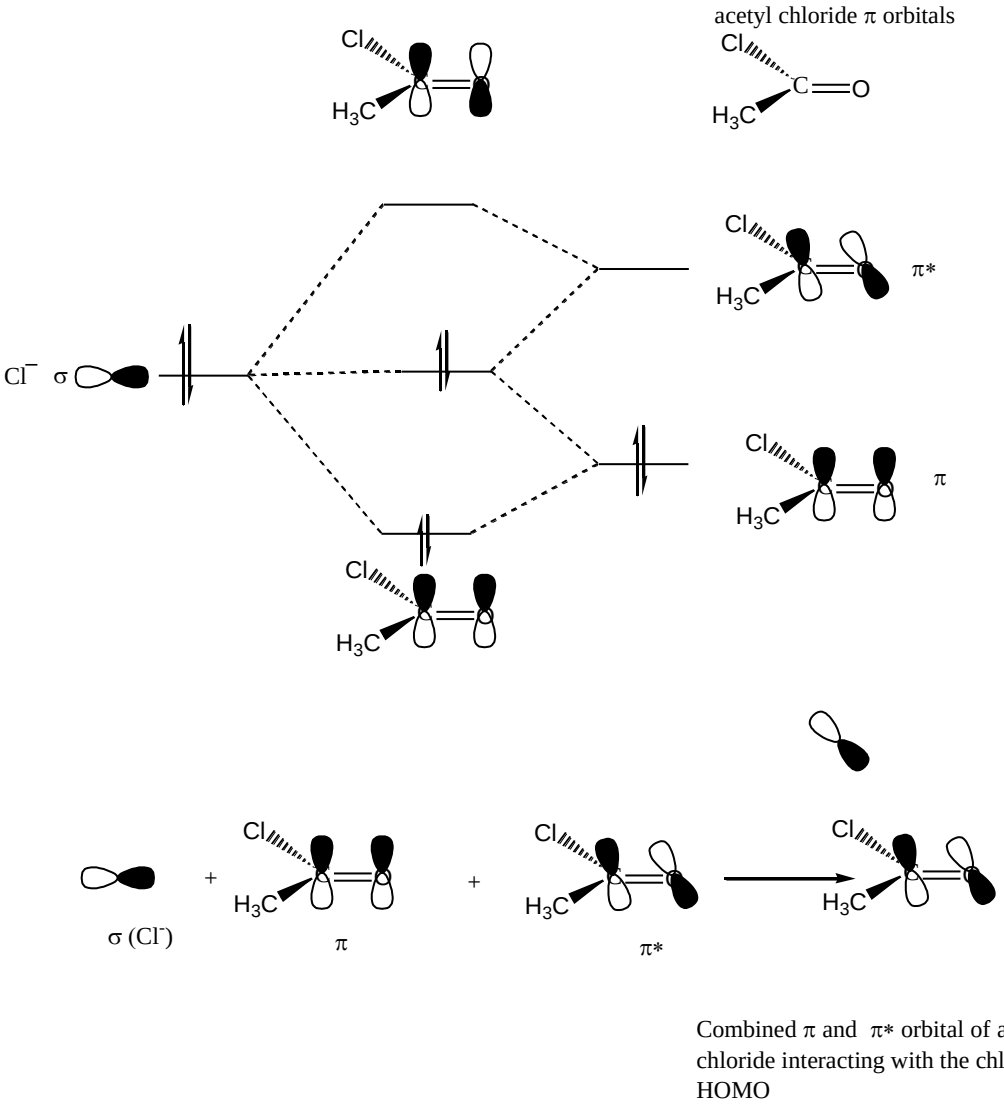

Figure 2.16.3: Molecular energy diagram for degenerate chloride exchange.

According to the FMOs model the highest occupied molecular orbital (HOMO) of the nucleophile is in an in-phase combination with the lowest unoccupied molecular orbital (LUMO) π* orbital of the carbonyl group and is in out-of-phase combination with the filled π orbital. As the nucleophile gets closer to the carbonyl carbon, the carbonyl carbon begins to move out of the plane it shares with oxygen and the other two substituents, and the π* orbitals (empty sp^3 –type orbital on the carbon) begins to overlap with the lone pair orbitals of the nucleophile (Bürgi, *et al*., 1974; Bürgi, *et al*., 1973). As the nucleophile gets closer to the carbon, the carbon moves further out of the CH_3COCl plane and the s-character of the orbital increases while its orbital energy decreases. In turn, there is greater interaction

between the carbon orbital and the HOMO of the nucleophile that leads to a more interaction with the carbonyl π orbital (Bürgi, *et al*., 1973; Liotta, *et al*., 1984). Liotta . has devised a theoretical model to explain the approach angle by maximizing favourable orbital interactions (nucleophile HOMO/carbonyl LUMO) and minimizing unfavourable orbital interactions (nucleophile HOMO/carbonyl HOMO) (Liotta, *et al*., 1984). Chloride being a better nucleofuge, the tetrahedral intermediate should be short lived. The nucleophilic attack occurs within Bürgi-Dunitz trajectory. The following section briefly explain Bürgi-Dunitz trajectory. The above findings have been used in this study to explain some outcomes.

2.16.3 The Bürgi-Dunitz Trajectory

The Bürgi-Dunitz trajectory has been used as a model for explaining and predicting nucleophilic attack on carbonyls (Bürgi, *et al*., 1974; Gawley and Aube, 1996). Nucleophiles approach the carbon and oxygen plane at an angle that is typically about 105±5˚ rather than perpendicular to the carbonyl π system (Figure 2.16.4). This specific angle of approach by nucleophile during its attack on the carbonyl carbon is known as Bürgi-Dunitz trajectory.

Bürgi-Dunitz trajectory

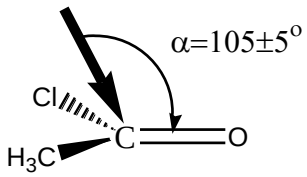

Figure 2.16.4: Bürgi-Dunitz trajectory.

Addition of a nitrogen nucleophile to a carbonyl has been found to have an average Bürgi-Dunitz angle 107˚ while addition of an oxygen nucleophile to a carbonyl has been found to have an average Bürgi-Dunitz angle 110˚ (Bürgi, *et al*., 1974; Bürgi, *et al*., 1974).

The Bürgi-Dunitz angle depends not upon the nature of the nucleophile but, instead, is an intrinsic property of carbonyl centers. Originally described vaguely as 105 ± 5°, (Bürgi, *et al*., 1974) the angle has come to be recognized as 107°. This result, the product of SCF-LCAO-MO calculations, is quite close to the tetrahedral angle (109.5°) and supports the existence of a tetrahedral intermediate in such reactions. The angle is a product of the overlap between the LUMO of the carbonyl function and HOMO of the nucleophile. The π*-orbital is perpendicular to the C=O bond, and optimally so, too, would be the angle of nucleophilic attack, which would produce the most energetically optimal overlap between its HOMO and the LUMO of the carbonyl center. However, the lone pairs of oxygen and the atom's high electronegativity interact with that of the basic nucleophile to force the angle of attack to 107° (Figure 2.16.5).

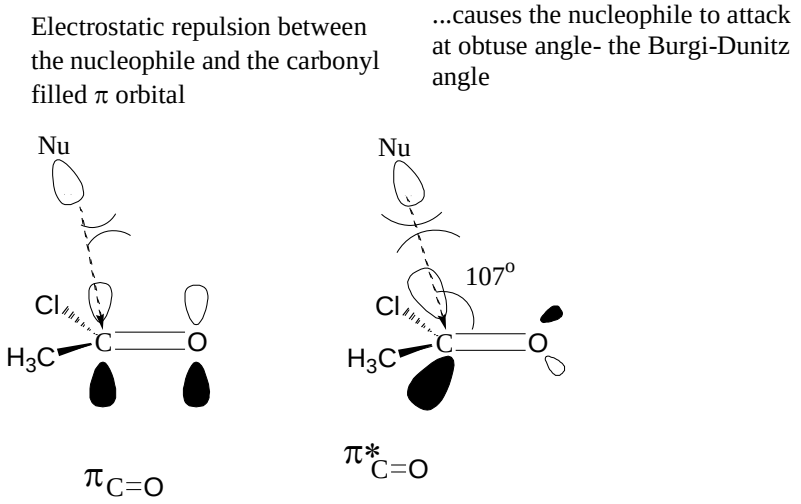

Figure 2.16.5: Orbital interaction for esterification of acetyl chloride.

A similar theory explains the esterification of carboxylic acid with methanol, except carboxylic acid is protonated to become an extremely powerful electrophile (Fig 2.16.6) and hydroxyl group is not a good leaving group.

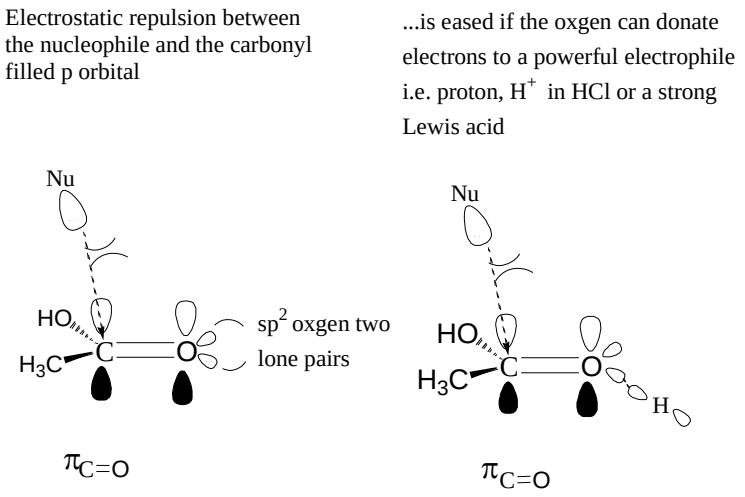

Figure 2.16.6: Orbital interaction for acid-catalyzed esterification.

2.17.0 Experimental Work on Methanolysis of Acetyl Chloride

The exact mechanism of the methanolysis of acetyl chloride is not known with certainty even in solvolytic media owing to the possibility of addition. However, it is generally agreed that the nucleophilic attack is the rate determining step (Baker, 1941).

There has been much recent interest, both theoretical and experimental, concerning the mechanism of solvolysis of acyl halides. It has been emphasized that concerted mechanisms can closely resemble the carbonyl addition mechanism, with a classification as concerted because the tetrahedral intermediate is too unstable to exist (Song and Jencks, 1989). A study (Bentley, *et al.*, 1996) of the alcoholysis and hydrolysis of acetyl chloride in terms of kinetics and product selectivities has been rationalized in terms of a single reaction channel involving an in-plane S_N2 nucleophilic attack.

Kinetics (Ba-Saif, *et al.*, 1987; Bentley, *et al.*, 1985; Hudson and Moss, 1962; Kevill and Kim, 1988; Kim and Caserio, 1981) and theoretical (Blake and Jorgensen, 1987; Guthrie, 1991; Yamabe and Minato, 1983) evidence for concerted mechanisms has been accumulating, especially for nucleophilic substitutions at acyl carbons having a good leaving

group. There are two possible mechanisms (Bentley and Shim, 1993), the first one involves nucleophilic attack by one alcohol molecule assisted by a second alcohol molecule or a polar solvent acting as a base. The second mechanism, involve nucleophilic attack by methanol via a carbocationic reaction within S_N2-S_N1 mechanistic spectrum, that is a solvent –separated ion pair intermediate (S_N1) or a concerted nucleophilic attack (S_N2).

The intermediacy of a tetrahedral species is usually considered to be the rule for acyl transfer process, and the classical perception (March, 1992) (Scheme **1.9.1**) is that concerted S_N2 – type mechanisms (Lowry and Richardson, 1987) occur only in exceptional cases. The generality of the tetrahedral intermediate has been in question especially with good leaving groups; the lifetime of the tetrahedral intermediates would be too short to exist.

Nearly two decades ago it was suggested that solvolysis of CH_3COCl in the presence of an electrophilic catalyst such as phenol may proceed via an ion pair, $(CH_3CO^+)\cdots(ClHOPh^-)$, and that solvolysis in methanol involves a loose S_N2 transition state with high carbocation character (Bentley and Harris, 1986; Bentley, *et al*., 1996; Kevill and Kim, 1988). A more recent experiment (Bentley, *et al*., 1996) also suggests that the rate of methanolysis of acetyl chloride exhibits a high sensitivity to changes in solvent ionizing power, a behaviour consistent with S_N1-like C-Cl bond cleavage. This is a particularly illuminating example since classical mechanisms still typically show the hydrolysis or alcoholysis of an acid halide or ester to involve a tetrahedral intermediate (March, 1992).

Experimental support for concerted mechanisms of acyl transfer has been evidenced by a number of groups. The esterification of acyl halides with alcohols has been the subject of many kinetics investigations (Ferreire and Miller, 1976; Hudson and Saville, 1955; Norris, *et*

al., 1935). Studies have been done on esterification of aliphatic acyl chlorides, benzoyl chlorides and some of its derivatives the influence of different kind of alcohols has also been investigated (Norris and Ashdown, 1925). Furthermore, a review has been presented by Norris and Cortese (Norris and Cortese, 1927).

Experimental results have shown that for stoichiometric concentrations of alcohol and acyl chloride, a simple kinetic law cannot be presupposed as is generally done in the literature. From the stoichiometry, the overall reaction is expected to be second order; however different orders have been reported from experimental data. Depending on reactant ratio and solvent used, the thermokinetic investigation of the esterification of acetyl chloride (Willms, *et al*., 2000) has shown the kinetic law (Eqn. 2.17.1) with alcohol (ROH) exhibiting a partial order of 1.5-1.9.

$$r = k[AcCl]\cdot[ROH]^{x} \qquad (2.17.1)$$

$$x=1.5\text{-}1.9$$

The fractional order with respect to alcohol in this rate law is a consequence of a mixed kinetic law (Eqn. 2.17.2) consisting of two terms with partial order 1 and 2 for the alcohol respectively (Willms, *et al*., 2000).

$$r = k_1[AcCl]\cdot[ROH]^2 + k_2[AcCl]\cdot[ROH] \qquad (2.17.2)$$

This law has been reported by several authors (Ashdown, 1930; Hudson and Saville, 1955; Ross, 1970). It has been interpreted as the involvement of two mechanisms. The kinetics of ester formation during the reaction of acetyl chloride with methanol in acetonitrile has been analyzed in terms of second-order and third-order contribution to the overall kinetics (first-order and second-order in methanol) (Kevill and Kim, 1988). However, addition of tetraethyl ammonium chloride has been found to cause a large acceleration and the kinetics were then found to be dominated by a new third-order term, first order in acetyl chloride, methanol and

the chloride ion. This gives a hint that the second methanol molecule, or solvent acts as a base.

The mixed reaction kinetics and varying activation parameters found by experiments give a hint of a more complicated mechanism. The classical mechanism cannot explain the mixed reaction mechanism (March, 1992). However, the mechanism proposed by Kevill may explain those observations (Kevill and Kim, 1988). The mechanism is presented in Scheme **2.19.1**. Computational study of this reaction may shed some light on the molecular level understanding of the mechanisms involved.

2.17.1 Computational Chemistry Work on Methanolysis of Acetyl Chloride

Earlier theoretical gas-phase studies by Yamabe and Minato (Yamabe and Minato, 1983) showed that rather simple acyl transfer reaction between chloride ion and acetyl chloride take place in a concerted fashion in the absence of a tetrahedral intermediate (see Figure 2.17.1)

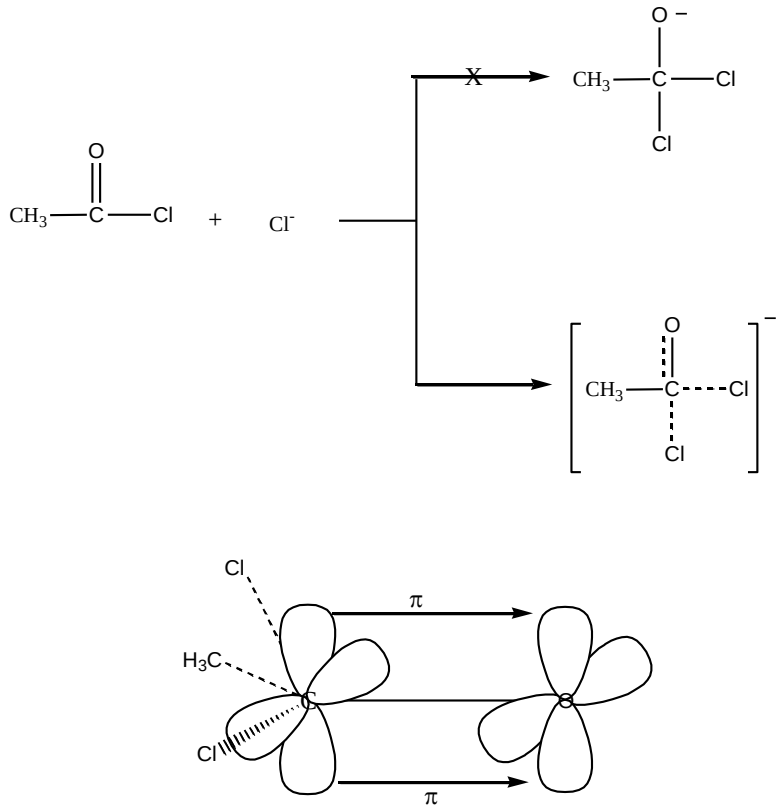

Figure 2.17.1 Concerted mechanism and orbital interactions in the absence of a tetrahedral intermediate.

Blake and Jorgenson (Blake and Jorgensen, 1987) also reported *ab initio* calculations on the degenerate exchange reactions of Cl^- with HCOCl and CH_3COCl and found tetrahedral transition states for both nucleophilic displacement reactions. Koo and co-workers (Koo, *et al*., 2004) have reported on acyl transfer mechanisms for a variety of carbonyl compounds including thiocarbonyl, sulfonyl, and phosporyl derivatives. They found that the backside σ attack pathway was only favoured over a π route when the carbon-bound leaving group had a low-lying σ* orbital.

Different from the S_N2 reaction of the alkyl substrate, the nucleophilic displacement on the unsaturated carbon needs the σ*-π* orbital mixing during the reaction. In the latter case, the σ* level determines the mechanism (concerted or stepwise). In other words, if the C-L bond is weak, the concerted process is likely, and vice versa.

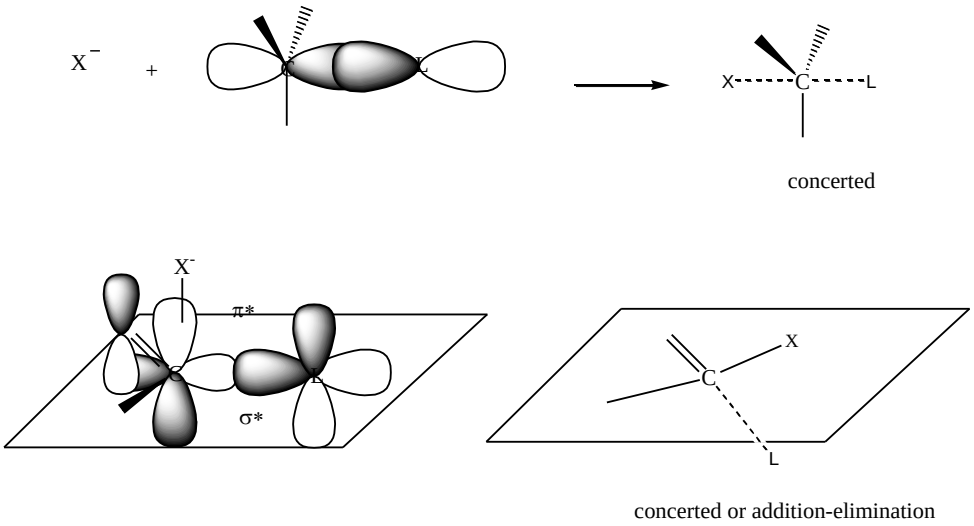

Figure 2.17.2: S_N2 reaction of the alkyl substrate and nucleophilic displacement on the unsaturated carbon.

Jali and Kruger (Jali and Kruger, 2005) reported by computational study that methanolysis of acetyl chloride could occur by a concerted mechanism involving the four-membered and six-membered systems. However, the gas phase activation energies for four-membered transition states were much higher than experimental ones. Those results were contrary to experimental findings. Previous experimental studies (Hudson and Saville, 1955) have shown that the reaction does not proceed by elimination of a covalent HCl from an addition intermediate (Eqn 2.17.1).

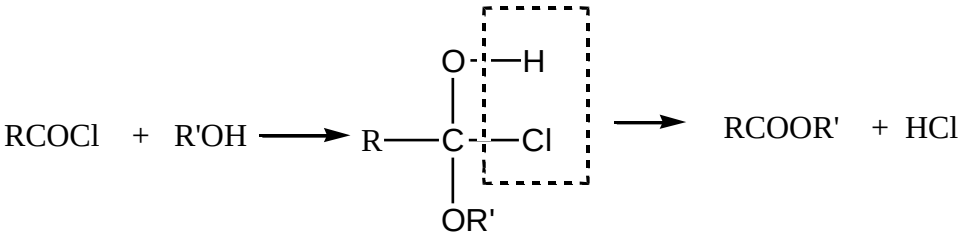

(Eqn 2.17.1)

The formation of the transition state was found to be accompanied by considerable increase in polarity thus requiring further solvation. However, in an effort to reconcile the experimental values and those they found theoretically, the calculations were repeated in this

study. In their computation results, they only gave Gibbs free energy, while this study gave not only Gibbs free energy but also enthalpy and entropy changes.

2.18.0 Experimental Work on Acid-Catalyzed Esterification

Kinetics of esterification between organic acids and alcohols has been extensively studied. There are two different opinions about the ways in which H^+ performs its catalytic effect. One opinion is that the organic acid is activated initially (Royals, 1954), that is the organic acid molecule gets a hydrogen ion from the catalyst before it is esterified with a molecule of primary or secondary alcohol. In the case of tertiary alcohol, such as *t*-butyl alcohol, the hydroxyl group of the alcohol, rather than that of the acid is eliminated. The other opinion was introduced by Goldschmidt (Goldschmidt and Udby, 1907) and further explored by Smith (Smith, 1940; Smith and Burn, 1944). During the period of 1895-1928 Goldschmidt demonstrated the fact that in acid catalyzed esterification reactions, the H^+ ions from the catalyst form complexes with the alcohol molecules, and that the esterification proceeds through interaction of molecules of the complex with the molecules of organic acid. The rate of formation of ester in this case is thus proportional to the momentary concentration of the organic acid.

Smith (Smith and Hilton, 1939) studied the kinetics of hydrogen ion catalyzed esterification of seven *n*-organic acids in methyl alcohol. He has discussed the influence of acids and the length of the carbon chain of the acid on the rate of its esterification. Some of the reported experimental esterification activation energies of some carboxylic acids with methanol are summarized in table 2.18.1.

Table 2.18.1: Experimental activation energy of some carboxylic acid at 25°.

Carboxylic acid	Ea /kcal mol^{-1}	Reference:
CH_3COOH	10.2	(Williamson and Hinshelwood, 1934)
CH_3CH_2COOH	9.8	(Williamson and Hinshelwood, 1934)
C_6H_5COOH	15.5	(Hartman and Borders, 1937)
$C_6H_5CH_2COOH$	9.8	(Hartman and Borders, 1937)

The kinetics of acid acid-catalyzed esterification of substituted benzoic acids by methanol has been studied by several authors (Hartman and Borders, 1937; Hartman and Gassmann, 1940) Some of the results are summarized in Table 2.18.2 below.

Table 2.18.2: Experimental activation energy of substituted benzoic acid at 25°.

Substituent	E_a /kcal mol^{-1}	LogA (sec. units)
None	15.5	7.6
m-NO_2	14.6	6.6
m-Cl	14.6	6.8
m-CH_3	14.2	6.7
p-NO_2	14.7	6.7
p-Cl	14.6	6.8
p-CH_3	13.8	6.4
m-Br	14.6	6.8

The results of acid acid-catalyzed esterification of substituted benzoic acids by methanol obtained by Chapman (Chapman, *et al*., 1968) are summarized below (table 2.18.3).

Table 2.18.3: Experimental activation energy of *ortho*-substituted benzoic acid at 25°.

Substituent	E_a [b] /kcal mol^{-1}	$\Delta H^{\ddagger}$ /kcal mol^{-1}	$\Delta S^{\ddagger}$ /cal $mol^{-1}K^{-1}$	logA
None	16.1	15.4	-24.1	8.01
o-F	15.0	14.3	-27.7	7.22
o-Cl	15.6	14.9	-27.7	7.23
o-Br	14.9	14.3	-30.2	6.67
o-I	14.3	13.6	-32.8	6.11
o-CH_3	15.0	14.4	-29.6	6.8
o-Et	14.9	14.2	-31.1	6.47
o-Pr^i	14.9	14.2	-31.2	6.45

The difference between the catalysts employed by different workers seems to be the most likely cause of the discrepancy usually reported from experiment. However, these results will be discussed in light of the current study.

In the case of uncatalyzed reactions, a second-order dependence of the rate of esterification with respect to the carboxylic acid concentration has been observed (Chemat, *et al*., 1997), due to autocatalysis of the esterification by the acid. When the concentration of alcohol is in tenfold excess of the concentration of acid, the rate for the uncatalyzed reaction is given by eqn. (2.18.1).

$$r = k_{uncat}[alcohol]\cdot[carboxylic-acid]^2 = k_{obs,uncat}[carboxylic-acid]^2 \qquad (2.18.1)$$

$k_{obs,uncat}$ can be measured and would be a pseudo-second-order rate constant, because the acid is not only a reactant but also a catalyst.

The rate of reaction, for the catalyzed reaction is given by eqn. (2.18.2), in which k_{cat} is the rate constant for the catalyzed reaction.

$$r = k_{cat}[alcohol]\cdot[carboxylic-acid] = k_{obs,cat}[carboxylic-acid] \qquad (2.18.2)$$

For acid catalyzed reaction eqn. (2.18.2) is always written as eqn. (2.18.3).

$$r = k_{cat}[alcohal]\cdot[carboxylic-acid]\cdot[H^+] \qquad (2.18.3)$$

Studies have been done on chemoselective process which distinguish phenylacetic and benzoic acids, sp^3-C and sp^2-C acids as well as between sp^3-C and sp-C tethered carboxylic acids (Lee, *et al*., 2001). The sp^3-C tethered carboxylic acids were found to be more reactive followed by sp-C and the least reactive are sp^2-C tethered carboxylic acids.

2.18.1 Computational Chemistry Work on Acid-Catalyzed Esterification

Computational studies of hydrolysis of esters have been done (Sturm, 1999). Very few studies have been done on esterification. A theoretical study of gas-phase esterification of monocarboxy fragments of armchair (10,10) and zigzag (16,10) single-walled nanotubes (SWNTs) with methanol has been reported (Basiuk, 2002). The esterification reaction was found to pass through a 4-memebered transition state having high activation energy (E_a~42.2 kcal mol^{-1}). Gas-phase esterification might be a promising approach to selective derivatization of different forms of carbon nanotubes. From the literature, it seems that there is no systematic computational study done on acid-catalyzed esterification. The development of molecular modeling methods for predicting the influence of the steric environment on the reactivity may provide a substantial advance in the field of chemoselective esterification.

2.19 Scope of the study

The review of literature on [1,7]-H shift in Z,Z-1,3,5-heptatriene systems and esterification reactions presented above indicates the wide-ranging applications of these reactions.

The first reaction being an equilibrium reaction, to shift the equilibrium to the right side is a major challenge and call for molecular level understanding of the reaction. Methanolysis of acetyl chloride provide a borderline S_N2-S_N1 mechanism with mixed reaction kinetics. The role of the counter ion in acid catalyzed esterification has not been established.

In order to understand these reactions it is most essential to have a knowledge of intrinsic kinetics of the reaction. From the review of literature it was evident that in spite of several published reports on this subject, there was a need to undertake a detailed study on features like kinetics of these reactions. Therefore, the objective of the present study was to study

these reactions by computational methods to get molecular level understanding of the underlying mechanisms. The results presented in this thesis would be very valuable as a basic information in the design of [1,7]-H shift in Z,Z-1,3,5-heptatriene systems and esterification reactions and processes.

In order to get molecular level understanding of the mechanism controlling the reaction barriers for the [1,7]-H shift in Z,Z-1,3,5-heptatriene systems (Fig. **2.19.1**), density functional studies using the B3LYP functional (Becke, 1988; Becke, 1993; Lee, *et al*., 1988; Stevens, *et al*., 1994) with 6-31+G(d) basis sets was performed in this study. This method produces satisfactory results (Hess, 2001) for the experimental activation energies for the [1,5]-H shift in 1,3-pentadiene and antrafacial [1,7]-H shift in previtamin D (E_a=19.5 kcal/mol (Hess, *et al*., 1985) systems. Antrafacial [1,7]-H shift, in frontier orbital terms, involves an interaction between the HOMO (highest occupied molecular orbitals) and the LUMO (lowest occupied molecular orbitals) (a "filled-empty" interaction). The mechanism of the rate enhancement or retardation by substituent groups in Z,Z-1,3,5-heptatriene systems in Figure **2.19.1** has also been examined in relation to activation barriers.

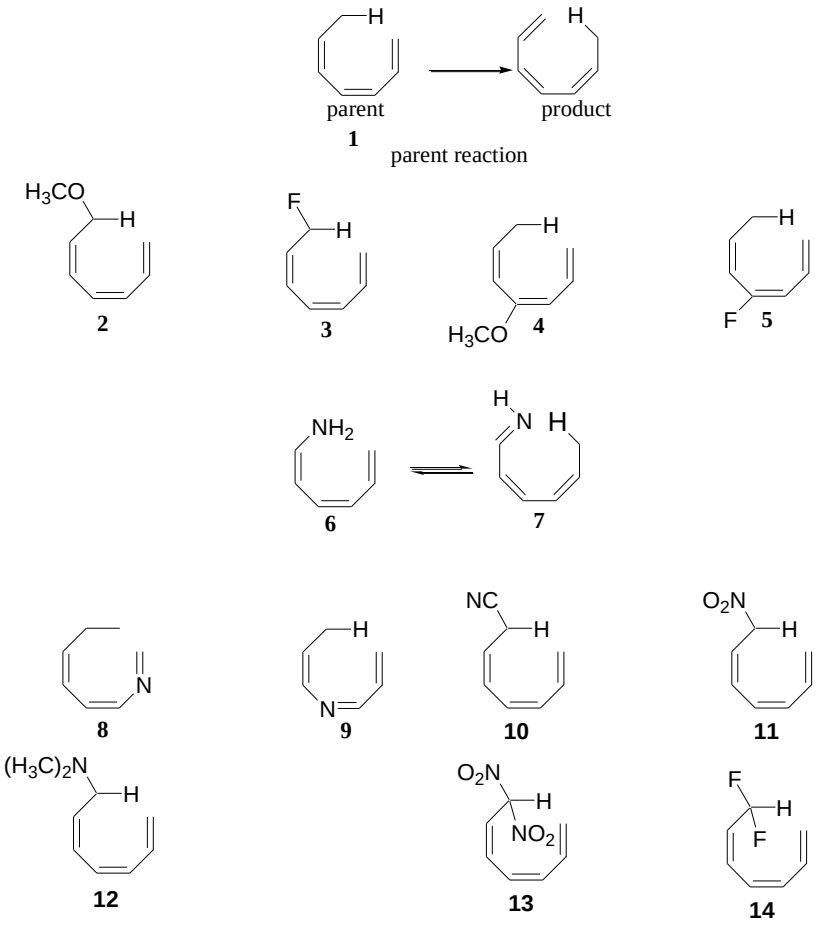

Figure 2.19.1: Compounds studied, 1-14, and parent reaction.

For the methanolysis of acetyl chloride, the mixed reaction kinetics and varying activation parameters found by experiments give a hint of a more complicated mechanism. The classical mechanism (Scheme **1.9.1**) cannot explain the mixed reaction mechanism (March, 1992). However, the mechanism proposed by Kevill (Scheme **2.19.1**) may explain those observations (Kevill and Kim, 1988).

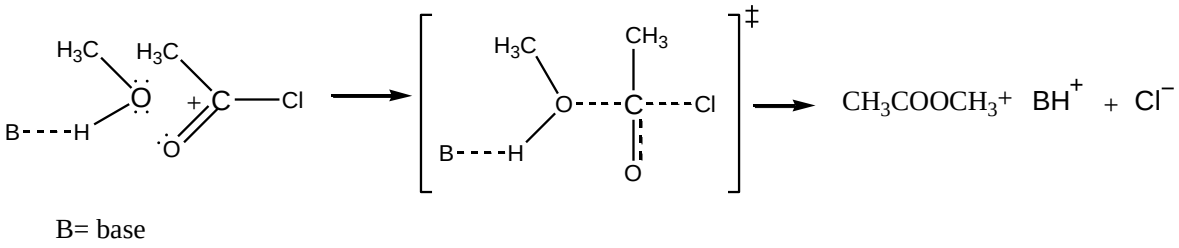

B= base

Scheme 2.19.1: Mechanism for methanolysis of acetyl chloride proposed by Kevill (Kevill and Kim, 1988).

This work studied the mechanism of methanolysis of acetyl chloride as proposed by Kevill by DFT calculations. Computational study of the reaction may shed some light on the molecular level understanding of the mechanisms involved. These calculations provide the first comprehensive mechanistic study of the methanolysis of acetyl chloride.

This work studied also the mechanism of acid-catalyzed esterification by DFT calculations, taking into account the counter ion as shown in scheme **2.19.2**. These calculations provide the first comprehensive mechanistic study of the acid-catalyzed esterification.

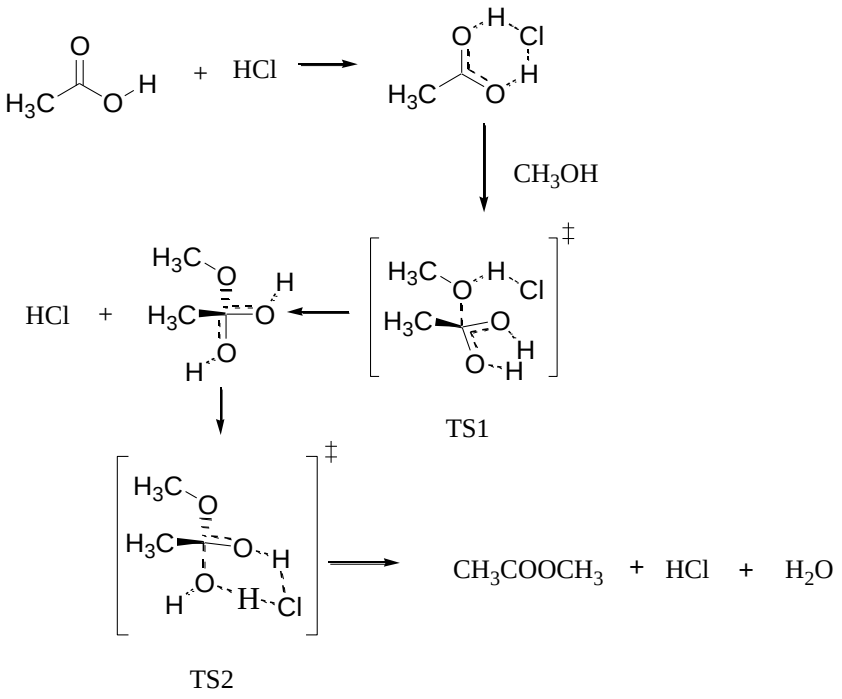

Scheme 2.19.2: Proposed mechanism for acid-catalyzed esterification.

Study was done for auto catalysis according to scheme **2.19.3.**

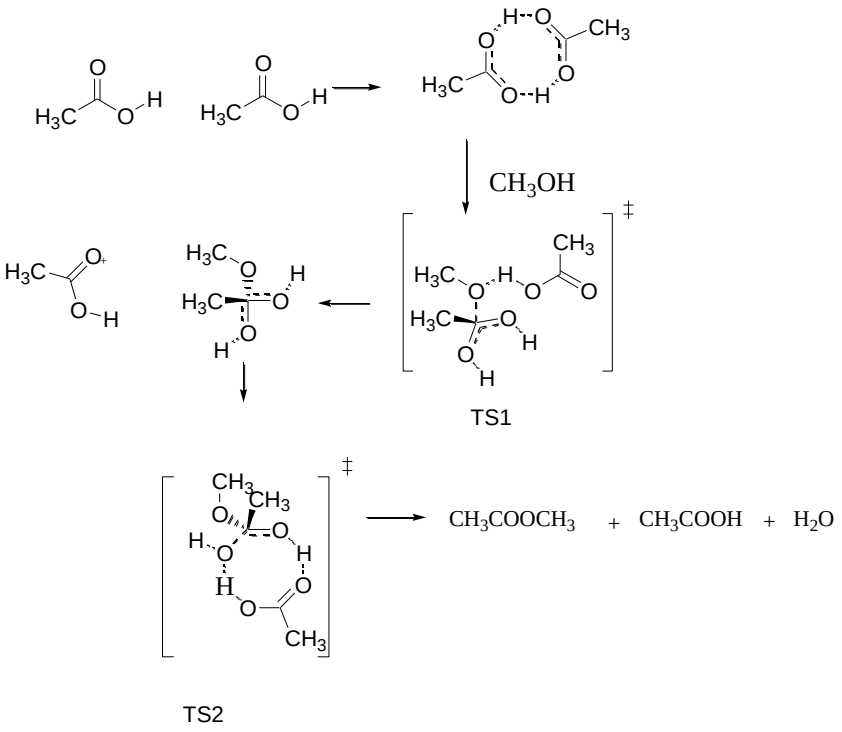

Scheme 2.19.3: Proposed mechanism of autocatalysis in esterification.

CHAPTER THREE

3 METHODOLOGY

3.1.0 Computational Methods

All calculations were performed using the Gaussian 03 series of programs (M. J. Frisch, *et al*., 2003). All geometries were fully optimized by use of the B3LYP functional (Becke, 1988; Lee, *et al*., 1988; Parr and Yang, 1989) with 6-31+G(d) basis sets. Vibrational frequency calculations were performed for all species to characterize them as minima, transition state structures, or possible higher saddle points on the potential energy surface. Zero-point vibrational corrections were determined from the harmonic vibrational frequencies to convert the total energies E to ground state energies E_0. IRC calculations were performed to verify that the transition structures were indeed first-order saddle points on the reaction pathways that had only one imaginary frequency modes. Enthalpies and Gibbs free energies at 298 K were calculated using the ideal gas approximation as implemented in Gaussian 03. Activation energies, E_a, and the Arrhenius factors, A were computed using Equations 3.1.1 and 3.1.2, respectively. These equations have been derived from the transition state theory (Glasstone, *et al*., 1941; Laidler, 1941).

$$E_a = \Delta H^{\ddagger} + RT \tag{3.1.1}$$

$$A = \left(e \frac{k_B T}{h} \right) \exp\left(\Delta S^{\ddagger} / R \right) \tag{3.1.2}$$

where E_a is the activation energy, $\Delta H^{\ddagger}$ is the activation enthalpy, $\Delta S^{\ddagger}$ is the activation entropy, T is the absolute temperature, R the gas constant, k_b is the Boltzmann constant, h is the Plank's constant, and A is the Arrhenius factor.

The integral equation formalism (IEF) (Cancès and Mennucci, 1998; Cancès, *et al*., 1997; Mennucci, *et al*., 1997) version of the polarizable continuum model (PCM) (Cammi and Tomasi, 1995; Tomasi, *et al*., 1981) was used as a continuum solvation model.

This study was carried out using the GAUSSIAN 03 program installed on a Pentium IV desktop computer.

This chapter outlines a brief presentation of the methods used in this study. This presentation follows the outline used by Foresman and Frisch (Foresman and Frisch, 1996) in their textbook "Exploring Chemistry with Electronic Structure Methods". Where nothing else is indicated the material in this chapter was adopted from Foresmann and Frisch and the Gaussian 03 manual (M. J. Frisch, *et al*., 2003).

The scheme below represents the steps that were used to run Gaussian calculations:

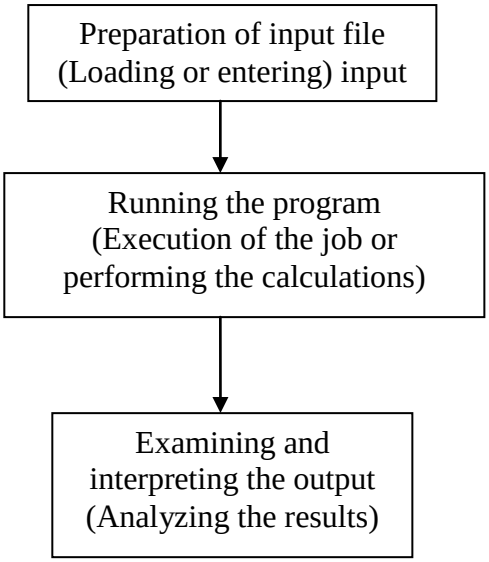

Scheme 3.1.1: Steps used in this study.

Each of these steps is briefly discussed below;

3.2.0 Preparation of the Input File

In this study, GaussView was used to build and edit the structures of molecules, which were saved as Gaussian job file (gjf). For the IRC job, the output of transition search structures were used as input file. The inputs were viewed as graphical structure, Cartesian coordinate or Z-matrix.

In this section the detailed method used is presented. The [1,7]-sigmatropic hydrogen shifts of 7-flouro-Z,Z-1,3,5-heptatriene (scheme 3.2.1) is used to illustrate the method. The reactant and products were optimized and the transition state searched.

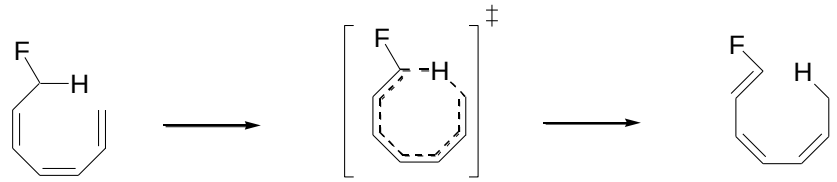

Reactant Transition state Product

Scheme 3.2.1: The [1,7]-sigmatropic hydrogen shifts of 7-flouro-Z,Z-1,3,5-heptatriene.

The complete input file for optimization and frequency calculations of 7-flouro-1,3,7-heptatriene is presented below and the meaning of each term explained.

% Section (Link 0 command)

```
%chk=ParentB3LYP6-31.chk
%mem=700mb
%nproc=1
%nosave
```

Route Section

```
# B3LYP/6-31+G(d)   opt   freq
```

Title Section

```
ParentB3LYP6-31
```

Charge and Multiplicity

```
0 1
```

Molecule specification

```
C                -1.72041694   -1.25764339   -0.03836931
C                -2.15758368    0.06092701   -0.05987152
C                 1.53615745    0.18720391   -0.30370318
C                -1.39595730    1.25645323   -0.32987325
C                -0.44412383    1.84332438    0.48959804
H                 1.33763353    0.36226999   -1.36825317
H                -2.32666875   -1.95753852    0.52938936
H                -3.20569675    0.19493024   -0.33947715
H                -1.92152525    1.97582132   -0.95397102
H                -0.20149580    2.88680075    0.32724996
H                -0.33645540    1.55984447    1.52817976
C                -0.31075589   -1.67083847   -0.03948515
H                -0.19928053   -2.74263507    0.12067959
C                 0.85147084   -0.98315498    0.28216064
H                 1.60045822   -1.67837773    0.65395652
H                 1.02184480    1.06949095    0.10501688
F                 2.89760468    0.19019595   -0.06727870
```

3.2.1 Link 0 Command or % Section

Defines the locations of scratch files and job resource limits.

- %chk contain the job name.
- The **%Mem** command controls the amount of dynamic memory to be used by *Gaussian*. By default, 6 megawords are used. In this study 500 to 700 MB were used, since the RAM for processor used was 1 GB.
- %nproc number of processors to be used. In this work one processor was used.
- %nosave command tells the program to delete the checkfile after that step is concluded.

3.2.2 Route Section

This section specifies the theoretical procedure; basis set and desired type of calculation. It may also contain other keywords and contains instructions for running the calculations. The first line of the route section always begins with a pound sign (#). It includes the procedure keyword and basis set.

- B3LYP/6-31+G(d) means A Density Functional Method due to Lee, Yang and Parr which incorporates a 3- Parameter Function due to Axel Becke used with 6-31+G(d) basis sets.
- opt freq command for both optimization and frequency calculation.

3.2.3 Title Section

The title section consists of one or more lines of descriptive information about the job. It is included in the output and in the archive entry.

3.2.4 Specifying Molecular Structures

Gaussian 03 accepts molecule specifications in several different formats:

- Cartesian coordinates
- Z-matrix format (internal coordinates)
- Mixed internal and Cartesian coordinates

3.2.5 Charge and Multiplicity

All molecule specifications require that the charge and spin multiplicity be specified (as two integers) on the first line of this section. The charge is a positive or negative integer specifying the total charge on the molecule. Thus, 1 or +1 would be used for a singly charged cation, -1 designates a singly-charged anion, and 0 represent a neutral molecule.

The spin multiplicity is given by the equation 2S+1, where S is the total spin for the molecule. Paired electrons contribute nothing to this quantity. They have a net spin of zero since an alpha electron has a +½ and a beta electron has a spin of -½. Each unpaired electron contributes +½ to S.

3.2.6 Cartesian Coordinate Input

Cartesian coordinate input consists of a series of lines of the form:

Atomic-symbol X-coordinate Y-coordinate Z-coordinate

For example, the molecular structure of 7-flouro-Z,Z-1,3,5-heptatriene given in Cartesian coordinates is given in section 3.2.0.

3.2.7 Z-Matrix Format (Internal Coordinate) Input

The other syntax for supplying molecular structures to Gaussian 03 is the Z-matrix. A Z-matrix specifies the locations of atoms and bonds between atoms using bond lengths, bond angles, and dihedral (torsion) angles. Each atom in the molecule is described on a separate input line within the Z-matrix. For example, here is the molecular structure of 7-flouro-1,3,7-heptatriene given in Z-matrix.

```
C
C           1       B1
C           1       B2      2       A1
C           2       B3      1       A2      3       D1
C           4       B4      2       A3      1       D2
H           3       B5      1       A4      2       D3
H           1       B6      2       A5      4       D4
H           2       B7      1       A6      4       D5
H           4       B8      2       A7      1       D6
H           5       B9      4       A8      2       D7
H           5       B10     4       A9      2       D8
C           1       B11     2       A10     4       D9
H           12      B12     1       A11     2       D10
C           12      B13     1       A12     2       D11
H           14      B14     12      A13     1       D12
H           3       B15     1       A14     2       D13
F           3       B16     1       A15     2       D14

 B1          1.38931818
 B2          3.57257086
 B3          1.44300333
 B4          1.38633975
 B5          1.09696242
 B6          1.08616037
 B7          1.09301289
 B8          1.08775463
 B9          1.08354427
 B10         1.08194516
 B11         1.46897096
 B12         1.08941611
 B13         1.38821308
 B14         1.08745066
 B15         1.10000000
 B16         1.38182634
 A1         84.36722632
 A2        128.54463192
```

A3	127.04936223
A4	88.37544665
A5	116.36064870
A6	114.96424964
A7	113.59375402
A8	118.21908682
A9	121.65629451
A10	124.67389265
A11	112.01290468
A12	131.59742232
A13	109.82514420
A14	82.56427088
A15	152.40874253
D1	8.92370307
D2	-71.42384335
D3	-76.85581223
D4	157.96204463
D5	150.92134240
D6	138.78523350
D7	-159.61008530
D8	-13.58143970
D9	12.45003867
D10	171.96615177
D11	19.19791110
D12	151.00922797
D13	21.94381944
D14	149.61260391

All the inputs in this study were put in Cartesian coordinates and necessary sections supplied as per the above example.

3.3.0 Execution of the Job

This was done by using the appropriate route section command. The route commands for different jobs are described below.

3.3.1 Input for Geometry Optimizations and Frequency Jobs

The geometry optimization and frequency calculations were executed simultaneously. The following route section command was used in all those calculations.

```
# B3LYP/6-31+G(d) opt freq
```

3.3.2 Input for Locating Transition Structures

The following route section commands were used to located transition state:

```
# B3LYP/6-31+G(d)   opt=(ts,noeigentest,calcfc)   freq
```

For gas phase systems

- ts is the command for transition sate search
- NoEigenTest suppresses testing the curvature in Berny optimizations.
- CalcFC Specifies that the force constants be computed at the first point.
- freq command for frequency calculations

```
# B3LYP/6-31+G(d) opt=(calcfc,ts,noeigentest) freq
scrf=(iefpcm,read,solvent=dichloromethane)
```

For dichloromethane solvents systems

The other terms are as defined for gas phase.

- Iefpcm indicate that the integral equation formalism continuum model solvent method was used.
- solvent=dichloromethane indicate the solvent used was dichloromethane, with dielectric constant ε=8.93
- Read, this command request to read the additional parameters from the input stream

The following additional information was added after molecule specification.

RADII=UAHF
SCFVAC
TSARE=0.4

- RADII=UAHF command the use of the United Atom Topological Model applied on radii optimized for the specified level.
- SCFVAC Performs the gas phase calculation before that in solution.

- TSARE Set the average area of the tesserae generated on each sphere in the cavity surface, in units of $Å^2$ (*area*=0.4).

```
# B3LYP/6-31+G(d) opt=(calcfc,ts,noeigentest) freq
scrf=(iefpcm,read,solvent=acetone)
For acetone solvents systems
```

Definitions as for the above, except the solvent is acetone with dielectric constant ε=20.7

3.4.0 Locating Results in Gaussian 03 output

Gaussian output files were opened by a graphical user inter-phase program, GaussView to get the output structures and animate them where necessary. However, output files were also opened in notepad or word document. The files run from few to hundreds of pages. Few sections that are pertinent to this work will be discussed.

3.4.1 Locating the Charge Distribution in Gaussian 03 Output

Natural population analysis was carried out in terms of localized electron-pair "bonding" units. Here are the charges computed by natural population analysis (the essential output is extracted). The scheme assigns charges very differently, placing most of the negative charges on one carbon atom. Its more detailed analysis also includes the number of core electrons, valence electrons and Rydberg electrons located in diffuse orbitals. It also partitions the charges on each atom among the atomic orbitals. Here is the output for 7-flouro-1,3,7-heptatriene.

```
Summary of Natural Population Analysis:

                                     Natural Population
               Natural  -----------------------------------------------
   Atom  No    Charge         Core      Valence    Rydberg      Total
 ------------------------------------------------------------------------
```

```
      C    1   -0.24000      1.99909     4.22460    0.01631     6.24000
      C    2   -0.24722      1.99908     4.23134    0.01679     6.24722
      C    3   -0.02687      1.99911     4.00849    0.01927     6.02687
      C    4   -0.27174      1.99914     4.25510    0.01750     6.27174
      C    5   -0.41733      1.99917     4.40391    0.01425     6.41733
      H    6    0.22153      0.00000     0.77721    0.00126     0.77847
      H    7    0.24394      0.00000     0.75485    0.00121     0.75606
      H    8    0.24280      0.00000     0.75614    0.00106     0.75720
      H    9    0.23847      0.00000     0.76042    0.00111     0.76153
      H   10    0.22822      0.00000     0.77104    0.00074     0.77178
      H   11    0.22479      0.00000     0.77412    0.00109     0.77521
      C   12   -0.26094      1.99906     4.24510    0.01678     6.26094
      H   13    0.24583      0.00000     0.75298    0.00119     0.75417
      C   14   -0.24360      1.99907     4.22796    0.01657     6.24360
      H   15    0.24662      0.00000     0.75238    0.00100     0.75338
      H   16    0.22046      0.00000     0.77795    0.00159     0.77954
      F   17   -0.40497      1.99996     7.39598    0.00903     9.40497
 =======================================================================
   * Total *    0.00000     15.99368    43.86959    0.13673    60.00000

                                Natural Population
 --------------------------------------------------------
   Core                      15.99368 ( 99.9605% of  16)
   Valence                   43.86959 ( 99.7036% of  44)
   Natural Minimal Basis     59.86327 ( 99.7721% of  60)
   Natural Rydberg Basis      0.13673 (  0.2279% of  60)
 --------------------------------------------------------

    Atom  No          Natural Electron Configuration
 ----------------------------------------------------------------------------
--
      C    1      [core]2S( 0.97)2p( 3.25)4p( 0.01)
      C    2      [core]2S( 0.97)2p( 3.26)4p( 0.01)
      C    3      [core]2S( 1.04)2p( 2.96)3d( 0.01)4p( 0.01)
      C    4      [core]2S( 0.99)2p( 3.27)4p( 0.01)
      C    5      [core]2S( 1.07)2p( 3.34)4p( 0.01)
      H    6            1S( 0.78)
      H    7            1S( 0.75)
      H    8            1S( 0.76)
      H    9            1S( 0.76)
      H   10            1S( 0.77)
      H   11            1S( 0.77)
      C   12      [core]2S( 0.97)2p( 3.27)4p( 0.01)
      H   13            1S( 0.75)
      C   14      [core]2S( 0.99)2p( 3.23)4p( 0.01)
      H   15            1S( 0.75)
      H   16            1S( 0.78)
      F   17      [core]2S( 1.86)2p( 5.54)
```

3.4.2 Locating the Molecular orbitals and energies in Gaussian 03 output

The Pop=Reg keyword in the route section requested data about molecular orbitals be included in the output. They appear at the beginning of the population analysis section. Below is the relevant part of the output for 7-flouro-1,3,7-heptatriene.

```
   Molecular Orbital Coefficients
                          26        27        28        29        30
                        (A)--O    (A)--O    (A)--O    (A)--O    (A)--O
   EIGENVALUES --     -0.35173  -0.34616  -0.32697  -0.28687  -0.23573
 1 1   C  1S          -0.00273  -0.00662   0.01326  -0.00682  -0.00145
 2        2S           0.00869   0.01535  -0.02739   0.01606   0.00269
 3        2PX         -0.10912  -0.18129  -0.11893  -0.06458  -0.15219
 4        2PY         -0.11511  -0.01170  -0.03957  -0.10979  -0.02107
 5        2PZ          0.03241   0.00752  -0.18001  -0.10790  -0.22243
 6        3S           0.00666   0.03473  -0.06856   0.03974   0.00113
 7        3PX         -0.04565  -0.08747  -0.08388  -0.05963  -0.12238
 8        3PY         -0.04713  -0.00484  -0.01093  -0.05153  -0.00863
 9        3PZ          0.00235  -0.00526  -0.09026  -0.05731  -0.14627
10        4S           0.32930  -0.03640   0.18570   0.24617  -0.20954


                          31        32        33        34        35
                        (A)--V    (A)--V    (A)--V    (A)--V    (A)--V
   EIGENVALUES --     -0.06354  -0.00592   0.00013   0.01499   0.01829
 1 1   C  1S           0.00564  -0.00153  -0.02890   0.00798   0.00458
 2        2S          -0.01417   0.01305   0.07736  -0.03348  -0.03069
 3        2PX          0.15435   0.04967   0.03995  -0.00755  -0.02275
 4        2PY          0.05945   0.04801   0.07182  -0.05513  -0.07903
 5        2PZ          0.22006   0.08729  -0.02160   0.02577   0.02075
 6        3S          -0.04727  -0.06330   0.23367   0.01594   0.06755
 7        3PX          0.17829   0.00693   0.07824   0.03781  -0.04336
 8        3PY          0.03588   0.12342   0.06592  -0.07972  -0.11703
 9        3PZ          0.21101   0.13011  -0.04554  -0.02190   0.04430
10        4S          -0.21305   0.15786   2.59868   3.02342  -1.17296
11        4PX          0.27981  -0.22743  -0.38168  -0.23752  -0.12661
```

The atomic contributions for each atom in the molecule are given for each molecular orbital, numbered in order of increasing energy (the MO's energy is given in the row labeled EIGENVALUES preceding the orbital coefficients). The symmetry of the orbital and whether it is an occupied orbital or a virtual (unoccupied) orbital appears immediately under the orbital number.

The highest occupied molecular orbital (HOMO) and the lowest unoccupied molecular orbital (LUMO) may be identified by finding the point where the occupied/virtual code letter in the symmetry designation changes from O to V.

For 7-flouro-1,3,7-heptatriene, molecular orbital number 30 is the HOMO, and molecular orbital number 31 is the LUMO. Figure 4.1.8 (labeled as it appear in chapter 4) show the HOMO and LUMO of 7-flouro-1,3,7-heptatriene.

Figure 4.1.8: The Homo (left, E=-235 Hartree) and the Lumo (right, E=-063 Hartree) of the 7-flouro-1,3,7-heptatriene

3.4.3 Locating the Thermochemical Parameters in Gaussian 03 Output

Gaussian predicts various important thermodynamic quantities at the specified temperatures and pressure, including the thermal energy correction, heat capacity and entropy. These items are broken down into their source component in the output. Here is the output for 7-flouro-1,3,7-heptatriene (Reactant).

	E (Thermal) KCal/Mol	CV Cal/Mol-Kelvin	S Cal/Mol-Kelvin
Total	93.480	30.609	91.805
Electronic	0.000	0.000	0.000
Translational	0.889	2.981	40.058
Rotational	0.889	2.981	28.788
Vibrational	91.703	24.647	22.960

Here is the output for 7-flouro-1,3,7-heptatriene (Transition Structure).

	E (Thermal) KCal/Mol	CV Cal/Mol-Kelvin	S Cal/Mol-Kelvin
Total	90.317	28.086	83.310
Electronic	0.000	0.000	0.000
Translational	0.889	2.981	40.058

Rotational	0.889	2.981	28.550
Vibrational	88.539	22.124	14.702

Here is the output for 1-flouro-1,3,7-heptatriene (Product)

	E (Thermal) KCal/Mol	CV Cal/Mol-Kelvin	S Cal/Mol-Kelvin
Total	93.314	31.164	92.407
Electronic	0.000	0.000	0.000
Translational	0.889	2.981	40.058
Rotational	0.889	2.981	28.787
Vibrational	91.537	25.202	23.562
Vibration 1	0.598	1.968	4.107

Gaussian also predicts the zero-point energy and absolute enthalpy and Gibbs free energies. Here is the zero-point energy and thermal corrected properties output from frequency calculation for 7-flouro-1,3,7-heptatriene (Reactant).

Zero-point correction=	0.140292 (Hartree/Particle)	ZPE
Thermal correction to Energy=	0.148970	
Thermal correction to Enthalpy=	0.149914	
Thermal correction to Gibbs Free Energy=	0.106294	
Sum of electronic and zero-point Energies=	-371.808540	$E_0=E_{elec}+ZPE$
Sum of electronic and thermal Energies=	-371.799862	$E=E_0+E_{vib}+E_{rot}+E_{transl}$
Sum of electronic and thermal Enthalpies=	-371.798918	H=E+RT
Sum of electronic and thermal Free Energies=	-371.842537	G=H-TS

Here is the zero-point energy and thermal corrected properties output from frequency calculation for transition structure of 7-flouro-1,3,7-heptatriene (TS).

Zero-point correction=	0.136711 (Hartree/Particle)	ZPE
Thermal correction to Energy=	0.143929	
Thermal correction to Enthalpy=	0.144873	
Thermal correction to Gibbs Free Energy=	0.105290	
Sum of electronic and zero-point Energies=	-371.783913	$E_0=E_{elec}+ZPE$
Sum of electronic and thermal Energies=	-371.776695	$E=E_0+E_{vib}+E_{rot}+E_{transl}$
Sum of electronic and thermal Enthalpies=	-371.775751	H=E+RT
Sum of electronic and thermal Free Energies=	-371.815334	G=H-TS

Here is the zero-point energy and thermal corrected properties output from frequency calculation for transition structure of 1-flouro-1,3,7-heptatriene (Product).

Zero-point correction=	0.139820 (Hartree/Particle)	ZPE
Thermal correction to Energy=	0.148705	
Thermal correction to Enthalpy=	0.149650	
Thermal correction to Gibbs Free Energy=	0.105744	
Sum of electronic and zero-point Energies=	-371.812952	$E_0=E_{elec}+ZPE$
Sum of electronic and thermal Energies=	-371.804067	$E=E_0+E_{vib}+E_{rot}+E_{transl}$
Sum of electronic and thermal Enthalpies=	-371.803122	H=E+RT
Sum of electronic and thermal Free Energies=	-371.847028	G=H-TS

The raw zero-point energy and thermal energy corrections are listed first, followed by the predicted energy of the system taking them into account. All values are in Hartrees.

The thermal energies for the systems studied are listed in Appendix I:

Table A-1 SI for [1,7]-sigmatropic hydrogen shift.

Table A-2 SI for esterification of acetyl chloride.

Table A-3 SI for acid-catalyzed esterification of carboxylic acids.

3.4.5 Locating the Transition Structures in Gaussian 03 Output

Optimizations to the transition states were done. Frequency calculations on the optimized structures were done to confirm that they were first-order saddle point (with only one imaginary frequency). Finally the IRC calculations were done to verify that the transition structures do connect the reactants and the products of the desired reaction.

3.5.0 Examining and Interpreting the Output

The outputs were visualized using GaussView. The relevant sections of the output file were extracted and interpreted individually, as illustrated in various sections.

3.5.1 Computing Thermochemical Parameters of Reactions

Thermochemical Parameters were calculated using the following general formula.

Parameters of Reactions =(Parameters of products)-(Parameters of Reactants)

In this example:

Enthalpy of reaction, (ΔH)

ΔH= -371.803122-(-371.798918)= -0.004491 Hartree
= -0.004491x627.5095 kcal/mol
= -2.64 kcal/mol

Free energy of reaction, (ΔG)

ΔG=-371.847028-(-371.842537)= -0.004491 Hartree
= -0.004491x627.5095 kcal/mol
= -2.818145165 kcal/mol

Entropy of reaction, (ΔS)

ΔS=92.407-91.805= 0.602 cal/mol-Kelvin

The calculated thermodynamic parameters tables presented in chapter four were calculated as illustrated above.

3.5.2 Predicting the Activation Parameters

Activation parameters were calculated using the following general formula.

Activation parameters=(Parameters of Transition Structure)-(Parameters of Reactants)

In this example:

Activation enthalpy, ($\Delta H^{\ddagger}$)

$\Delta H^{\ddagger}$=-371.775751-(-371.798918)= 0.023167 Hartree
=0.023167x627.5095 kcal/mol
=14.54 kcal/mol

Activation free energy, ($\Delta G^{\ddagger}$)

$\Delta G^{\ddagger}$=-371.815334-(-371.842537)= 0.027203 Hartree
=0.027203 x627.5095 kcal/mol
=17.07 kcal/mol

Activation entropy, ($\Delta S^{\ddagger}$)

$\Delta S^{\ddagger}$=83.310-91.805
=-8.495 cal/mol-Kelvin

The calculated thermodynamic parameters tables presented in results and discussion were calculated as illustrated above.

The next chapter presents the results and discussion of the systems studied.

CHAPTER FOUR

4 RESULTS AND DISCUSSION

Section 4.1 gives the results for [1,7] Sigmatropic Hydrogen Shift in Z,Z-1,3,5-Heptatriene Systems (as indicated in Fig**. 2.19.1**), section 4.2 the results for esterification of acetyl chloride with methanol (as indicated in Scheme **2.19.1**) and section 4.3 acid-catalyzed esterification (as indicated in Scheme **2.19.2**).

The raw thermochemical data are presented in Appendix **1**. The accompanying CD (Appendix **2**) contains the input and output files. The geometries of the structures can be viewed by using the GaussView program.

The colour codes used throughout the text are: the black, grey (small), red, green, deep blue and light blue balls are carbon, hydrogen, oxygen, chlorine, nitrogen, and fluorine atoms, respectively. For molecular orbital (LUMO and HOMO) the two isosurfaces colored red and green represent alpha and beta orbitals, respectively, as calculated. The numbering of the structures is as in Figure **2.19.1.**

4.1.0 [1,7] Sigmatropic Hydrogen Shift in Z,Z-1,3,5-Heptatriene Systems

4.1.1 The rearrangement of 1,3,5- heptatriene (parent) system

Although the results of B3LYP/6-31g(d,p) calculation of [1,7]-H shift in the parent 1,3,5-heptatriene **1** have previously been published (Hess, 2001; Mousavipour, *et al*., 2007), some issues pertinent to this study will be addressed. The results for the degenerate rearrangement

of the unsubstituted systems are similar to previous reported calculations in previtamin D – vitamin D interconversion.

The optimized geometries of the reactant (Z,Z-1,3,5-heptatriene) and the corresponding transition state treated at the B3LYP/6-21+g(d) are shown in Figure 4.1.1.

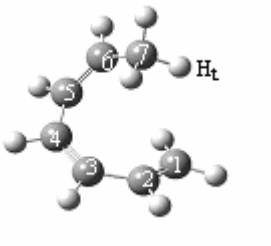

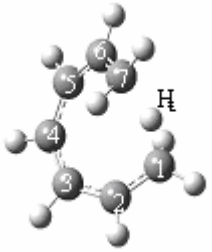

C(7)-Ht=1.1015
C(1)-Ht=2.7739
C(1)-C(2)=1.3451
C(2)-C(3)=1.4661
C(7)-Ht-C(1)=109.95

1

C(7)-Ht=1.37112
C(1)-Ht=1.3712
C(1)-C(2)=1.4135
C(2)-C(3)=1.3986
C(7)-Ht-C(1)=151.07

1‡

Figure 4.1.1: Optimized structures of parent *cis* heptatriene (left) and the [1,7]-H shift transition structure (right). Some selected bond lengths (in Å) and angles (in deg).

The transition state, a Hückel (4n) π-electron array, has the C_s symmetry and an antarafacial topology predicted by Woodward and Hoffmann (Woodward and Hoffmann, 1969). An IRC connects this transition state to a local minimum *cis* heptatriene. However, the global minimum is a *trans* conformation and according to the Curtin-Hammett principle the *trans* C_s conformation must be taken into account for comparison with experiment, as was pointed out by Carpenter . in another density functional analysis of pericyclic reactions (Carpenter and Sosa, 1994).

The activation energy (E_a) for this transformation was found to be 15.35 kcal mol^{-1} from the cissoids conformation, but 20.49 kcal mol^{-1} from *trans*-heptatriene, close to the experimental

value of 20.9 kcal mol^{-1} (Havinga and Schlatmann, 1961). It was therefore concluded that the B3LYP/6-31+G(d) method yields satisfactory results for this reaction. The negative actvation entropy, -8.23 cal/$mol^{-1}K^{-1}$ indicate a more odered transition state. For the study of the following analogues, the activation energy will be given relative to the *cis*-reactant for convenience.

The imaginary frequency at the transition state reflects the simultaneous breaking of C(7)-Ht bond and formation of C(1)-Ht bond. At transition state C(1)-Ht is 1.3712 Å and C(7)-Ht is 1.3711 Å, an indication of a symmetrical transition. The transition structure has two double bonds having the necessary *cisoid* configuration. The sharpness of the potential energy surface in the region is manifested in the high imaginary frequency of transition state (1361 icm^{-1}).

In sigmatropic reactions, a σ-bond (in other words a substituent) moves across a conjugated system to a new site. For [1,7]-H shift, C-Ht σ-bond moves across the π-orbitals of the triene system. From FMO theory, the interaction involves the interaction of the HOMO of the nucleophile and the LUMO of the electrophile. In this reaction, the interaction of the HOMO of the σ-bond and the LUMO of the triene is bonding for the hydrogen to shift in antarafacial manner. HOMO-LUMO interactions are discussed for each reaction.

The HOMO and LUMO of the parent molecule are shown in figure **4.1.2.** The HOMO of the reactant, shown on the left in figure 4.1.2, gives a weak interaction between the prototropic proton (H_t) and the bond of C=C.

Figure 4.1.2: The HOMO (left) and the LUMO of the parent Z,Z-1,3,5-heptatriene.

In an attempt to establish the mechanism of rate enhancement or retardation by substituent groups, the systems in Figure **2.19.1** were studied and the calculated activation parameters are summarized in table **4.1.1.**

Table 4.1.1: Calculated thermodynamic parameters for [1,7]-H shift in Z,Z-1,3,5-heptatriene systems-gas phase.

Reaction	$\Delta G^{\ddagger}$ /kcal mol^{-1}	$\Delta H^{\ddagger}$ /kcal mol^{-1}	$\Delta S^{\ddagger}$ /cal mol^{-1}K^{-1}	E_a /kcal mol^{-1}
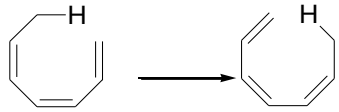	17.22	14.76	-8.23	15.35
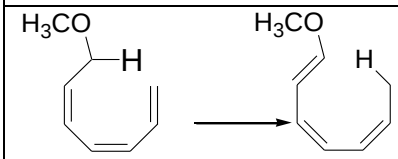	14.35	12.10	-7.57	12.69
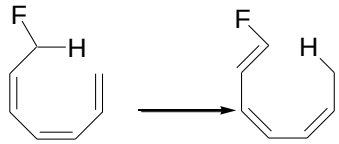	17.07	14.54	-8.50	15.13
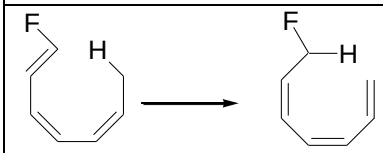	*19.89*	*17.18*	*-9.10*	*17.77*
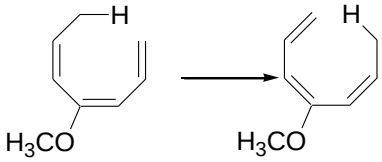	18.32	15.06	-11.04	15.65

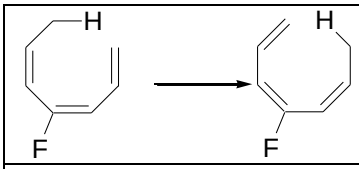	17.50	14.94	-8.56	15.53
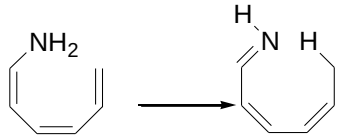	12.82	11.20	-5.43	11.79
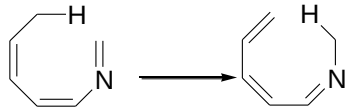	20.11	17.27	-9.53	17.86
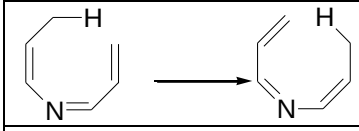	25.24	22.35	-9.69	22.94
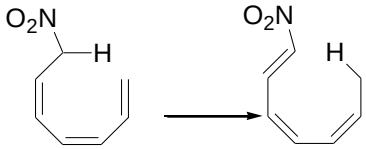	14.65	11.67	-10.02	12.26
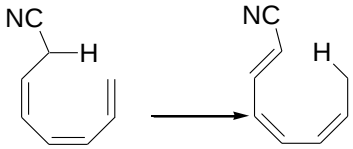	14.11	11.55	-8.61	12.14
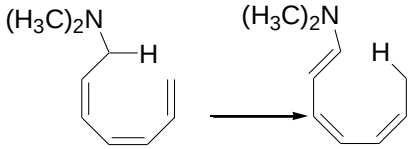	14.35	12.03	-7.78	12.63

Unless noted otherwise, all results in the following sections refer to B3LYP/6-31+G(d).

To find the contribution of the Coulombic forces, the total electron population on each atom was calculated by NBO methods. The NBO calculations are presented in table **4.1.2**. The overall electron deficiency is seen concentrated on Ht, where the electron population is lowest, and therefore it is here that the nucleophile will attack. The overall excess of electrons is again concentrated on C(1), and therefore it is here the electrophile will attack. Thus, as the reaction takes place, the charge-charge attraction of C(1) and Ht will have little nucleophilic or electrophilic character. Each reaction is discussed on its own.

Table 4.1.2: Calculated Natural Bond Orbital (NBO) charges (B3LYP/6-31+G(d)) on carbon atoms of the triene systems and migrating H on studied structures[a].

Structure	C(1)	C(2) or N(2)	C(3)	C(4) or (N4)	C(5)	C(6)	C(7)	Ht
Parent	-0.4167	-0.2694	-0.2574	-0.2307	-0.2836	-0.1912	-0.7262	0.2505
7-methoxy	-0.4208	-0.2711	-0.2548	-0.2337	-0.2738	-0.2067	-0.1417	0.2183
7-flouro	-0.4173	-0.2717	-0.2472	-0.2400	-0.2609	-0.2436	-0.2436	0.2205
4-methoxy	-0.4367	-0.2582	-0.3097	0.3064	-0.3150	-0.1755	-0.7277	0.2559
4-fluoro	-0.4261	-0.2612	-0.3294	0.4082	-0.3229	-0.1639	-0.7292	0.2560
7-nitro	-0.4167	-0.2729	-0.2441	-0.2434	-0.2474	-0.2386	-0.3398	0.2781
7-cyano	-0.4195	-0.2696	-0.2475	-0.2400	-0.2576	-0.1967	-0.6026	0.2941
7-amine	-0.4806	-0.2701	-0.3028	-0.2157	-0.3899	0.0081	-0.8372	0.4177
2-imine	-0.0721	-0.4415	-0.0579	-0.3018	-0.2812	-0.2044	-0.7259	0.2474
4-imine	-0.3925	-0.3056	0.0561	-0.4480	-0.0904	-0.1982	-0.7286	0.2472

[a]numbering as shown below.

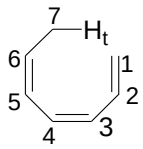

The chemical reactivity (activation energy) has been discussed in terms of HOMO-LUMO interaction, Coulombic interaction, strength of bond being made or broken and loss of conjugation for each substituent or heteroatom.

4.1.2 Electron-Donating Substituents

Methoxy analogue **2** and **4** (see Figure **2.19.1)** were studied, which withdraw electrons by induction and allows participation of the free electron pairs on the oxygen by resonance, thus increasing the electron density in the triene system. In **2** the degeneracy of transformation is broken; the effect on the activation energy decrease of 1.66 kcal/mol is significant as shown

in Figure 4.1.3. The activation entropy change by 0.66 cal $mol^{-1}K^{-1}$ while activation enthalpy decreases`by 0.66 kcal/mol.

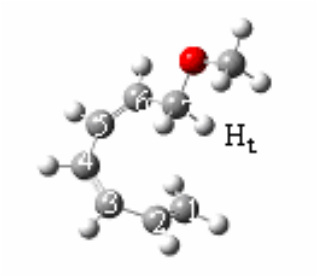

C(7)-Ht=1.10776
C(1)-Ht=2.62806
C(1)-C(2)=1.34484
C(2)-C(3)=1.46631
C(7)-Ht-C(1)= 118.17

2

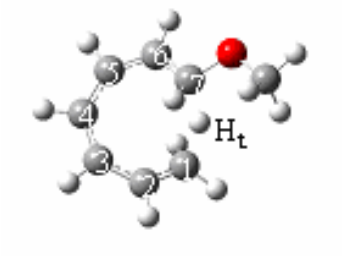

C(7)-Ht=1.35322
C(1)-Ht=1.39796
C(1)-C(2)=1.40833
C(2)-C(3)= 1.40386
C(7)-Ht-C(1)= 151.53

2‡

Figure 4.1.3: Optimized structures of 7-methoxy parent (left) and the TS (right). Some selected bond lengths (in Å) and angles (in deg).

The imaginary frequency at the transition state reflects the simultaneous breaking of C(7)-Ht bond and formation of C(1)-Ht bond. At transition state C(1)-Ht is 1.39796 Å and C(7)-Ht is 1.35322 Å, an indication of an early transition state. The sharpness of the potential energy surface in the region is manifested in the high imaginary frequency of transition state (1332 icm^{-1}).

The decrease in the activation energy can be rationalized by the analysis of the molecular orbitals of the reactant, giving a measure of the interaction between LUMO and HOMO. The HOMO and the LUMO of the reactant, shown on the left in figure 4.1.4, gives a strong interaction between the prototropic proton and the bond of C=C.

Figure 4.1.4: The HOMO (left) and the LUMO (right) of the 7-methoxy parent.

NBO charge distribution (Table 4.1.3) show reduction of the electron density around C(7), thus more electronegative methoxy-substituent tend to destabilize the C(7)-Ht, on the other hand, there is an increase of electron density in C(1), this effectively lower the activation energy. This lowers the activation energy, and hence, makes it more reactive than the parent.

In **4** where the degeneracy of transformation is not broken, the effect on the activation energy with an increase of 0.30 kcal/mol is small as shown in Figure 4.1.4. The activation entropy increase in magnititude by 2.81 cal mol^{-1} K^{-1}, while activation entropy increases by 1.30 kcal/mol. This indicates that the substituent effects in the reactant and the transition structure are comparable.

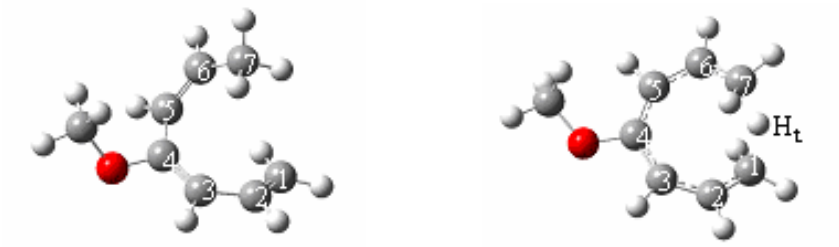

C(7)-Ht=1.10058	C(7)-Ht=1.36402
C(1)-Ht=2.89427	C(1)-Ht=1.39093
C(1)-C(2)=1.34600	C(1)-C(2)=1.41188
C(3)-C(4)= 1.46226	C(3)-C(4)=1.39492
C(7)-Ht-C(1)= 108.24	C(7)-Ht-C(1)=151.34222
4	**4‡**

Figure 4.1.5: Optimized structures of 4-methoxy parent (left)and the TS (right). Some selected bond lengths (in Å) and angles (in deg).

There is increase of electron density in C(1) and C(7). The HOMO –LUMO are shown in Figure 4.1.6.

Figure 4.1.6: The HOMO (left) and the LUMO (right) of the 4-methoxy parent.

The effect of electron-donating substituents on the reaction was also studied for the analogues **3** and **5** shown in Figure 4.1.5. In **3** the degeneracy of transformation is broken.

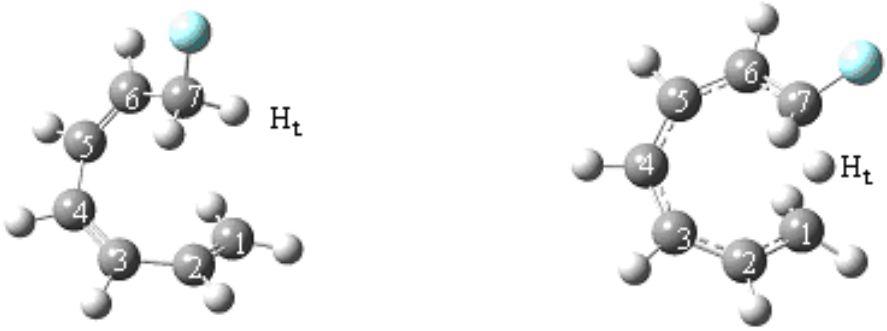

C(7)-Ht=1.09857
C(1)-Ht=2.77150
C(1)-C(2)=1.34378
C(2)-C(3)=1.46838
C(7)-Ht-C(1)=111.54

3

C(7)-Ht=1.36779
C(1)-Ht=1.36516
C(1)-C(2)=1.41270
C(2)-C(3)= 1.39942
C(7)-Ht-C(1)= 151.79

3‡

Figure 4.1.7: Optimized structures of 7-fluoro parent (left) and the TS (right). Some selected bond lengths (in Å) and angles (in deg).

The activation energy decreases by 0.26 kcal/mol relative the parent reaction. The activation enthalpy decreases by 0.22 kcal/mol while the activation entropy increases in magnitude by 0.27 cal mol^{-1} K^{-1}. The inductive effect and mesomeric effect cancel each other. The HOMO

–LUMO are shown in Figure 4.1.8. There is strong interaction between the HOMO and LUMO.

Figure 4.1.8: The HOMO (left) and the LUMO (right) of the 7-fluoro parent.

The following reaction (Scheme 4.1.9**)** was also considered to study the reversibility of the reaction,

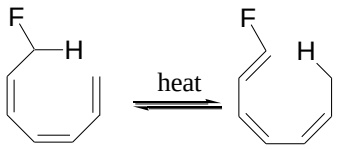

3 3b

Scheme 4.1.9: The reversibility of the reaction.

The activation parameters for the forward reaction is $\Delta G^{\ddagger}$=17.07 kcal mol^{-1}, $\Delta H^{\ddagger}$= 14.54 kcal/mol, $\Delta S^{\ddagger}$=-8.50 cal mol^{-1} K^{-1} while the backward reaction $\Delta G^{\ddagger}$=19.89 kcal mol^{-1}, $\Delta H^{\ddagger}$= 17.18 kcal/mol $\Delta S^{\ddagger}$=-9.10 cal mol^{-1} K^{-1}. For the reverse reaction, the fluorine in C(1) decreases the electron density, thereby making it less nucleophilic, hence the equilibrium lies far to the right. Though the reaction may not be reversible, using the relation, $\Delta G^{\ddagger} = -RT \ln K^{\ddagger}$, the product can be determined.

Substitution of fluorine at C(4) in structure **5**, increases the activation energy by 0.18 kcal/mol. The fluorine increase the electron density on both C(1) and C(7). The two effects nearly cancel each other.

C(7)-Ht=1.10087
C(1)-Ht=2.82450
C(1)-C(2)=1.34465
C(2)-C(3)=1.46314
C(7)-Ht-C(1)=109.03235

5

C(7)-Ht=1.37367
C(1)-Ht=1.37367
C(1)-C(2)=1.41256
C(2)-C(3)=1.39667
C(7)-Ht-C(1)=142.08000

5‡

Figure 4.1.9: Optimized structures of 4-fluoro parent (left) and the TS (right). Some selected bond lengths (in Å) and angles (in deg).

The HOMO –LUMO are shown in Figure 4.1.10., There is a stron interaction between HOMO and LUMO.

Figure 4.1.10: The Homo (left) and the Lumo of the 4-fluoro parent.

4.1.3 Electron-Withdrawing Substituents

The effect of electron-withdrawing substituents on the reaction was studied for the analogues **10** and **11** shown in Figure 4.1.11 and 4.1.13.

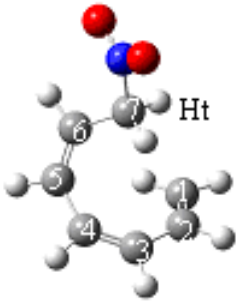

C(7)-Ht=1.09893
C(1)-Ht=2.79048
C(1)-C(2)=1.34412
C(2)-C(3)=1.46815
C(7)-Ht-C(1)=110.12152

11

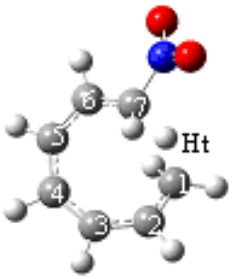

C(7)-Ht=1.36004
C(1)-Ht=1.38296
C(1)-C(2)=1.40685
C(2)-C(3)= 1.40495
C(7)-Ht-C(1)= 151.00984

11‡

Figure 4.1.11: Optimized structures of 7-nitro parent (left) and the TS (right). Some selected bond lengths (in Å) and angles (in deg).

The activation energy decreases by 3.09 kcal/mol relative to the parent reaction. The activation enthalpy decrease by 3.69 3.09 kcal/mol while activation entropy increase in magnitude by 1.79 cal mol^{-1} K^{-1}. There is a notable increase in charge deficiency on Ht, (+ 0.27806), thus destabilizing C(7)-Ht bond. There is an increase in conjugation moving from reactant to product. The HOMO, shows strong interaction with C(1), but surprisingly the LUMO is concentrated on the nitro group (Figure 4.1.12).

Figure 4.1.12: The Homo (left) and the Lumo (right) of the 7-nitro parent.

For the cyano substituent on C(7) the charge deficiency on Ht increases to +0.29409. The activation energy decreases by 3.21 kcal/mol. There is increase in conjugation, moving from reactant to product (Figure 4.1.13).

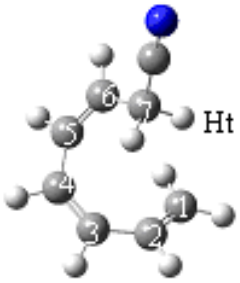

C(7)-Ht=1.10231
C(1)-Ht=2.68614
C(1)-C(2)=1.34458
C(2)-C(3)=1.46711
C(7)-Ht-C(1)=116.51059

10

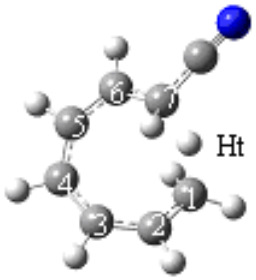

C(7)-Ht=1.35843
C(1)-Ht=1.39227
C(1)-C(2)=1.40512
C(2)-C(3)= 1.40560
C(7)-Ht-C(1)=151.75880

10‡

Figure 4.1.13: Optimized structures of 7-cyano parent (left) and the TS (right). Some selected bond lengths (in Å) and angles (in deg).

The HOMO-LUMO are shown in Figure 4.1.14.

Figure 4.1.14: The Homo (left) and the Lumo (right) of the 7-cyano parent.

The nitro and cyano groups withdraw electrons without any electron donation by resonance, and this effectively decreases the activation energy relative to the parent reaction. There is a notable electron density decrease in Ht (table 4.1.3).

4.1.4 Heteroanalogues

A series of nitrogen analogues have also been studied to clarify the ability of the lone pair to participate in the π electron system and its effect on the transformation. Substituting a nitrogen atom for one of the selected carbons in the chain leads to the four analogues **6-9** studied. **6** can be transformed to **7** via the [1,7] hydrogen shift. The activation energy is calculated to be 11.79 kcal/mol (see Figure 4.1.6). The reaction can be rationalized by

considering the bond dissociation energies (BDE) from the literature. The π bond of C=N is stronger than the π bond of C=C by 10.2 kcal/mol (Cottrell, 1958; Janz, 1967). The BDE of a vinylic C-H bond is 85 kcal/mol (Kerr, 1966), whereas the BDE of a vinylic N-H bond is 92 kcal/mol (Janz, 1967), thus a difference of 7 kcal/mol in favour of the N-H bond. The BDE analysis gives a shift of the equilibrium by 3.2 kcal/mol. Although not all the relevant bonds have been considered in this BDE analysis, the approximated value is in good agreement with the calculated one. The activation energy is lowered by a significant amount due to the involvement of the lone pair of the nitrogen atom in the aromatic π system of the transition structure as shown by the Homo-Lumo analysis, whereas a repulsive n-π interaction prevails in the reactant.

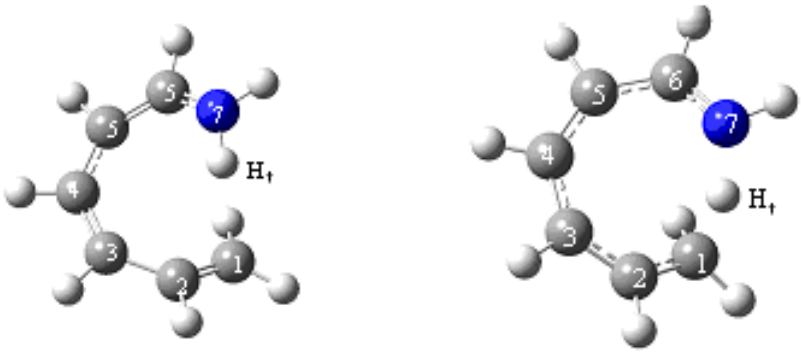

6 **6‡**

Figure 4.1.15: Optimized structures of 7-amine parent (left) and the TS (right). Some selected bond lengths (in Å) and angles (in deg).

The HOMO–LUMO are shown in Figure 4.1.16. There is noted a strong interaction between HOMO and LUMO.

Figure 4.1.16: The Homo (left) and the Lumo (right) of the 7-amine parent.

Substitution of C(2) with N, figure 4.1.17, the activation energy increase by 2.51. The charge in C(1) decrease tremendously to -0.0721, making it less nucleophilic.

C(7)-Ht=1.09999
C(1)-Ht=3.31584
C(1)-N(2)=1.27114
N(2)-C(3)=1.40345
C(7)-Ht-C(1)= 100.05

8

C(7)-Ht=1.37187
C(1)-Ht=1.34122
C(1)-N(2)=1.35461
N(2)-C(3)= 1.33047
C(7)-Ht-C(1)= 150.28

8‡

Figure 4.1.17 Optimized structures of 2-imine parent (left) and the TS (right). Some selected bond lengths (in Å) and angles (in deg).

The HOMO and LUMO are shown in Figure 4.1.18.

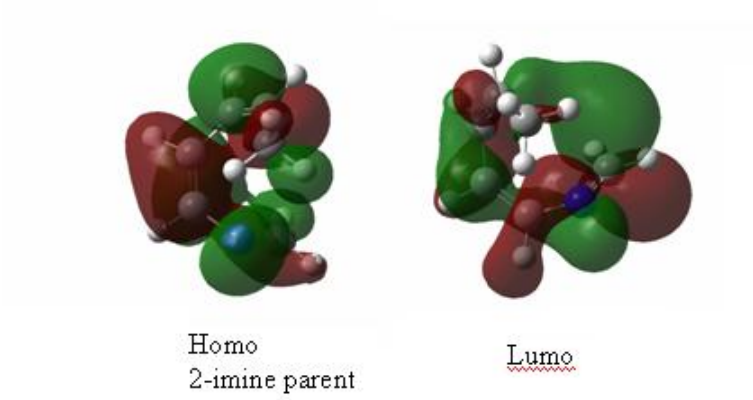

Figure 4.1.18: The Homo (left) and the Lumo (right) of the 2-imine parent.

Substitution of C(4) with N, the activation energy increase by 7.59 kcal/mol. There is a notable charge decrease at C(1) but an increase in C(7), thereby stabilizing C(7)-Ht bond.

C(7)-Ht=1.09968	C(7)-Ht=1.37470
C(1)-Ht=5.80201	C(1)-Ht=1.37470
C(1)-C(2)=1.34383	C(1)-C(2)=1.41273
C(2)-C(3)=1.47558	C(2)-C(3)=1.40351
C(3)-N(4)=1.28845	C(3)-N(4)=1.33479
C(7)-Ht-C(1)=67.39	C(7)-Ht-C(1)=146.28341
9	**9‡**

Figure 4.1.19: Optimized structures of 4-imine parent (left) and the TS (right). Some selected bond lengths (in Å) and angles (in deg).

The HOMO –LUMO are shown in Figure 4.1.20.

Figure 4.1.20: The Homo (left) and the Lumo (right) of the 4-imine parent.

4.1.5 Steric Effects in Sigmatropic Hydrogen Shift in Z,Z-1,3,5-Heptatriene Systems

Transition states with substituents in *endo*-positions with respect to triene systems were located (Table **4.1.3**) in order to study the steric effects. This shows the role of the electrostatic repulsion of the substituent and the triene π system. The substituent toward the triene system into its *endo*- position destabilizes the transition state by about 4.77 and 1.94 kcal/mol for methoxy group and fluorine atom respectively.

Table 4.1.3: Calculated thermodynamic parameters, substituents-*endo* position -gas phase.

Reaction	$\Delta G^{\ddagger}$ /kcal mol^{-1}	$\Delta H^{\ddagger}$ /kcal mol^{-1}	$\Delta S^{\ddagger}$ /cal mol^{-1}K^{-1}	E_a /kcal mol^{-1}
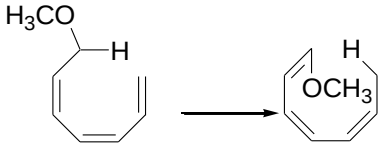	19.09	16.87	-7.44	17.46
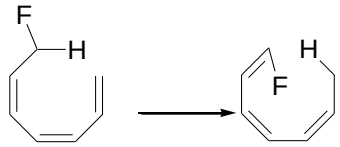	19.35	16.48	-9.66	17.07
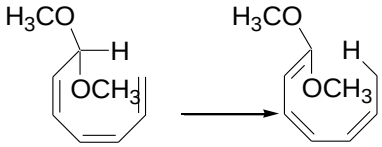	17.10	14.12	-10.00	14.71
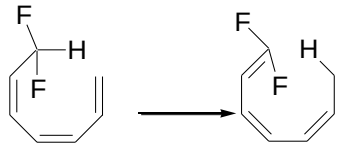	20.64	17.49	-10.55	18.08

4.1.6 Solvent Systems of Sigmatropic Hydrogen Shift in Z,Z-1,3,5-Heptatriene Systems

Solvation models were incorporated in the calculation in an attempt to reproduce and explain the experimental results. The solvation model employed in this study is the Integral Equation Formalism Polarized Continuum Model (IEFPCM) (Cancès and Mennucci, 1998; Cancès, *et al*., 1997; Mennucci, *et al*., 1997). Transition structures of the reaction were located and

optimized at the same level of theory. Two solvents, dichloromethane (non polar) and acetone (polar) were used. Only the parent reaction was studied in the solvent system. The results are presented in Table **4.1.4**

Table 4.1.4: Calculated thermodynamic parameters [1,7]-H shift-solvent phase.

Structure	$\Delta G^{\ddagger}$ /kcal mol^{-1}	$\Delta H^{\ddagger}$ /kcal mol^{-1}	$\Delta S^{\ddagger}$ /cal $mol^{-1}K^{-1}$	E_a /kcal mol^{-1}
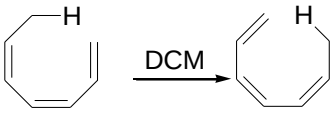	15.15	14.66	-8.35	15.25
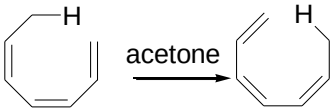	17.15	14.64	-8.40	15.23

In dichloromethane solvent, the activation energy by 0.10 kcal/mol while in acetone decrease by 0.12 kcal/mol. This is in agreement with experimental observations that these reactions are not much affected by solvent.

4.2.0 Esterification

In this study two esterification reactions were analyzed, the results of esterification of acetyl chloride with methanol (methanolysis of acetyl chloride) are given in section 4.2 while those of acid-catalyzed esterification of carboxylic acids with methanol are in section 4.3.

4.2.0 Esterification of Acetyl Chloride with Methanol

4.2.1 Degenerate Chloride Ion Exchange

Degenerate chloride ion exchange has been reported at B3LYP/6-31G(d) (Fox, *et al*., 2004) and has been shown to be concerted without a tetrahedral intermediate. However, in this work, the calculations have been repeated at B3LYP/6-31+G(d), to explain some pertinent aspect that were not addressed in previous reports. At the B3LYP/6-31+G(d) level of the theory the degenerate exchange of Cl^- with CH_3COCl does proceed by a concerted pathway involving π attack with a relatively low activation barrier (8.58 kcal/mol). The out-of-plane S_N2 pathway is a first-order saddle point that has C_s symmetry. The incoming nucleophile and leaving group are each bonded to distinct, ~sp^3 carbon orbitals of the approximate tetrahedral transition state (see Figure 4.2.1). The Cl^- ion attacks within the Bürg-Dunitz trajectory, 111.9˚. The C-Cl bonds are atypically long (2.179 Å), an indication of a loose transition structure. The two chloride atoms deviate from sp^3 with Cl-C-Cl angle of 99.95º.

O(1)-C(2)=1.19192	O(1)-C(2)=1.19453
C(2)-Cl(3)=1.87781	C(2)-Cl(3)=2.17945
C(2)-C(4)=1.48084	C(2)-C(4)=1.51290
C(4)-H(5)=1.12346	C(4)-H(5)= 1.08767
H(5)-Cl(6)=2.26497	H(5)-Cl(6)=2.87748
Cl(6)-H(5)-C(4)= 161.91	Cl(6)-H(5)-C(4)= 79.25
Cl(6)-C(2)-Cl(3)=105.62	Cl(6)-C(2)-Cl(3)= 99.95
Cl(6)-C(2)-O(1)= 119.31	Cl(6)-C(2)-O(1)= 111.86

Figure 4.2.1: Optimized structures of reactive intermediates (left) and TS (right). Some selected bond lengths (in Å) and angles (in deg).

No evidence for the existence of a tetrahedral intermediate was observed. In general, a "concerted" reaction involves two (or more) bond making or breaking processes that occur synchronously as the reaction proceeds. This implies that there is no discrete or discernible intermediates with finite lifetime along the reaction coordinate. The calculated thermodynamic parameters are presented in table 4.2.1.

Table 4.2.1 Calculated thermodynamic parameters-gas phase for degenerate chloride ion exchange[a].

Reaction	$\Delta G^{\ddagger}$ /kcal mol^{-1}	$\Delta H^{\ddagger}$ /kcal mol^{-1}	$\Delta S^{\ddagger}$ /cal mol^{-1}K^{-1}	E_a /kcal mol^{-1}
$CH_3COCl + Cl^- \longrightarrow [H_3C(Cl)(Cl)C{=}O]^{-\ddagger}$	10.35	7.99	-7.95	8.58

[a] All activation parameters are calculated relative to reactive intermediate

4.2.2 Methanolysis of Acetyl Chloride

For the methanolysis of acetyl chloride, a base is normally required to remove the acidic proton of the nucleophilic alcohol. The reaction can possibly proceed via three different reaction pathways. Firstly, a cyclic four and/ or six-membered ring transition state reaction (Jali and Kruger, 2005) and or an acyclic transition state reaction. Below are examples of the acyclic and cyclic four- and six-membered ring transition states studied

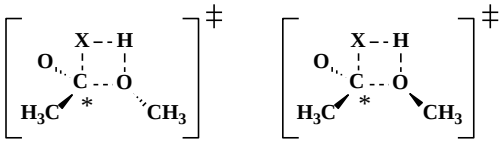

TS-4.1.1- X **TS-4.1.2 -X**

a) One step 4-membered cyclic transition state structures, X=Cl

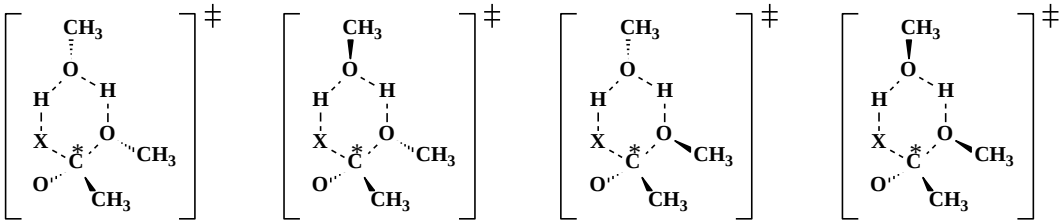

TS-6.1.1-X **TS-6.1.2-X** **TS-6.1.3-X** **TS-6.1.4-X**

b) One step 6-membered cyclic transition state structures, X=Cl

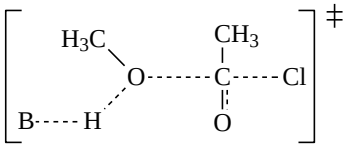

c) acyclic transition state structures proposed by Kevill

Figure 4.2.2: Possible transition states structures studied.

Computational study was done for these conceivable transition structures.

4.2.3 One Step 4-Membered Cyclic Transition State Mechanism

As the alcohol performs a nucleophilic attack on the carboxylic carbonyl, the proton of the incoming alcohol is transferred in a concerted process to the chlorine atom of acetyl chloride. The imaginary frequency (266.024 icm^{-1}) at the transition state reflects the formation of C(2)-O(5) bond and transfer of H(4) to Cl(3). The oxygen atom of the nucleophilic methanol

attacks within the Bürg-Dunitz trajectory, 113.58˚ (Fig 4.2.2). The C-Cl bonds are atypically long (2.53904Å), an indication of a loose transition structure. The oxygen and chloride atoms deviate from sp^3 with O-C-Cl angle of 77.79º.

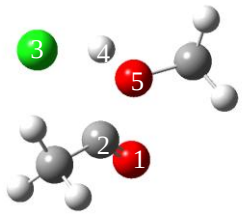

O(1)-C(2)= 1.17181
C(2)-Cl(3)= 2.53904
Cl(3)-H(4)= 1.91098
H(4)-O(5)= 1.02790
O(5)-C(2)-O(1)= 113.57563
O(5)-C(2)-Cl(3)= 77.79329

Figure 4.2.3: Optimized structures of 4-membered cyclic TS. Some selected bond lengths (in Å) and angles (in deg).

The calculated thermodynamic parameters are presented in table 4.2.2. The energy difference is due to steric effect of the methyl group.

Table 4.2.2: Calculated[a] transition state energies for the esterification of acetyl chloride with methanol for one step 4-membered cyclic transition state mechanism.

Structure	$\Delta G^{\ddagger}$ /kcal mol^{-1}	$\Delta H^{\ddagger}$ /kcal mol^{-1}	$\Delta S^{\ddagger}$ /cal $mol^{-1}K^{-1}$	E_a [b] /kcal mol^{-1}	lnA [c]
TS-4.1.1-Cl	28.24	16.26	-40.18	16.85	10.27
TS-4.1.2-Cl	32.94	21.19	-39.39	21.78	10.66

a All activation parameters are calculated as difference between TS and acetyl chloride and methanol

The activation enthalpy of 16.85 kcal/mol is much higher than the reported experimental value 9.25 kcal/mol. This structure is highly strained and does not explain the second order kinetics found from experiment. These confirm theoretically that this mechanism is less likely to occur.

4.2.4 One Step 6-Membered Cyclic Transition State Mechanism

For the concerted 6-membered cyclic transition states, a hydrogen-bonded alcohol molecule mediates the translocation of the proton by the Grotthus-type mechanism (Gutman and Nachliel, 1997). The important role of the second methanol is that it functions as a proton relay station for the proton transfer from the donating oxygen atom of the nucleophilic methanol to the accepting oxygen of the acetic acid or chlorine atom of the acetyl chloride (figure 4.2.4). Furthermore, it may play an important role in reducing the strain energy, since 6-membered cyclic transition state is less strained compared to 4-membered transition one.

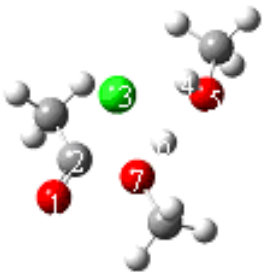

O(1)-C(2)=1.18033
C(2)-Cl(3)=2.47315
Cl(3)-H(4)=2.10384
H(4)-O(5)=0.99608
O(5)-H(6)=1.53912
H(6)-O(7)=1.03427
O(7)-C(2)-O(1)=112.55289
O(7)-C(2)-Cl(3)=92.87164

Figure 4.2.4: Transition- state (TS) structures for TS-6.1.1-Cl.

The imaginary frequency (167.579 icm^{-1}) at the transition state reflects the formation of C(2)-O(7) bond and transfer of H(6) to O(5). The methanol oxygen attacks within the Bürg-Dunitz trajectory, of 112.55˚. The C-Cl bonds are atypically long (2.47315Å), an indication of a loose transition structure. The oxygen and chloride atoms deviate from sp^3 with O-C-Cl angle of 99.87º. The calculated activation parameters are presented in table 4.2.3. The difference in energy could be attributed to steric effects of the methoxy group.

Table 4.2.3: Calculated[a] transition state energies for the esterification of acetyl chloride with methanol for one step 6-membered cyclic transition state mechanism.

Structure	$\Delta G^{\ddagger}$ /kcal mol^{-1}	$\Delta H^{\ddagger}$ /kcal mol^{-1}	$\Delta S^{\ddagger}$ /cal $mol^{-1}K^{-1}$	E_a [b] /kcal mol^{-1}	lnA [c]
TS-6.1.1-Cl	24.97	8.95	-53.71	9.54	3.47
TS-6.1.2-Cl	25.16	9.22	-53.71	9.81	3.37
TS-6.1.3-Cl	27.01	10.43	-55.63	11.02	2.50
TS-6.1.4-Cl	28.88	12.54	-54.81	13.13	2.88

a Energies All activation parameters are calculated as difference between TS and acetyl chloride and two hydrogen bonded methanol

In the 6-membered cyclic transition state mechanism, the ester bond at transition state is shorter than in 4-membered cyclic transition state mechanism. This explains why this mechanism has lower enthalpy of activation ($\Delta H^{\ddagger}$). The distance H(4) and Cl(3) is too large (2.104 Å) for a cyclic transition state, this suggests that the second methanol molecule acts as a base.

Close examination of the reported 6-membered system, shows that indeed, these were not cyclic but acyclic. The transition state could well be represented by the structures shown in Figure 4.2.2(c).

4.2.5 Acyclic Transition State Mechanism

In nonpolar solvent, the base is a second alcohol molecule, while for the polar solvent, the solvent could still act as a base.

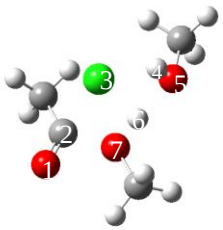

O(1)-C(2)=1.18033
C(2)-Cl(3)=2.47315
Cl(3)-H(4)=2.10384
H(4)-O(5)=0.99608
O(5)-H(6)=1.53912
H(6)-O(7)=1.03427
O(7)-C(2)-O(1)=112.55289
O(7)-C(2)-Cl(3)=92.87164

Figure 4.2.5: Transition- state (TS) structures for second methanol molecule as a base.

The Cl^- ion attacks within the Bürg-Dunitz trajectory, 112.6˚. The C-Cl bonds is atypically long (2.473 Å), an indication of a loose transition structure. The O-C bond is 1.681 Å while the Cl- H bond is 2.104, showing that the proton is not transferred to chlorine atom.

4.2.6 Role of Specific Solvation on Acetyl Chloride Methanolysis/ Hydrolysis

In the presence of a polar solvent, for example acetone or acetonitrile, the solvent molecule may assist as a base and the order with respect to methanol is 1. A mechanism has been proposed in which, for over-all reaction, a first-formed tetrahedral intermediate is deprotonated by either a solvent molecule (second-order kinetics) or a second methanol molecule (third-order kinetics) to give a tetrahedral intermediate which collapses to products.

4.2.7 Base-Catalyzed Acyl Transfer Reactions with Ammonia and Pyridine

Generally a base such as pyridine is added and its function is believed to be to consume the evolved hydrogen chloride. However, when the base is included it appears in the rate equation. This study found that the base assists in the removal of the prototropic proton of

the nucleophilic alcohol. Calculations were done for NH_3 and pyridine as a base and the resulting transition state structures are shown in Figure 4.2.6. These calculations clearly show the function of the base in removing the proton of the nucleophilic methanol.

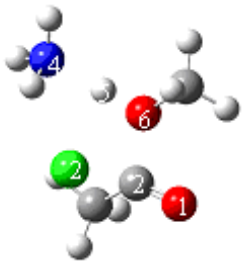

O(1)-C(2)=1.18610
C(2)-Cl(3)=2.39221
Cl(3)-N(4)=3.16202
N(4)-H(5)=1.51905
H(5)-O(6)=1.07717
O(6)-C(2)=1.67050
O(6)-C(2)-O(1)=112.59054
O(6)-C(2)-Cl(3)=93.99374

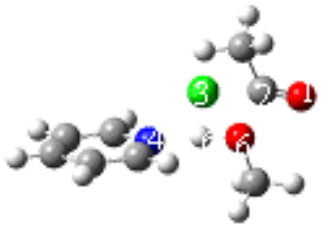

O(1)-C(2)=1.19020
C(2)-Cl(3)=2.41755
Cl(3)-N(4)=3.59053
N(4)-H(5)=1.48778
H(5)-O(6)=1.09113
O(6)-C(2)=1.61337
O(6)-C(2)-O(1)=113.55199
O(6)-C(2)-Cl(3)=92.46758

Figure 4.2.6: Transition state structures (a) NH_3 as base b) Pyridine as base.

The calculated thermodynamic parameters when the base is methanol, ammonia and pyridine are shown in table 4.2.4.

It must be considered how these observations relate to the concerted loose S_N2 transition state (Scheme **2.19.1**) which has been proposed for the methanolysis of the parent compound, acetyl chloride (Kevill and Kim, 1988).

Table 4.2.4: Calculated thermodynamic parameters-gas phase for various bases[a].

Structure	$\Delta G^{\ddagger}$ /kcal mol^{-1}	$\Delta H^{\ddagger}$ /kcal mol^{-1}	$\Delta S^{\ddagger}$ /cal mol^{-1}K^{-1}	E_a /kcal mol^{-1}
$CH_3COCl + 2CH_3OH \rightarrow$ 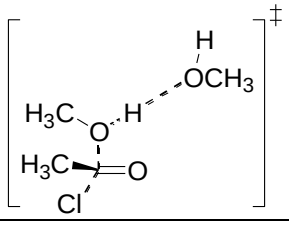	24.97	8.95	-53.71	9.54
$CH_3COCl + CH_3OH + NH_3 \rightarrow$ 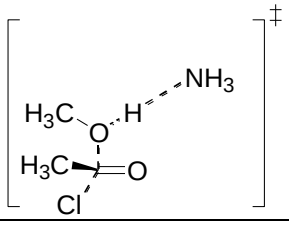	25.92	9.67	-54.50	10.26
$CH_3COCl + CH_3OH + py \rightarrow$ 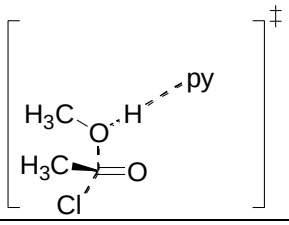	26.65	10.80	-53.16	11.93

[a] All activation parameters calculated relative to acetyl chloride and hydrogen-bonded methanol-base.

The leaving group effects in the present study were investigated along the halogen series, calculations were done for acetyl fluoride and acetyl bromide. The results are presented in table **4.2.5**. The reactivity increases down the group.

Table 4.2.5: Calculated thermodynamic parameters-gas phase for halogen series[a].

Structure	$\Delta G^{\ddagger}$ /kcal mol^{-1}	$\Delta H^{\ddagger}$ /kcal mol^{-1}	$\Delta S^{\ddagger}$ /cal mol^{-1}K^{-1}	E_a /kcal mol^{-1}
$CH_3COF + 2CH_3OH$ 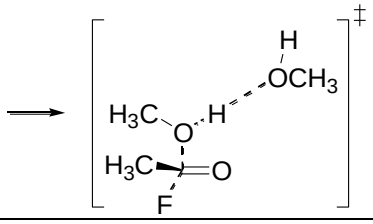	33.68	17.35	-54.75	17.94
$CH_3COCl + 2CH_3OH$ 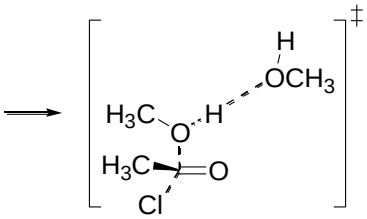	24.97	8.95	-53.71	9.54
$CH_3COBr + 2CH_3OH$ 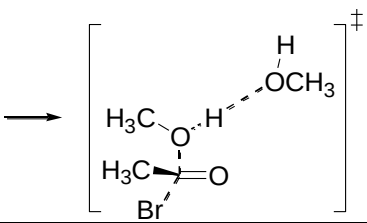	19.04	2.54	-55.36	3.13

[a] All activation parameters calculated relative to acetyl halide and hydrogen-bonded methanol-base.

The results suggest that, the breaking of the bond of the leaving group is a rate-controlling factor as well as the formation of the bond to the attacking nucleophile. Bromide is a better leaving group than chloride and fluoride, while fluoride is not a better leaving group. The results show that the better the leaving group the faster the reaction, which agree with the experimental findings. This can be attributed to the disparity in bond strength.

4.2.8 Solvent Systems in Methanolysis

Solvation models were incorporated in the calculation in an attempt to reproduce and explain the experimental results. The solvation model employed in this study is the Integral Equation Formalism Polarized Continuum Model (IEFPCM). Transition structures of the reaction were located and optimized at the same level of theory. Two solvents dichloromethane (none

polar) and acetone (polar) were used. Attempt to get a transition state in dichloromethane failed, (this was due to choice of basis set- for hf/3-21g, it worked, but not for B3LYP/6-31+G(d)) only the results in acetone are reported here. Only the acetyl chloride with methanol (second methanol molecule as a base) reaction was studied in the solvent system.

Table 4.2.6: Calculated thermodynamic parameters-solvent phase.

Structure	$\Delta G^{\ddagger}$ /kcal mol^{-1}	$\Delta H^{\ddagger}$ /kcal mol^{-1}	$\Delta S^{\ddagger}$ /cal $mol^{-1}K^{-1}$	E_a /kcal mol^{-1}
$CH_3COCl + 2CH_3OH$ Acetone → 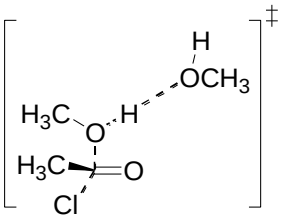	23.29	10.28	-43.61	10.87

Computational results of the esterification of acetyl chloride with methanol are a direct result of the preference for Bürgi-Dunitz trajectories in nucleophilic attack on carbonyl groups.

Nucleophilic substitution, in frontier orbital terms, involves an interaction between the HOMO of the nucleophile and the LUMO of the electrophile (substrate) - a "filled-empty" interaction.

The LUMO of the acetyl chloride is shown in Fig **4.2.7**. This LUMO is almost exclusively the C=O π^* orbital, meaning that the bond that breaks on nucleophilic attack is the C=O double bond. Notice also that the nucleophile must attack at Bürgi-Dunitz trajectory to the plane of the carbonyl.

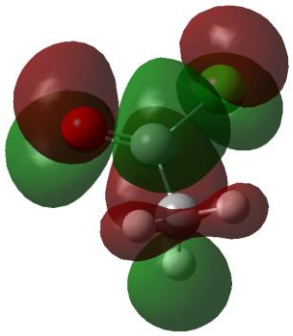

Figure 4.2.7: LUMO for acetyl chloride.

Hence there is no way an attacking nucleophile can break the C-Cl bond directly. In short, a tetrahedral intermediate must form because the orbital construction of the substrate won't permit any other pathway. The concerted mechanism observed can be rationalized by the lifetime of the zwitterions formed.

4.2.9 Zwitterions

The difficulty in drawing any definite conclusion as to what mechanism is correct stems in part from the fact that they are very similar. The zwitterionic mechanism becomes equivalent to the single-step mechanism when the lifetime of the zwitterion-intermediate approaches zero. This has been somewhat obscured in the literature where the zwitterion mechanism has been written without hydrogen bonds to base molecules. The calculations would suggest that while the zwitterion mechanism is not necessarily wrong the single-step mechanism is more suited to conveying the nature of the reaction taking place. From the quantum mechanical calculations potential reaction-barriers were also identified. The mechanism was found to have no intrinsic barrier.

4.2.10 Bases

A base molecule can by definition undergo the following reaction:

$$B + H_2O \rightleftharpoons BH^+ + OH^- \qquad (4.2.1)$$

Amine molecules are all bases and they are usually the strongest bases present in the system. Water itself is a weak base, the hydroxyl-ion (OH^-) is a strong base, but usually present in small quantities. There is however nothing in the experimental data to suggest that such protonation takes place.

In this study the reactions of acid halides with methanol have been studied by use of gas-phase calculations. The results show that methanolysis proceeds through a loose transition state with a concerted S_N2 mechanism. The nucleophilic methanol attacks the carbonyl carbon at Bürgi-Dunitz trajectory and a base assists in removing the proton of the nucleophilic alcohol. The base could be the usual base, for example pyridine or either a second molecule of methanol or solvent molecule. The conclusion reached is that the reactions can be explained by third-order mechanisms, in which one methanol molecule acts as a nucleophile and another acts as a general base. These findings agree with earlier suggestions by Fox (Fox, *et al.*, 2004) that the methanolysis of acetyl chloride does not proceed through the generally assumed addition-elimination pathway with discrete tetrahedral intermediate but is consistent with ionization of Cl^-.

4.3.0 Acid-Catalyzed Esterification

To get more insight into the mechanism of acid-catalyzed esterification, DFT calculations were done as per scheme 2.18.4. Computational studies of hydrolysis of esters have been done (Sturm, 1999), but to our knowledge, no systematic study has been done on acid-catalyzed esterification. Hydrochloric acid was the acid of choice in this study, due to its simplicity. The auto-catalysis (scheme **2.19.2**) was also examined where a second molecule of the carboxylic acid catalyzes the reaction and the results are presented.

4.3.1 HCl Catalyzed Esterification

The first step is the protonation of the carboxylic acid by HCl, to get a protonated complex (Figure 4.3.1), where the counter ion chloride is taken into consideration. The C=O is elongated to 1.28 Å. As the nucleophilic alcohol attacks the complex formed, the counter ion of the catalyzing acid pick the proton of the nucleophilic alcohol. This results in a concerted tetrahedral transition state. The diol formed reacts with the regenerated acid to form the ester.

For the reaction of acetic acid with methanol, the imaginary frequency (319.559 icm^{-1}) at the transition state reflects the simultaneous breaking of O(7)-H(8) bond and formation of O(7)-C(3) bond). The methanol oxygen attacks within the Burg-Dunitz trajectory, 107.06˚. The O(7)-H(8) bonds are atypically elongated (1.18426Å), and H(8) is very close to Cl(6). This results in the formation of a diol and HCl.

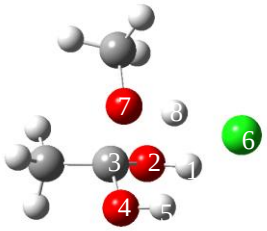

H(1)-O(2)= 1.06534	H(1)-O(2)= 0.98079
O(2)-C(3)= 1.28228	O(2)-C(3)= 1.37592
C(3)-O(4)= 1.28235	C(3)-O(4)= 1.36628
C(4)-H(5)= 1.06524	C(4)-H(5)= 0.98173
H(5)-Cl(6)= 1.83065	H(5)-Cl(6)= 2.41274
H(1)-Cl(6)= 1.83048	H(1)-Cl(6)= 2.51481
	O(7)-C(3)= 1.55708
	O(7)-H(8)= 1.18426
	H(8)-Cl(6)= 1.60359
Cl(6)-H(1)-O(2)= 157.19	Cl(6)-H(1)-O(2)= 133.09
Cl(6)-H(5)-O(4)= 157.19	Cl(6)-H(5)-O(4)= 136.90
	O(7)-C(3)-O(2)= 107.06
	O(7)-C(3)-O(4)= 103.48

Figure 4.3.1: CH_3COOH-HCl opt (left) and TS1 (right).

The NBO calculations for acetic acid (CH_3COOH), protonated acetic acid ($CH_3C(OH)OH^+$) and the acetic acid -HCl complex (CH_3COOH-HCl), are shown below in table 4.3.1 (the numbering as shown in Figure 4.3.2). The complex is stabilized by the counter ion.

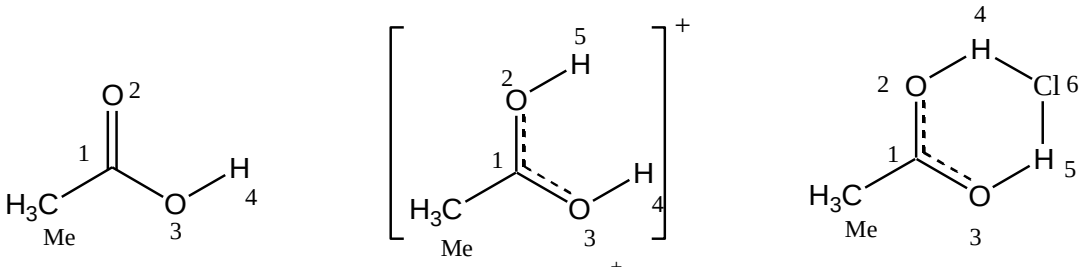

a) CH_3COOH b) $CH_3C(OH)OH^+$ c) CH_3COOH-HCl

Figure 4.3.2: Acetic acid, protonated acetic and acetic acid -HCl complex.

Table 4.3.1: Calculated Natural Bond Orbital (NBO) charges (B3LYP/6-31+G(d)) on carbon atoms of the acetic acid (CH_3COOH), protonated acetic acid ($CH_3C(OH)OH^+$) and the complex (CH_3COOH-HCl).

Structure	Me	C(1)	O(2)	O(3)	H(1)	H(2)	Cl(6)
CH_3COOH	0.02528	0.80477	-0.61607	-0.73207	0.51805		
$CH_3C(OH)OH^+$	0.17745	0.93021	-0.57353	-0.63069	0.53457	0.56200	
CH_3COOH-HCl	0.07642	0.88012	-0.65446	-0.65403	0.48063	-0.48069	-0.61045

The charge of the carbonyl carbon in acetic acid is 0.80477, upon protonation by H^+ it increase to 0.93021, thus making it a better nucleophile. When the whole molecule of HCl is considered, the charge of carbonyl is 0.88012, which is still higher than in acetic acid. Moreover, this system is stabilized by the Chloride counter ion.

The hydrogen ion is a catalyst. The reaction rate is increased because it is easier for the nucleophile to attack the carbon when the electron density of the latter has been decreased (Jencks, 1972).

The diol forms an intermediate with HCl with subsequent formation of a second transition state TS2 (Figure 4.3.3), where finally water is eliminated to form the desired product.

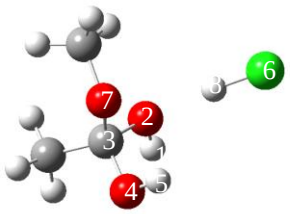

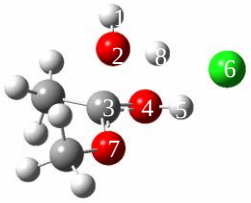

H(1)-O(2)= 0.97193
O(2)-C(3)= 1.44702
C(3)-O(4)= 1.38973
C(4)-H(5)= 0.97435
H(5)-Cl(6)= 3.78991
H(1)-Cl(6)= 3.55244
O(7)-C(3)= 1.39370
O(7)-H(8)= 2.96269
H(8)-Cl(6)= 1.31630

H(1)-O(2)= 0.97557
O(2)-C(3)= 1.76932
C(3)-O(4)= 1.32444
C(4)-H(5)= 1.00635
H(5)-Cl(6)= 2.14256
O(2)-H(8)= 1.10567
O(7)-C(3)= 1.33957
O(7)-H(8)= 2.60488
H(8)-Cl(6)= 1.72744
O(7)-C(3)-O(2)= 100.33820
O(7)-C(3)-O(4)= 112.89973

Figure 4.3.3: $CH_3C(OH)_2$-HCl opt (left) and TS2 (right).

The calculated activation energy 6.93 kcal/mol is in reasonable agreement with the one obtained experimentally (10.2 kcal/mol) (Williamson and Hinshelwood, 1934).

Similar calculations were repeated for benzoic, propanoic, phenylacetic acid with methanol and the results are presented in table 4.3.2.

The optimized structures for the benzoic acid are shown below.

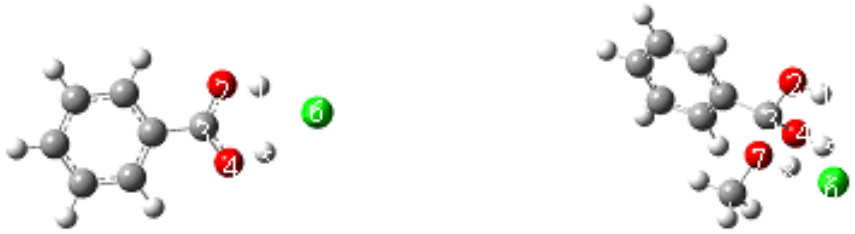

H(1)-O(2)= 1.05817	H(1)-O(2)= 0.95544
O(2)-C(3)= 1.28875	O(2)-C(3)= 1.40654
C(3)-O(4)= 1.28874	C(3)-O(4)= 1.39880
C(4)-H(5)= 1.05819	C(4)-H(5)= 0.95532
H(5)-Cl(6)= 1.84251	H(5)-Cl(6)= 2.74969
H(1)-Cl(6)= 1.84255	H(1)-Cl(6)= 2.87272
	O(7)-C(3)= 1.55000
	O(7)-H(8)= 1.06190
	H(8)-Cl(6)= 1.44875
Cl(6)-H(1)-O(2)= 157.80	Cl(6)-H(1)-O(2)= 125.03
Cl(6)-H(5)-O(4)= 157.80	Cl(6)-H(5)-O(4)= 125.47
	O(7)-C(3)-O(2)= 108.31
	O(7)-C(3)-O(4)= 106.78

Figure 4.3.4: C_6H_5COOH-HCl opt (left) and C_6H_5COOH-TS1 (right).

The calculated activation energy 10.86 kcal/mol is in reasonable agreement with the one obtained experimentally (15.5 kcal/mol). Similar calculations were also done for phenyl acetic acid.

The influence of substituents on reactivity often provides information about the reaction mechanism. Experimental findings have been rationalized with the reaction classical mechanism suggested by Fisher. This study used theoretical investigation using DFT calculations. The calculated thermochemical parameters are summarized in table 4.3.2 for some selected acids. The trend agrees closely with the experimental finding where acetic, propanoic and phenyl acetic acids have close activation energies while benzoic acid has higher activation energy.

Table 4.3.2: Calculated thermodynamic parameters-gas phase of HCl as a catalyst.

Reaction	$\Delta G^{\ddagger}$ /kcal mol^{-1}	$\Delta H^{\ddagger}$ /kcal mol^{-1}	$\Delta S^{\ddagger}$ /cal mol^{-1}K^{-1}	E_a /kcal mol^{-1}
CH_3COOH-HCl + CH_3OH 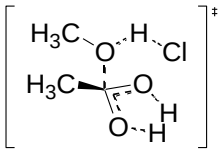	20.56	6.34	-47.70	6.93
CH_3CH_2COOH-HCl + CH_3OH 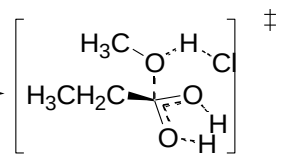	20.58	6.39	-47.62	6.98
C_6H_5COOH-HCl + CH_3OH 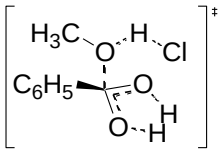	23.89	10.86	-43.70	11.45
$C_6H_5CH_2COOH$-HCl + CH_3OH 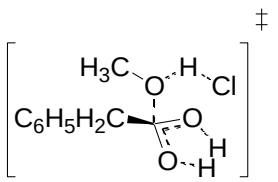	20.95	7.00	-46.80	7.59

The thermodynamics parameter for the second step for the esterification of acetic acid and methanol are shown in table 4.3.3. It is clear that this is not the rate determining step.

Table 4.3.3: Calculated thermodynamic parameters for TS2.

Reaction	$\Delta G^{\ddagger}$ /kcal mol^{-1}	$\Delta H^{\ddagger}$ /kcal mol^{-1}	$\Delta S^{\ddagger}$ /cal mol^{-1}K^{-1}	E_a /kcal mol^{-1}
$(CH_3)_2C(OH)_2OH$ + HCl 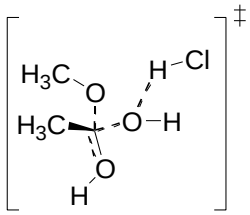	16.42	5.75	-38.57	6.34

To get more insight into the mechanism of the reaction, the chemoselective esterification process was investigated, to demonstrate the rate of esterification of sp^3-C, sp^2-C and sp-C tethered carboxylic acids. Propanoic acid, propenoic and propynoic acid were used in this study; the results are shown in table **4.3.4**.

The trend shows that sp^3-C tethered carboxylic acid undergoes esterification more readily, than sp^2-C tethered carboxylic acid. The ease with which sp-C tethered carboxylic acid is compared to sp^2-C tethered may be attributed to the acidity of ethyne moiety.

Table 4.3.4: Calculated thermodynamic parameters- sp^3-C, sp^2-C and sp-C tethered carboxylic acids-gas phase, as HCl catalyst.

Reaction	$\Delta G^{\ddagger}$ /kcal mol^{-1}	$\Delta H^{\ddagger}$ /kcal mol^{-1}	$\Delta S^{\ddagger}$ /cal $mol^{-1}K^{-1}$	E_a /kcal mol^{-1}
CH_3CH_2COOH-HCl + CH_3OH 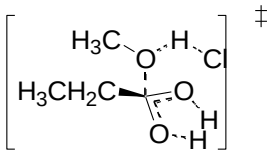	20.58	6.39	-47.62	6.98
$CH_2CHCOOH$-HCl + CH_3OH 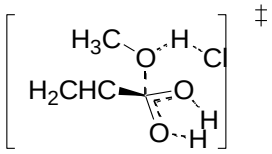	22.29	9.42	-43.13	10.04
CHCCOOH-HCl + CH_3OH 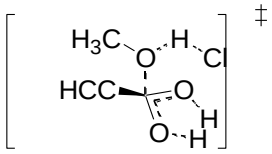	20.63	8.21	-41.66	8.80

4.3.2 Effects of Substituents on Benzene Ring

The effect of the reactivity due to substituents on the benzene ring was studied, and the results are presented on table 4.3.4. Only the *para*-positions were considered. There was no clear trend observed with halogen. Electron donating methyl group at *para*-position was found to increase the activation energy. This reduces the electrophilic character of the carbonyl carbon.

Table 4.3.5: Calculated thermodynamic parameter for Hammett effects.

Reaction	$\Delta G^{\ddagger}$ /kcal mol^{-1}	$\Delta H^{\ddagger}$ /kcal mol^{-1}	$\Delta S^{\ddagger}$ /cal $mol^{-1}K^{-1}$	E_a [b] /kcal mol^{-1}
C_6H_5COOH-HCl + CH_3OH → 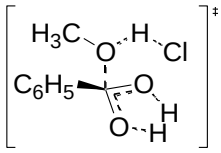	23.89	10.87	-43.70	11.46
p-F-C_6H_5COOH-HCl + CH_3OH → 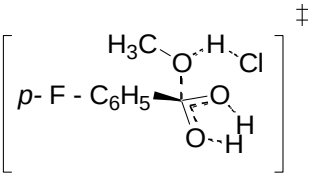	23.95	10.81	-44.10	11.4
p-Cl-C_6H_5COOH-HCl + CH_3OH → 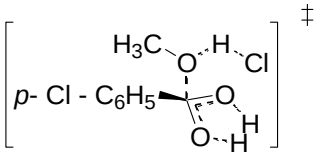	23.73	10.54	-44.26	11.13
p-Br-C_6H_5COOH-HCl + CH_3OH → 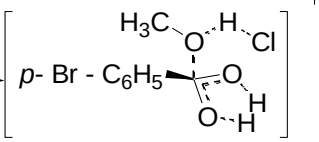	23.01	10.08	-43.39	10.67
p-CH_3-C_6H_5COOH-HCl + CH_3OH → 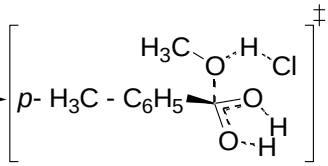	23.95	12.27	-39.17	12.86

4.3.3 Solvent Systems in Esterification

Solvation models were incorporated in the calculation in an attempt to reproduce and explain the experimental results. The solvation model employed in this study is the Integral Equation Formalism Polarized Continuum Model (IEFPCM). Transition structures of the reaction were located and optimized at the same theory level. Two solvents dichloromethane (none polar) and acetone (polar) were used. Only the parent reaction was studied in the solvent system. The results are summarized in table **4.3.6**.

Table 4.3.6: Calculated thermodynamic parameters for acid-catalyzed esterification-solvent phase.

Structure	$\Delta G^{\ddagger}$ /kcal mol^{-1}	$\Delta H^{\ddagger}$ /kcal mol^{-1}	$\Delta S^{\ddagger}$ /cal mol^{-1}K^{-1}	E_a /kcal mol^{-1}
1-DCM	23.14	9.87	-44.48	10.46
1-Acetone	23.02	9.94	-43.88	10.53

The calculated activation energy (10.5 kcal mol^{-1}) in solvent systems is in a very close agreement with the experimental value (10.2 kcal mol^{-1}).

4.3.4 Auto-Catalyzed

The transition structure for autocatalysis is presented in figure **4.3.5**. The activation energy (see table **4.3.7**) is exceedingly higher, compared to the catalyzed reaction. Hence this reaction is very slow, and takes long to reach equilibrium.

H(1)-O(2)= 1.00278
O(2)-C(3)= 1.32736
C(3)-O(4)= 1.23129
O(4)-H(5)= 1.70472
H(5)-O(6)= 1.00278
H(1)-O(8)= 1.70471

H(1)-O(2)= 1.00207
O(2)-C(3)= 1.33705
C(3)-O(4)= 1.32904
C(4)-H(5)= 1.00431
H(5)-O(6)= 1.71225
H(1)-Cl(6)= 1.74467
O(10)-C(3)= 1.80005
O(10)-H(9)= 1.07245
H(9)-O(8)= 1.43882
O(10)-C(3)-O(2)= 103.38162
O(10)-C(3)-O(4)= 100.06307

Figure 4.3.5: CH_3COOH dimer (left) and auto-catalysis TS1 (right).

The activation parameters obtained for these modeled reactions were in acceptable agreement with the experimental data.

Table 4.3.7: Calculated thermodynamic parameters-gas phase, autocatalysis.

Reaction	$\Delta G^{\ddagger}$ /kcal mol^{-1}	$\Delta H^{\ddagger}$ /kcal mol^{-1}	$\Delta S^{\ddagger}$ /cal mol^{-1}K^{-1}	E_a /kcal mol^{-1}
$2CH_3COOH + CH_3OH \rightarrow$ 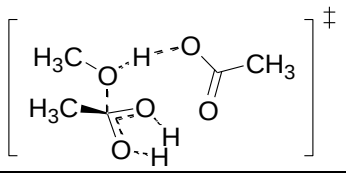	35.21	20.39	-49.72	20.98

From the foregoing calculations, the general mechanism for esterification may be summarized as in the scheme below. The carboxylic acid forms a complex with the acid catalyzing the reaction. As the nucleophilic alcohol attacks the complex formed the conjugate base of the catalyzing acid picks the proton of the nucleophilic alcohol. The diol formed reacts with the regenerated acid to form the ester (see scheme 4.3.1).

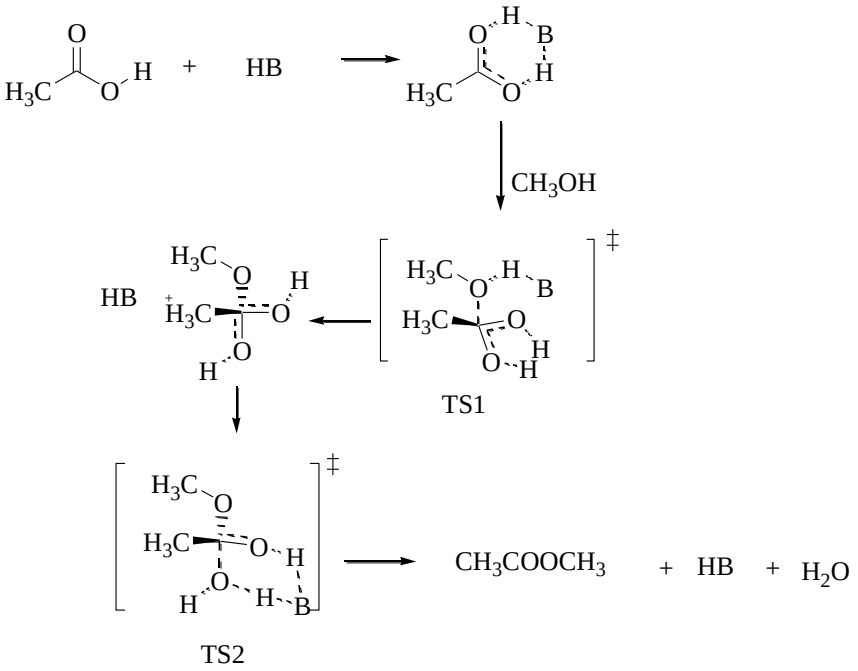

Scheme 4.3.1: General mechanism for acid-catalyzed reaction.

CHAPTER FIVE

5 CONCLUSION AND RECOMMENDATIONS

5.1.0 Conclusion

This study applied quantum chemistry to the reactions studied with the purpose of predicting and interpreting the experimental data. From the finding of this study, the following conclusions were made:

5.1.1 [1,7] – Hydrogen Shift

Substituents or heteroatoms in Z,Z-1,3,5-heptatriene have a substantial effect on the [1,7]-H shift reaction. As a general trend, electron-donating substituents increase the π electron density of the aromatic transition structure and stabilize it, therefore decreasing the activation energy, whereas electron-withdrawing substituents have the inverse effect. However, when electron-donating and –withdrawing properties of a given substituent are considered, both inductive and mesomeric effects need to be taken into account. Other factors that affect the activation energy in [1,7]- H shift in 1,3,5-heptatriene systems include: HOMO/LUMO interaction, electron density, strength of bond formed or broken, loss of conjugation or loss of aromaticity, steric effects and entropy.

5.1.2 Methanolysis of Acetyl Chloride

The study revealed that methanolysis of acetyl chloride is a concerted reaction and proceeds with no discernible tetrahedral intermediate typical of an addition-elimination pathway. The nucleophilic attack by an alcohol molecule is assisted by a second alcohol molecule or a polar solvent acting as a base. This occurs by S_N2-S_N1 boderline reaction resulting in the mixed reaction kinetics observed experimentally.

5.1.3 Acid-Catalyzed Esterification

During an acid catalyzed esterification reaction, the carboxylic acid forms a reactive complex with the catalyzing acid. When the nucleophilic alcohol attacks the reactive complex, the counter ion of the catalyzing acid, deprotonates the nucleophilic alcohol to form a diol. The diol then reacts further with the acid to form the products.

5.1.4 Auto-Catalyzed Esterification

The theoretical study explains the second-order reaction kinetics in uncatlyzed esterification reaction of carboxylic acid. As reported in the literature the esterification is favoured by using excess amounts of carboxylic acid. This observation could be explained in terms of autocatalysis of the carboxylic acid.

5.1.5 Solvent Systems

Density functional theory calculations at B3LYP/6-31+G(d) level incorporated with IEFPCM was able to give qualitatively good results of the reactions investigated. The study successfully reproduced the experimentally determined activation energies.

5.2 Recommendations

This study has adequately demonstrated the fact that computational methods can be used to facilitate the understanding of reaction pathways and kinetics. Accordingly, there is need to use these theoretical techniques in conjunction with available experimental data so as to shed more light on the mechanistic pathways and kinetics of [i,j] sigmatropic reactions at various temperatures, other pericyclic reactions e.g cycloaddition and electrocyclic reactions and trans-esterification reactions. In addition these techniques can also be used to determine free energies of solution and reactivity of organic molecules in various solvent systems. While the work has been focused on the gas phase system the same techniques could also be used to determine optimal solvents required for the processes.

Further work could be done on heterogeneous (zeolite) acid-catalyzed esterification, this is in line toward *green chemistry*. It is important nowadays not just getting the product but how green is the process.

REFERENCES

Aafaqi, R., Mohamed, A.R. and Bhatia, S. (2004) Kinetics of Esterification of Palmitic Acid with Isopropanol Using p-Toluene Sulfonic Acid and Zinc Ethanoate Supported Over Silica Gel as Catalysts, *J. Chem. Technol. Biotechnol*, 1127.

Ahlrichs, R., Bar, M., Haser, M., Horn, H. and Komel, C. (1989) Electronic Structure Calculations on Workstation Computers: The Program SystemTurbomole, *Chem. Phys. Lett.*, **162**, 165-169.

Allinger, N. (1977) Conformational Analysis. 130. MM2. A Hydrocarbon Force Field Utilizing V1 and V2 Torsional Terms, *J. Am. Chem. Soc.*, **99**, 8127-8134.

Altiokka, M. R. and Citak, A. (2003) Kinetics Study of Esterification of Acetic Acid with Isobutanol in the Presence of Amberlite Catalyst, *Appli. Catal. A. Gen.*, **239**, 141-148.

Ashdown, A. A. (1930) The Rate of Reaction of Certain Alcohols with para-Nitrobenzoyl Chloride in Anhydrous Ether Solution, *J. Am. Chem. Soc.*, **52**, 268-279.

Ayturk, E., Hamamci, H. and Karakas, G. (2003) Production of Lactic Acid Esters Catalyzed by Heteropoly Acid Supported Over Ion-Exchange Resins, *Green Chem.*, **5**, 460-466.

Ba-Saif, S., Luthra, A. K. and Williams, A. (1987) Concertedness in Acyl Group Transfer in Solution: A single Transition State in Acetyl Group Transfer between Phenolate Ion Nucleophiles, *J. Am. Chem. Soc.*, **109**, 6362-6368.

Baker, J. W. (1941) Mechanism and Kinetics of Aromatic Side-Chain Substitution. Interpretation of Reaction Data by the Method of Relative Energy Levels, *Trans. Faraday Soc.*, **37**, 632-644.

Basiuk, V. A. (2002) Reactivity of Carboxylic Groups on Armchair and Zigzag Carbon Nanotube Tips: A Theoretical Study of Esterification with Methanol, *Nano lett.*, **2**, 835-839.

Becke, A.D. (1988) Density-Functional Exchange-Energy Approximation with Correct Asymptotic Behaviour, *Phys. Rev. A*, **38**, 3098-3100.

Becke, A. D. (1993) Density Functional Thermochemistry. III. Fhe Role of Exact Exchange, *J. Chem. Phys.*, **98**, 5648.

Bell, S. and Crighton, J. S. (1984) Locating Transition States, *J. Chem. Phys.*, **80**, 2464-2475.

Bender, M. L. (1960) Mechanisms of Catalysis of Nucleophilic Reactions of Carboxylic Acid Derivatives, *Chem. Rev.*, **60**, 53-113.

Bentley, T. W., Carter, G. E. and Harris, H. C. (1985) Competing S_N2 and Carbonyl Addition Pathways for Solvolysis of Benzoyl Chloride in Aqueoes Media, *J. Chem. Soc. Perkin Trans 2*, 983.

Bentley, T. W. and Harris, H. C. (1986) Solvolyses of para-Substituted Benzoyl Chloride in Trifluoroethanol and in Highly Aqueous Media, *J. Chem. Soc. Perkin Trans 2*, 619.

Bentley, T. W., Llewenllyn, G. and McAlister, J. A. (1996) S_N2 Mechanism for Alcoholysis, Aminolysis, and Hydrolysis of Acetyl Chloride, *J. Org. Chem.*, **61**, 7927-7932.

Bentley, T. W. and Shim, C. S. (1993) Dual Reaction Channels for Solvolyses of Acyl Chlorides in Alcohol-Water Mixtures, *J. Chem. Soc. Perkin Trans*, **2**, 1659-1663.

Blake, J. F. and Jorgensen, W. L. (1987) Ab initio Study of the Displacement Reactions of Chloride Ion with Formyl and Acetyl Chloride *J. Am. Chem. Soc.*, **109**, 3856.

Blondin, G. A., Kulkarni, B. D. and Nes, W. R. (1964) Concerning the Nonphotochemical Biosynthesis of Vitamin D3 in Fish, *J. Am. Chem. Soc.*, **86**, 2528-2529.

Born, M. (1920) Volumen und Hydratationswarme der Lonen, *Z. Physik*, **1**, 45-48.

Born, M. and Oppenheimer, R. (1927) Zur Quantentheorie der Molekeln, *Ann. Phys.*, **84**, 457-484.

Boys, S. F., Cook, G.B., Reeves, C. M. and Shavitt, I. (1956) Automatic Fundamental Calculations of Molecular Structure, *Nature*, **178**, 1207.

Breslow, R., Hoffman, J. J. M. and Perchonock, C. (1973) Relative Reactivities of the 5-Halocyclopentadienes in Diels-Alder and 1,5 Shift Reactions, *Tetrahedron Lett.*, **14**, 3723-3726

Buenker, R. J. and Peyerimhoff, S. D. (1969) *Ab Initio* SCF Calculations for Azulene and Naphthalene *Chemical Physics Letters*, **3**, 37-42.

Bürgi, H. B., Dunitz, J. D., Lehn, J. M. and Wipff, G. (1974) Stereochemistry of Reaction Paths at Carbonyl Centres *Tetrahedron*, **30**, 1563-1572

Bürgi, H. B., Dunitz, J. D. and Shefter, E. (1973) Geometric Reaction Coordinates. II. Nucleophilic Addition to a Carbonyl Group, *J. Am. Chem. Soc.*, **95**, 5065-5067.

Bürgi, H. B., Dunitz, J. D. and Shefter, E. (1974) Chemical Reaction Paths. IV. Aspects of O--C=O Interactions in Crystals, *Acta Cryst.*, **B30**, 1517-1527.

Cammi, R. and Tomasi, J. (1995) Remarks on the Use of the Apparent Surface Charges (ASC) Methods in Solvation Problems: Iterative Versus Matrix-Inversion Procedures and the Renormalization of the Apparent Charges, *J. Comput. Chem.*, **16**, 1449-1458.

Cancès, E. and Mennucci, B. (1998) New Applications of Integral Equations Methods for Solvation Continuum Models: Ionic Solutions and Liquid Crystals, *J. Math. Chem.*, **23**, 309.

Cancès, E., Mennucci, B. and Tomasi, J. (1997) A New Integral Equation Formalism for the Polarizable Continuum Model: Theoretical Background and Applications to Isotropic and Anisotropic Dielectrics, *J. Chem. Phys.*, **107**, 3032-3041.

Carpenter, J. E. and Sosa, C. P. (1994) Density Functional Studies of Representative Pericyclic Reactions, *J. Mol. Struct: THEOCHEM*, **311**, 325-300.

Ceperley, D. M. and Alder, B. J. (1980) Ground State of the Electron Gas by a Stochastic Method, *Phys. Rev. Lett.*, **45**, 566-569.

Chapman, N. B., Rodgers, M. G. and Shorter, J. (1968) The Separation of Polar and Steric Effects. Part Vi. The Kinetics of the Acid-Catalyzed Esterification of Substituted Benzoic Acids by Methanol, *J. Chem. Soc.*, 158.

Chemat, F., Poux, M. and Galema, S.A. (1997) Esterification of Stearic Acid by Isomeric Forms of Butanol in a Microwave Oven Under Homogeneous and Heterogeneous Reaction Conditions, *J. Chem. Soc., Perkin Trans.*, **2**, 2371-2374.

Clark, T. (1985) *A Handbook of Computational Chemistry*. John Wiley & Sons Inc., Chichester.

Cottrell, T. L. (1958) *The Strengths of Chemical Bonds*. Academic Press, New York.

Coulson, C. A. (1952) *Valence*. Oxford University Press, London.

Coutot, P. and Rumin, R. (1970) Photoisomérisation en Série Cyclohexadiénique-1,3. VI. Nouveaux Exemples D'ouverture Photochimique Stéréospécifique et Migration Sigmatropique [1,7] D'hydrogène par voie Thermique *Tetrahedron Lett.*, **11**, 1849-1852.

Cramer, C. J. (2004) *Essentials of Computational Chemistry: Theories and Models*. John Wiley & Sons, Ltd, West Sussex England.

Dearing, A. (1988) Computer-Aided Molecular Modelling: Research Study or Research Tool? , *J. Comput.-Aided Mol. Design.*, **2**, 179-189.

Dewar, M. J. S. (1969) *The Molecular Orbital Theory of Organic Chemistry*. McGraw-Hill, New York.

Dewar, M. J. S. (1971) Aromaticity and Pericyclic Reactions, *Angew. Chem., Int. Ed. Engl.* , **10**, 761-776.

Epiotis, N. D. (1973) Configuration Interaction and Organic Reactivity. III. Sigmatropic Reactions and Ionic Rearrangements *J. Am. Chem. Soc.*, **95**, 1206-1214.

Eyring, H., Walter, J. and Kimball, G.E. (1944) *Quantum Chemistry* Wiley, New York.

Fernbach, S. and Taub, A.H. (1970) *Computers and their`Role in the Physical Sciences*. Routledge.

Ferreire, P. C. and Miller, J. (1976) Comparison of Methanolysis of a Series of p-Benzyloxybenzoyl Chlorides with that of Benzoyl, p-Phenoxybenzoyl, and p-Methoxybenzoyl Chlorides, *J. Chem. Soc., Perkin Trans. 2*, 1648 - 1651.

Fock, V. (1928) Näherungsmethode zur Lösung des quantenmechanischen Mehrkörperproblems (Approximate method for solution of quantum many body), *Z. Physik*, **61**, 126-148.

Foresman, J. B. and Frisch, Æ. (1996) *Exploring Chemistry with Electronic Structure Methods*. Gaussan, Inc., Pittsburgh.

Foster, J. P. and Weinhold, F. (1980) Natural Hybrid Orbitals *J. Am. Chem. Soc.*, **102**, 7211-7218.

Fox, J. M., Dmitrenko, O., Liao, L. and Bach, R.D. (2004) Computational Studies of Nucleophilic Substitution at Carbonyl Carbon: the S_N2 Mechanism versus the Tetrahedral Intermediate in Organic Synthesis, *J. Org. Chem.*, **69**, 7317-7328.

Frey, H. M. and Walsh, R. (1969) Thermal Unimolecular Reactions of Hydrocarbons *Chem. Rev.*, **69**, 103-124.

Fukui, K. (1970) *Theory of Orientation and Stereochemistry*. Springer-Verlag, Hiedelberg.

Fukui, K. (1971) Recognition of Stereochemical Paths by Orbital Interaction, *Acc. Chem. Res.*, **4**, 57-64.

Gawley, R. E. and Aube, J. (1996) *Principles of Asymmetric Synthesis*. Pergamon, Elsevier Science Ltd., Tarrytown, NY.

Gilchrist, T. L. and Storr, R.C. (1972) *Organic Reactions and Orbital Symmetry*. Cambridge University Press.

Gill, G. B. Q. (1968) The application of the Woodward–Hoffmann orbital symmetry rules to concerted organic reactions, *Q. Rev. Chem. Soc.* , **22**, 338 - 389.

Glasstone, S., Laidler, K. J. and Eyring, H. (1941) *The Theory of Rate Processes*. McGraw-Hill, New York.

Goddard, I. W. A. (1972) Selection Rules for Chemical Reactions Using the Orbital Phase Continuity Principle *J. Am. Chem. Soc.*, **94**, 793-807.

Goldschmidt, H. and Udby, O.Z. (1907), *Physik. Chem.*, **60**, 728-755.

Gonzalez, C. and Schlegel, H. B. (1989) An Improved Algorithm for Reaction Path Following, *J. Chem. Phys.*, **90**, 2154-2161.

Gonzalez, C. and Schlegel, H. B. (1990) Reaction Path Following in Mass-Weighted Internal Coordinates, *J. Chem. Phys.*, **94**, 5523-5527.

Guthrie, J. P. (1991) Concerted Mechanism for Alcoholysis of Esters: An Examination of the Requirements *J. Am. Chem. Soc.*, **113**, 3941-3949.

Gutman, M. and Nachliel, E. (1997) Time-Resolved Dynamics of Proton Transfer in Proteinous Systems, *Annu. Rev. Phys. Chem.*, **48**, 329-356.

Halgren, T. A. and Lipscomb, W. N. (1977) The Synchronous-Transit Method for Determining Reaction Pathways and Locating Molecular Transition States, *Chem. Phys. Lett.*, **49**, 225-232.

Hall, G.G. (1951) The Molecular Orbital Theory of Chemical Valency VIII. A Method for Calculating Ionization Potentials, *Proc. R. Soc, London*, **A205**, 541-552.

Hartman, R. J. and Borders, A. M. (1937) Effect of Polar Groups upon Esterification Velocities of Substituted Benzoic Acids, *J. Am. Chem. Soc.*, **59**, 2107-2112.

Hartman, R. J. and Gassmann, A.G. (1940) Kinetics of the Esterification of Substituted Benzoic Acids, *J. Am. Chem. Soc.*, **62**, 1559 - 1560.

Hartree, D. R. (1928) The wave Mechanics of an Atom with a Non-Coulomb Central Field. Part I. Theory and Methods, *Proc. Cambridge. Philos. Soc*, **24**, 89-110.

Havinga, E. (1973) Vitamin D, Example and Challenge, *Experimenta*, **29**, 1181-1193.

Havinga, E. and Schlatmann, J. L. M. A. (1961) Remarks on the specificities of the photochemical and thermal transformations in the vitamin D field, *Tetrahedron*, **16**, 146-152.

Heimgartner, V. H., Hansen, H.-J. and Schmid, H. (1970) Thermisches Verhalten von o-Dipropenylbenzol, Beispiel einer aromatischen [1,7]-sigmatropischen H-Verschiebung. Vorläufige Mitteilung, *Helv. Chim. Acta.*, **53**, 173-176.

Heimgartner, V. H., Hansen, H.-J. and Schmid, H. (1972) Thermisches Verhalten von 1,2-Dipropenylbenzolen, *Helv. Chim. Acta.*, **55**, 1385-1403.

Heitler, W. (1945) *Elementary Wave Mechanics – with Applications to Quantum Chemistry*. Oxford, Claredon, London.

Heitler, W. and London, F. (1927) Quantum Chemistry, *Zeitschrift fur Physik*, **44**, 455.

Hendrick, J. B., Cram, D.J. and Hammond, G.S. (1970) *Organic Chemistry*. McGraw-Hill, New York.

Hess, B. A. (2001) Computational Support for Tunneling in Thermal [1,7]-Hydrogen Shift Reactions, *Org. Chem.*, **66**, 5897 - 5900.

Hess, B. A., Schaad, L. J. and Pancir, J. (1985) Theoretical studies of [1,n]-sigmatropic rearrangements involving hydrogen transfer in simple methyl-substituted conjugated polyenes, *J. Am. Chem. Soc.*, **107**, 149-154.

Hinchcliffe, A. (1996) *Modelling Molecular Structure*. Wiley, Chichester.

Hirst, D.M. (1990) *A Compuational Approach to Chemistry*. Blackwell, Oxford.

Hoeger, C. A., Johnston, A. D. and Okamura, W.H. (1987) Studies of vitamin D (calciferol) and its analogs. 30. Thermal [1,7]-sigmatropic hydrogen shifts: stereochemistry, kinetics, isotope effects and .pi.-facial selectivity, *J. Am. Chem. Soc.*, **109**, 4690-4698.

Hoeger, C. A. and Okamura, W. H. (1985) On the antarafacial stereochemistry of the thermal [1,7]-sigmatropic hydrogen shift, *J. Am. Chem. Soc.*, **107**, 268-270.

Hoffman, R. and Woodward, R. B. (1968) The conservation of orbital symmetry, *Acc. Chem. Res.*, **1**, 17-22.

Hohenberg, P. and Kohn, W. (1964) In Homogeneous Electron Gas, *Phys. Rev. B*, **136**, 864-871.

Hopkinson, G. A. and Judson, P. N. (1989) Artificial Intelligence in Information Systems, *Chem. Brit.*, **25**, 1122-1124.

Houk, K. N., Li, Y. and Evanseck, J.D. (1992) Transition Structures of Hydrocarbon Pericyclic Reactions, *Angew. Chem., Int. Ed. Engl.*, **31**, 682-708.

Hudson, R. F. and Moss, G.E. (1962) The Mechanism of Hydrolysis of Acid Chlorides. Part IX. Acetyl Chloride, *J. Chem. Soc.*, 5157-5163.

Hudson, R. F. and Saville, B. (1955) Solvent Participation in Nucleophilic Displacement Reactions. Part II. The Reaction Between Ethanol and Acid Chlorides, *J. Chem. Soc*, 4121-4129.

Hyde, R. M. and Livingstone, D.J. (1988) Perspectives in QSAR: Computer chemistry and pattern recognition, *J. Comput.-Aided Mol. Design.*, **2**, 145-155.

Jali, S. and Kruger, H. G. (2005) DFT Mechanistic Investigation of the Esterification Reaction of Methanol with Acetic Acid and Acetyl Chloride. University of KwaZulu-Natal.

Janz, G. J. (1967) *Thermodynamic Properties of Organic Compounds*. Academic Press, New York.

Jencks, W. P. (1972) General Acid-Base Catalysis of Complex Reactions in Water, *Chem. Rev.*, **72**, 705-718.

Kerr, J. A. (1966) Bond Dissociation Energies by Kinetic Methods, *Chem. Rev.*, **66**, 465-500.

Kevill, D. N. and Kim, C.-B. (1988) Nucleophilic Substitution at Trigonal Carbon. Part 3. Kinetics and Mechanism of the Reaction of Methanol and Phenol with Acetyl Chloride in Acetonitrile, *Bull. Soc. Chim. Fr.*, **2**, 383-390.

Kim, J. K. and Caserio, M. C. (1981) Acyl Transfer Reactions in the Gas phase. The Question of Tetrahedral Intermediates, *J. Am. Chem. Soc.*, **103**, 2124-2127.

Klamt, A., Jones, V., Burger, T. and Lohrenz, J.C.W. (1998) Refinement and Parametrization of COSMO-RS, *J. Phys. Chem. A*, **102**, 5074-5085.

Klamt, A. and Schüürmann, G. (1993) A New Approach to Dielectric Screening in Solvents with Explicit Expressions for the Screening Energy and its Gradient, *J. Am. Chem. Soc. Perkin Trans 2*, 799-805.

Koch, W. and Holthausen, M. C. (2000) *A Chemist's Guide to Density Functional Theory*. Wiley-VCH Verlag GmBH, Weinheim.

Kohn, W. and Sham, L. J. (1965) Self-Consistent Equations Including Exchange and Correlation Effects, *Phys. Rev.*, **140**, 1133-1138.

Koo, I. S., Lee, I., Oh, J., Yang, K. and Bentley, T.W. (2004) Substituent effects on the kinetic solvent isotope effect in solvolyses of arenesulphonyl chlorides, *J. Phys. Org. Chem.*, **6**, 223-227.

Laidler, K. J. (1941) *Theories of Chemical Reaction Rates*. McGraw-Hill, New York.

Leach, A. R. (2001) *Molecular Modeling. Principle and Applications*. Prentice Hall, London.

Lee, A. S.-Y., Yanga, H.-C. and Su, F.-Y. (2001) An Unprecedented and Highly Chemoselective Esterification Method, *Tetrahedron Lett.*, **42**, 3001-3303.

Lee, C., Yang, W. and Parr, R.G. (1988) Development of the Colle-Salvetti Correlation-Energy Formula into a Functional of the Electron Density, *Phys. Rev. B*, **37**, 785 - 789

Lee, C., Yang, W. and Parr, R.G. (1988) Development of the Colle-Salvetti Correlation-Energy Formula into a Functional of the Electron Density, *Phys. Rev. B*, **37**, 785-789.

Liotta, C. L., Burgess, E. M. and Ebershardt, W.H. (1984) Trajectory Analysis. Theoretical Model for Nucleophilic Attack at pi-Systems. The Stabilizing and Destabilizing Orbital Terms, *J. Am. Chem. Soc.*, **106**, 4849-4852.

Lotero, E., Liu, Y., Lopez, D. E., Suwannakarn, K., Bruce, D.A. and Goodwin, J.G.J. (2005) Synthesis of Biodiesel via Acid Catalysis, *Ind. Eng. Chem. Res.*, **44**, 5353-5363.

Lowry, T. H. and Richardson, K. S. (1987) *Mechanism and Theory in Organic Chemistry*. Harper and Row, New York.

M. J. Frisch, G. W. Trucks, H. B. Schlegel, G. E. Scuseria, M. A. Robb, J. R. Cheeseman, J. A. Montgomery, Jr., T.V., K. N. Kudin, J. C. Burant, J. M. Millam, S. S. Iyengar, J. Tomasi, V. Barone, B. Mennucci, M. Cossi, G. Scalmani, N. Rega, G. A. Petersson, H. Nakatsuji, M. Hada, M. Ehara, K. Toyota, R. Fukuda, J. Hasegawa, M. Ishida, T. Nakajima, Y. Honda, O. Kitao, H. Nakai, M. Klene, X. Li, J. E. Knox, H. P. Hratchian, J. B. Cross, C. Adamo, J. Jaramillo, R. Gomperts, R. E. Stratmann, O. Yazyev, A. J. Austin, R. Cammi, C. Pomelli, J. W. Ochterski, P. Y. Ayala, K. Morokuma, G. A. Voth, P. Salvador, J. J. Dannenberg, V. G. Zakrzewski, S. Dapprich, A. D. Daniels, M. C. Strain, O. Farkas, D. K. Malick, A. D. Rabuck, K. Raghavachari, J. B. Foresman, J. V. Ortiz, Q. Cui, A. G. Baboul, S. Clifford, J. Cioslowski, B. B. Stefanov, G. Liu, A. Liashenko, P. Piskorz, I. Komaromi, R. L. Martin, D. J. Fox, T. Keith, M. A. Al-Laham, C. Y. Peng, A. Nanayakkara, M. Challacombe, P. M. W. Gill, B. Johnson, W. Chen, M. W. Wong, C. Gonzalez, and J. A. Pople and (2003) Gaussian 03. Gaussian, Inc. , Pittsburgh PA.

Maitland, J. J. (1997) *Organic Chemistry*. W. W. Norton & Company Ltd, New York.

March, J. (1992) *Advanced Organic Chemistry*. Wiley, New York.

Marvell, E. N., Caple, G., Schatz, B. and Pippin, W. (1973) Electrocyclic Reactions *1 Stereochemistry of the Triene Electrocyclization, *Tetrahedron*, **29**, 3781-3789

McQuarrie, D. A. and Simon, J. D. (1999) *Molecular Thermodynamics*. University Science Book, California.

Melman, A. and Nahmany, M. (2004) Chemoselectivity in Reactions of Esterification, *Org. Biomol. Chem.*, **2**, 1563-1572.

Mennucci, B., Cancès, E. and Tomasi, J. (1997) Evaluation of Solvent Effects in Isotropic and Anisotropic Dielectrics and in Ionic Solutions with a Unified Integral Equation Method: Theoretical Bases, Computational Implementation, and Numerical Applications, *J. Phys. Chem. B*, **101**, 10506-10517.

Moriarty, R. M. and Paaren, H. E. (1980) The Stereochemical Course of the Previtamin-Vitamin Conversion with C-19-Substituted 7-Dehydrocholesteryl Derivatives, *Tetrahedron Lett.*, **21**, 2389-2392

Mousavipour, S. H., Ramos, A. R., Pañeda, R. M., Núñez, E. M., Vzquez, S. A. and Ríos, M. A. (2007) Direct-Dynamics VTST Study of the [1,7] Hydrogen Shift in 7-Methylocta-1,3(Z),5(Z)-triene. A Model System for the Hydrogen Transfer Reaction in Previtamin D_3, *J. Phys. Chem. A*, **111**, 719 -725.

Mulliken, R. S. (1955) Electronic Population Analysis on LCAO-MO Molecular Wave Functions I, *J. Chem. Phys.*, **23**, 1833-1846.

Norris, J. F. and Ashdown, A. A. (1925) The Reactivity of Atoms and Groups in Organic Compounds. I. The Relative Reactivities of the Hydroxyl-Hydrogen Atoms in Certain Alcohols, *J. Am. Chem. Soc.*, **47**, 837-846.

Norris, J. F. and Cortese, F. (1927) The Reactivity of Atoms and Groups in Organic Compounds. II. Second Contribution on the Relative Reactivities of the Hydroxyl-Hydrogen Atoms in Certain Alcohols, *J. Am. Chem. Soc.*, **49**, 2640-2650.

Norris, J. F., Fasce, E. V. and Staud, C. J. (1935) The Reactivity of Atoms and Groups in Organic Compounds. XVI. The Relative Effects of Substituents on the Rates at which Certain Acyl and Alkyl Chlorides React with Ethyl Alcohol, *J. Am. Chem. Soc.*, **57**, 1415-1425.

Onsager, L. (1936) Electric Moments of Molecules in Liquids, *J. Am. Chem. Soc.*, **58**, 1486-1493.

Otera, J. (2003) *Esterification: Methods, Reactions, and Applications*. Wiley, Chichester.

Parr, R. G. and Yang, W. (1989) *Density-Functional Theory of Atoms and Molecules*. Oxford University Press, New York.

Patai, S. (1966) *The Chemistry of the Carbonyl Group*. Interscience, New York.

Pauling, L. and Wilson, E. B. (1935) *Introduction to Quantum Mechanics – with Applications to Chemistry*. Dover Books, New York.

Peng, C. and Schlegel, H. B. (1993) Combining Synchronous Transit and Quasi-Newton Methods to Find Transition States, *Israel. J. Chem.*, **33**, 449-454.

Perdew, J. P. (1986) Density-Functional Approximation for the Correlation Energy of the Inhomogeneous Electron Gas, *Phys. Rev. B*, **33**, 8822-8824.

Pople, J. A. and David, L.B. (1970) *Approximate Molecular Orbital Theory*. McGraw Hill, New York.

Preuss, H. (1968) Das SCF-MO-P(LCGO)-Verfahren und seine Varianten, *International Journal of Quantum Chemistry*, **2**.

Reed, A.E., Weinstock, R.B. and Weinhold, F. (1985) Natural Population Analysis, *J. Chem. Phys.*, **83**, 735-746.

Richardson, W. G., Walker, T. E. H. and Hinkley R. K. (1971) *A Bibliograpghy of Ab Initio Molecular Wave Functions*. Clarendon Press, Oxford.

Roothaan, J. C. C. (1951) New Development in Molecular Orbital Theory, *Rev. Mod. Phys.*, **23**, 69-89.

Ross, S. D. (1970) Evidence for Hydrogen-Bonded Transition States in the Rate-Determining Step of the Reaction of Benzoyl Chlorides with Ethanol in Acetone and Chloroform, *J. Am. Chem. Soc.*, **92**, 5998-6002.

Roth, W. R., König, J. and Stein, K. (1970) Die Stereochemie Sigmatroper 1.5-Wasserstoffverschiebungen, *Chem. Ber.*, **103**, 426-439.

Royals, E. E. (1954) *Advanced Org. Chem*. Prentice Hall, Inc, New-York.

Saettel, N. J. and Wiest, O. (2000) Ab Initio Studies of [1,5] - H Shifts: Pentadiene and Beyond, *J. Org. Chem.*, **65**, 2331-2336.

Schaefer, H. F. I. (1984) *Quantum Chemistry*. Claredon Press, Oxford.

Schafer, A., Klamt, A., Sattel, D., Lohrenz, J.C.W. and Eckert, F. (2000) COSMO Implementation in TURBOMOLE: Extension of an Efficient Quantum Chemical Code Towards Liquid Systems, *Phys. Chem. Chem. Phys.*, **2**, 2187-2193.

Schrödinger, E. (1926) Ober das Verhaitnis der Heisenberg-Born-Jordanschen Quantenmechanik zu der Meinen, *Ann. Phys.*, **79**, 361-376.

Schweizer, E. E., Crouse, D. M. and Dairymple, D. L. (1969) Thermal Rearrangement of o-*cis*-Butadienylphenol to 2-Methyl-2H-1-Benzopyran, *Journal of the Chemical Society D: Chemical Communications* 354.

Sialom, B. and Mazur, Y. (1980) Influence of Fuorine and Oxygen Atoms at C-19 on the Previtamin D-Vitamin D Interconversion, *J. Org. Chem.*, **45**, 2201-2204.

Sicinski, R. R. (1992) The Synthesis of Provitamin D Analogue 19-(Phenylsulfonyl)androsta-5,7-diene-3β,17β-diyl 3-Acetate 17-Pivalate, *Acta Chim. Hung.*, **129**, 191.

Slater, J. C. (1931) Directed Valence in Polyatomic Molecules, *Phys. Rev.*, **37**, 481-489.

Smith, H. A. (1940) The Acid Catalyzed Esterification of Aliphatic Acids, *J. Am. Chem. Soc.*, **62**, 1136-1140.

Smith, H. A. and Burn, J. (1944) Kinetics of the Acid-Catalyzed of Phenyl- and Cychlohexyl-Substituted Aliphatic Acids in Methanol, *J. Am. Chem. Soc.*, **66**, 1494-1497.

Smith, H. A. and Hilton, B. (1939) Kinetics of the Catalyzed Esterification of Normal Aliphatic Acids in Methyl Alcohol, *J. Am. Chem. Soc.*, **61**, 254-260.

Smith, S. J. and Sutcliffe, B. T. (1997) The Development of Computational Chemistry in the United Kingdom, *Rev. in Comput. Chem.*, **70**, 271-316.

Solomons, T. W. G. and Fryhle, C. B. (2004) *Organic Chemistry*. John Wiley & Sons, Inc.

Song, B. D. and Jencks, W. P. (1989) Mechanism of Solvolysis of Substituted Benzoyl Halides, *J. Am. Chem. Soc.*, **111**, 8470-8479.

Sonntag, N. O. V. (1953) The Reactions of Aliphatic Acid Chlorides, *Chem. Rev.*, **52**, 237-416.

Stevens, P. J., Devlin, F. J., Chabalowski, C.F. and Frisch, M.J. (1994) Ab Initio Calculation of Vibrational Absorption and Circular Dichroism Spectra Using Density Functional Force Fields, *J. Phys. Chem.*, **98**, 11623-11627.

Stewart, R. and Yates, K. (1960) The Position of Protonation of the Carboxyl Group, *J. Am. Chem. Soc.*, **82**, 4059-4061.

Streitwieser, A., Heathcock, C. H. and Kosower, E. M. (1992) *Introduction to Organic Chemistry*. Macmillan Publishing Company, New York.

Sturm, P. (1999) Quantenchemische Betrachtung Zur Kinetic der Neutralen und Aalkalischen Esterhydrolyse. *Institute of Physical and Theoretical Chemistry*. Regensburg.

Tapia, O. and Goscinski, O. (1975) Self-Consistent Reaction Field Theory of Solvent Effects, *Mol. Phys.*, **29**, 1653-1661.

Tomasi, J., Cammi, R., Mennucci, B., Cappelli, C. and Corni, S. (2002) Molecular Properties in Solution Described with a Continuum Solvation Model, *Phys. Chem. Chem. Phys.* , **4**, 5697.

Tomasi, J., Mietus, S. and Scrocco, E. (1981) Electrostatic Interaction of a Solute with a Continuum - A direct Utilization of Ab Intio Molecular Potentials for the Provision of Solvent Effects, *Chem. Phys.*, **55**, 117-129.

Tomasi, J. and Persico, M. (1994) Molecular Interactions in Solution: An Overview of Methods Based on Continuous Distribution of the Solvent, *Chem. Rev.*, **94**, 2027-2094.

Turro, N. J. (1978) *Modern Photochemistry*. The Benjamin/Cumming Publishing Company, Inc., California.

Vosko, S. H., Wilk, L. and Nusair, M. (1980) Accurate Spin-Dependent Electron Liquid Correlation Energies for Local Spin Density Calculations: A Critical Analysis, *Can. J. Phys.*, **58**, 1200-1211.

Wiest, O. and Houk, K. N. (1996) Density Functional Theory Calculations of Pericyclic Reaction Transition Structures, *Top Curr. Chem.*, **183**, 1-24.

Williamson, A. T. and Hinshelwood, C. N. (1934) The Kinetics of Esterification. The Reaction Between Acetic Acid and Methyl Alcohol Catalyzed by Hydrions, *Transcations of the Faraday Society*, 1145-1159.

Willms, T., Anderson, H.L., Heldt, K. and Hinz, B. (2000) Thermokinetic Investigation of the Alcoholysis of Acetyl Chloride Part I, *Thermochimica Acta*, **364**, 35-45.

Willms, T., Anderson, H.L., Heldt, K. and Hinz, B. (2000) Thermokinetics Investigation of the Reaction of Acetly chloride with Different Alcohols: Part II, *Thermochimica Acta*, **364**, 47-58.

Woodward, R. B. and Hoffman, R. (1970) *The Conservation of Orbital Symmetry*. Verlag Chemie GmbH/Academic Press, Weinheim/Bergstr.

Woodward, R. B. and Hoffmann, R. (1965) Selection Rules for Sigmatropic Reactions, *J. Am. Chem. Soc.*, **87**, 2511-2513.

Woodward, R. B. and Hoffmann, R. (1969) The Conservation of Orbital Symmetry, *Angew. Chem., Int. Ed. Engl*, **8**, 781-853.

Yamabe, S. and Minato, T. (1983) Molecular Orbital Study on the Gas-Phase Nucleophilic Displacement on Acyl Chlorides, *J. Org. Chem.*, **48**, 2972-2975.

Yamabe, S., Minato, T. and Kawabata, Y. (1984) The Importance of the σ^*-π^* Orbital Mixing for the Nucleophilic Displacement on the Unsaturated Carbon, *Can. J. Chem.*, **62**, 235-240.

Ziegler, T. (1991) Approximate Density Functional Theory as Practical tool in Molecular Energetics and Dynamics, *Chem. Rev.*, **91**, 651-667.

Zimmerman, H. E. (1971) Mobius-Huckel Concept in Organic Chemistry. Application of Organic Molecules and Reactions, *Acc. Chem. Res.*, **4**, 272-280.

APPENDIX 1

Supportive information

Table A-1 SI. Absolute energies (Hartree) and entropies (cal $mol^{-1}K^{-1}$) from B3LYP/6-31+G(d) calculations of Z,Z-1,3,5-heptatriene systems and related heteroanalogues

Structure or #	E_e	E_0	H_{298}	G_{298}	S_{298}	ZPE
trans-parent	-272.572545	-272.564175	-272.563231	-272.605393	88.737	0.146824
cis-Parent	-272.56402	-272.555992	-272.555048	-272.59615	86.506	0.14745
Parent TS‡	-272.53885	-272.532463	-272.531519	-272.56871	78.277	0.14437
7-methoxy parent	-387.04886	-387.038465	-387.037521	-387.08503	99.988	0.18061
7-methoxy parent TS‡	-387.02825	-387.019188	-387.018244	-387.06216	92.421	0.17718
7-endo-methoxy parent TS‡	-387.020593	-387.011581	-387.010637	-387.054608	92.545	0.177341
4-methoxy parent	-387.0575	-387.046636	-387.045692	-387.09422	102.204	0.17966
4-methoxy parent TS‡	-387.03157	-387.022642	-387.021698	-387.0217	91.163	0.17703
7-fluoro parent	-371.80854	-371.799862	-371.798918	-371.84254	91.805	0.14029
7-fluoro parent TS‡	-371.78391	-371.776695	-371.775751	-371.81533	83.31	0.13671
7-endo-fluoro parent TS‡	-371.780651	-371.773599	-371.772654	-371.811686	82.149	0.137112
4-fluoro parent	-371.81732	-371.808474	-371.80753	-371.85094	91.353	0.13934
4-fluoro parent TS‡	-371.79185	-371.784662	-371.783718	-371.82305	82.789	0.1361
4-imine parent	-288.6221	-288.614144	-288.6132	-288.65466	87.25	0.13559
4-imine parent TS‡	-288.58474	-288.578529	-288.577585	-288.61444	77.558	0.13266
2-imine parent	-288.61539	-288.607364	-288.60642	-288.64786	87.219	0.13533
2-imine parent TS‡	-288.58605	-288.579843	-288.578899	-288.61581	77.687	0.13293
7-amine parent	-288.622371	-288.614805	-288.613860	-288.653570	83.576	0.137199
7-amine parent TS‡	-288.603243	-288.596954	-288.596010	-288.633139	78.144	0.133109
7-nitro parent	-477.068856	-477.058501	-477.057556	-477.106527	103.066	0.150875
7-nitro parent TS‡	-477.048783	-477.039910	-477.038966	-477.083177	93.051	0.147453
7-cyano parent	-364.805859	-364.796293	-364.795349	-364.841271	96.651	0.146531
7-cyano parent TS‡	-364.786007	-364.777892	-364.776948	-364.818780	88.042	0.143353
7-N(CH3)2 Parent	-406.450581	-406.438860	-406.437916	-406.488577	106.627	0.221300
7-N(CH3)2 Parent TS	-406.430122	-406.419684	-406.418740	-406.465707	98.850	0.217626
7,7-dimethoxy parent	-501.542547	-501.529456	-501.528512	-501.583060	114.805	0.213327
7,7-dimethoxy parent TS‡	-501.518641	-501.506955	-501.506011	-501.555807	104.806	0.209804
7,7-chloro parent	-471.062974	-471.053548	-471.052604	-471.098785	97.195	0.132399
7,7-chloro parent TS‡	-471.033546	-471.025670	-471.024726	-471.065893	86.643	0.128961

E_e	Electronic energy
E_0	Total energy plus zero-point vibrational energy
H_{298}	Enthalpy at 298 K
G_{298}	Gibbs free enthalpy at 298 K
S	Entropy at 298 K
ZPE	Zero point energy

Table A-2 SI. Absolute energies (Hartree) and entropies (cal $mol^{-1}K^{-1}$) from B3LYP/6-31+G(d) calculations of esterification of acetyl chloride with methanol

Structure or #	**E_e**	**E_0**	**H_{298}**	**G_{298}**	**S_{298}**	**ZPE**
Methanol	-115.673890	-115.670568	-115.669624	-115.696643	56.867	0.051303
Methanol-methanol	-231.355375	-231.347424	-231.346480	-231.389301	90.125	0.104968
RI-degenerate	-1073.703168	-1073.696427	-1073.695483	-1073.736522	86.374	0.047294
TS- degenerate	-1073.689580	-1073.683702	-1073.682758	-1073.720021	78.426	0.047645
CH_3COCl	-613.407439	-613.402801	-613.401857	-613.435301	70.388	0.052106
CH_3OH-NH_3	-172.206063	-172.199219	-172.198275	-172.237622	82.813	0.088941
CH_3OH-py	-363.889869	-363.880734	-363.879790	-363.927526	100.468	0.142117
TS-CH_3COCl-2MeOH	-844.746370	-844.734593	-844.733649	-844.784503	107.032	0.155249
TS-CH_3COCl-MeOH-py	-977.278763	-977.265384	-977.264440	-977.320362	117.698	0.190565
TS-CH_3COCl-MeOH-NH_3	-785.596159	-785.585670	-785.584725	-785.631621	98.701	0.138703

E_e	Electronic energy
E_0	Total energy plus zero-point vibrational energy
H_{298}	Enthalpy at 298 K
G_{298}	Gibbs free enthalpy at 298 K
S	Entropy at 298 K
ZPE	Zero point energy

Table A-3 SI. Absolute energies (Hartree) and entropies (cal $mol^{-1}K^{-1}$) from B3LYP/6-31+G(d) calculations of acid-catalyzed esterification

Structure or #	E_e	E_0	H_{298}	G_{298}	S_{298}	ZPE
Methanol	-115.673890	-115.670568	-115.669624	-115.696643	56.867	0.051303
CH_3COOH-HCl	-689.826053	-689.819723	-689.818779	-689.857452	81.395	0.071449
TS-CH_3COOH-HCl-MeOH	-805.487955	-805.479255	-805.478311	-805.521342	90.567	0.125691
HCl	-805.492972	-805.467113	-805.466169	-805.509685	44.615	0.125919
$(CH_3)_2(OH)OH$						
TS2-$(CH_3)_2(OH)OH$-HCl	-805.475931	-805.467113	-805.466169	-805.509685	91.589	0.126444
$CH_2CHCOOH$-HCl	-727.901810	-727.895048	-727.894104	-727.933582	83.088	0.077121
TS-$CH_2CHCOOH$-HCl -MeOH	-843.559395	-843.549662	-843.548718	-843.594720	96.821	0.129849
HCCCOOH-HCl	-726.655337	-726.649496	-726.648552	-726.685915	78.637	0.051889
TS-HCCCOOH-HCl -MeOH	-842.315281	-842.306052	-842.305108	-842.349697	93.846	0.106778
phCOOH-HCl	-881.520426	-881.511452	-881.510508	-881.556154	96.071	0.125489
TS-phCOOH-HCl-MeOH	-997.175756	-997.163778	-997.162834	-997.214737	109.240	0.177854
$phCH_2COOH$-HCl	-920.800536	-920.790055	-920.789111	-920.840085	107.285	0.153477
TS-$phCH_2COOH$-HCl-MeOH	-1036.461781	-1036.448536	-1036.447592	-1036.503352	117.356	0.206834
p-F-phCOOH-HCl	-980.770249	-980.760419	-980.759475	-980.807282	100.619	0.117008
TS-p-F-phCOOH-HCl-MeOH	-1096.425609	-1096.412833	-1096.411889	-1096.465762	113.385	0.169666
p-Cl-phCOOH-HCl	-1341.124603	-1341.114389	-1341.113444	-1341.162558	103.369	0.115552
TS-p-Cl-phCOOH-HCl-MeOH	-1456.780375	-1456.767233	-1456.766288	-1456.821394	115.979	0.168340
p-Br-phCOOH-HCl	-3452.656690	-3452.646555	-3452.645611	-3452.695200	104.368	0.116308
TS-p-Br-phCOOH-HCl-MeOH	-3568.313328	-3568.300131	-3568.299187	-3568.355179	117.846	0.168604
p-CH_3O-phCOOH-HCl						
TS p-CH_3O-phCOOH-HCl-MeOH	-1111.671151	-1111.656557	-1111.655613	-1111.713545	121.929	0.210441

E_e	Electronic energy
E_0	Total energy plus zero-point vibrational energy
H_{298}	Enthalpy at 298 K
G_{298}	Gibbs free enthalpy at 298 K
S	Entropy at 298 K
ZPE	Zero point energy

APPENDIX 2

Accompanying this thesis is a CD containing the Gaussian input file format (gjf), Gaussian output files and excel spreadsheet files used in data analysis. The geometries of the structures can be viewed by using the Gaussview program.